Pergamon

0306-4522(94)00481-1

Neuroscience Vol. 65, No. 1, pp. 119–160, 1995
Elsevier Science Ltd
IBRO
Printed in Great Britain

AFFERENT PROJECTIONS TO THE RAT LOCUS COERULEUS DEMONSTRATED BY RETROGRADE AND ANTEROGRADE TRACING WITH CHOLERA-TOXIN B SUBUNIT AND *PHASEOLUS VULGARIS* LEUCOAGGLUTININ

P.-H. LUPPI,*† G. ASTON-JONES,‡ H. AKAOKA,§ G. CHOUVET§ and M. JOUVET*

*Département de Médecine Expérimentale, U52 INSERM, URA 1195 CNRS, Université Claude Bernard, Lyon, France

‡Department of Psychiatry, Hahnemann University, Philadelphia, 19102, U.S.A.

§INSERM U171, Centre Hospitalier Lyon-Sud, Pierre-Bénite, France

Abstract—The aim of this study was to examine the afferents to the rat locus coeruleus by means of retrograde and anterograde tracing experiments using cholera-toxin B subunit and phaseolus leucoagglutinin. To obtain reliable injections of cholera-toxin B in the locus coeruleus, electrophysiological recordings were made through glass micropipettes containing the tracer and the noradrenergic neurons of the locus coeruleus were identified by their characteristic discharge properties. After iontophoretic injections of cholera-toxin B into the nuclear core of the locus coeruleus, we observed a substantial number of retrogradely labeled cells in the lateral paragigantocellular nucleus and the dorsomedial rostral medulla (ventromedial prepositus hypoglossi and dorsal paragigantocellular nuclei) as previously described.[6] We also saw a substantial number of retrogradely labeled neurons in (1) the preoptic area dorsal to the supraoptic nucleus, (2) areas of the posterior hypothalamus, (3) the Kölliker–Fuse nucleus, (4) mesencephalic reticular formation. Fewer labeled cells were also observed in other regions including the hypothalamic paraventricular nucleus, dorsal raphe nucleus, median raphe nucleus, dorsal part of the periaqueductal gray, the area of the noradrenergic A5 group, the lateral parabrachial nucleus and the caudoventrolateral reticular nucleus. No or only occasional cells were found in the cortex, the central nucleus of the amygdala, the lateral part of the bed nucleus of the stria terminalis, the vestibular nuclei, the nucleus of the solitary tract or the spinal cord, structures which were previously reported as inputs to the locus coeruleus.[10,13] Control injections of cholera-toxin B were made in areas surrounding the locus coeruleus, including (1) Barrington's nucleus, (2) the mesencephalic trigeminal nucleus, (3) a previously undefined area immediately rostral to the locus coeruleus and medial to the mesencephalic trigeminal nucleus that we named the peri-mesencephalic trigeminal nucleus, and (4) the medial vestibular nucleus lateral to the caudal tip of the locus coeruleus. These injections yielded patterns of retrograde labeling that differed from one another and also from that obtained with cholera-toxin B injection sites in the locus coeruleus. These results indicate that the area surrounding the locus coeruleus is divided into individual nuclei with distinct afferents.

These results were confirmed and extended with anterograde transport of cholera-toxin B or phaseolus leucoagglutinin. Injections of these tracers in the lateral paragigantocellular nucleus, preoptic area dorsal to the supraoptic nucleus, the ventrolateral part of the periaqueductal gray, the Kölliker–Fuse nucleus yielded a substantial to large number of labeled fibers in the nuclear core of the locus coeruleus. Anterograde transport of cholera-toxin B or phaseolus leucoagglutinin from the posterior hypothalamic areas yielded a moderate to small number of labeled fibers in the nuclear core of the locus coeruleus. These anterograde tracing experiments confirm that these areas send direct projections to the rat locus coeruleus. Importantly, fiber labeling from each of these areas was in most cases much denser in areas immediately surrounding the locus coeruleus than in the locus coeruleus proper. In particular, the lamina and the periaqueductal gray medial to the locus coeruleus where many dendrites of locus coeruleus noradrenergic cells are located contained a large number of fibers.

These data might indicate that a large number of the afferents to the noradrenergic neurons of the locus coeruleus terminate on dendrites outside the dense core of the nucleus. Further electrophysiological as well as ultrastructural studies are necessary to test this hypothesis.

†To whom correspondence should be addressed.

Abbreviations: DAB, 3,3′-diaminobenzidine; HRP, horseradish peroxidase; PAP, peroxidase-antiperoxidase; PB, phosphate buffer; PBST, PB saline containing 0.3% Triton X-100; PBST-Az, PBST and 0.1% sodium azide; PHA-L, *Phaseolus vulgaris* leucoagglutinin; PS, paradoxical sleep; TH, tyrosine hydroxylase; TMB, tetramethylbenzidine; WGA-HRP, wheatgerm agglutinin conjugated with HRP.

The rat locus coeruleus (LC) is a nucleus of the pontine tegmentum composed of a homogeneous compact noradrenergic cell group innervating nearly all the neuroaxis.[16] These neurons exhibit a regular tonic discharge during waking, decrease their activity during slow-wave sleep and almost stop firing during paradoxical sleep (PS).[4] During waking, these neurons are phasically activated by a variety of sensory

stimuli.[5] These and other data obtained by electrophysiological and pharmacological experiments suggest a crucial role of these cells in the control of behavioral state, including vigilance and attention, and a critical but permissive role in the generation of paradoxical sleep.[4,34,43] For several years, several groups have sought to understand the afferent control of LC neurons to reveal brain circuits involved in state and attention functions.

In early anatomical studies, using the retrograde tracer horseradish peroxidase (HRP) with diaminobenzidine (DAB) as a chromogen, it was reported that many CNS structures project to the LC.[10,13,45,57] In contrast, using the more sensitive retrograde tracers Fluoro-Gold and wheatgerm agglutinin conjugated with HRP (WGA-HRP) with tetramethylbenzidine (TMB) as a chromogen, Aston-Jones *et al.*[6] recently found that major inputs to the LC as indicated by numerous strongly labeled neurons emanate from two nuclei, the paragigantocellularis lateralis and prepositus hypoglossi, both in the rostral medulla. This conclusion was substantiated by confirmatory anterograde tracing as well as by electrophysiological studies showing prominent functional influences of these two nuclei on LC neurons. We recently reported in cats that subunit B from the cholera-toxin (CTb), when iontophoretically applied and visualized with streptavidin-HRP, is a highly sensitive retrograde and anterograde tracer.[41] Therefore, here we applied our method to rats in order to examine the afferents to the LC. Single cell recordings through the injection pipette were used to accurately place injections in the LC. We endeavoured to confirm the specificity of the retrogradely labeled afferents to the LC by means of (1) CTb control injections in the regions surrounding the LC and (2) injections of the anterograde tracers CTb and *Phaseolus vulgaris* leucoagglutinin (PHA-L) in the areas projecting to the LC. Preliminary results of this work have been reported.[39]

EXPERIMENTAL PROCEDURES

Retrograde tracing experiments

Male Sprague–Dawley rats (Taconic Farms Inc. or IFFA Credo) weighing 250–350 g were anesthetized with chloral hydrate (400 mg/kg, intraperitoneal) or Nembutal (60 mg/kg, intraperitoneal) and placed in a stereotaxic apparatus. A scalp incision was made, a hole was drilled in the skull overlying the LC, and the dura was reflected. The skull was placed at a 12° angle (nose tilted down) to avoid rupturing the overlying transerse sinus; coordinates were: 3.7 mm caudal to real lambda, 1.2 mm lateral to midline and 6.0 mm ventral from skull.

Preparation of cholera toxin B. To obtain reliable iontophoretic injections, it was necessary to replace the original buffer lyophilized with CTb by a phosphate buffer (PB) at pH 6.0.[41] For this purpose, 1 mg of lyophilized CTb was reconstituted with 1 ml of 0.1 M PB (pH 6.0) and then desalted, buffer exchanged and concentrated to 1% by two repeated 1 h-30-ultrafiltrations (1–0.1 ml) at 7000 r.p.m. with a centricon-10 microconcentrator (Amicon, U.S.A.).

Cholera toxin B injection protocol. Glass capillary tubes (1.5 or 1 mm O.D.) were heated, pulled and the tips broken to 3–5 μm diameter under microscopic control. These micropipettes were backfilled with the 1% solution of CTb in 0.1 M PB (pH 6.0). Electrophysiological recordings from these pipettes with a good signal to noise ratio aided in localizing LC by its distinctive spontaneous or foot pinch-evoked discharge characteristics.[7] To eject CTb, a pulsed positive current (4 or 7 s on, 4 or 7 s off, 0.5–2 μA, 5–15 min) was applied (Midgard CS-4 or Finntronics constant current source) to avoid heating or clogging the tip. At the end, the pipettes were left in place for 10–15 min to prevent leakage of the tracer along the pipette track. Animals were allowed to survive for one to seven days before perfusion. Using different injection times and currents we obtained either large ($n = 6$, 1–2 μA, 5–15 min) or small ($n = 8$, 0.5 μA, 5–15 min) injections centered in the LC. Control iontophoretic injections (0.5 μA, 10 min) were also made in nuclei adjacent to LC including Barrington's nucleus (Bar, $n = 3$), mesencephalic trigeminal nucleus (5 Me, $n = 2$), the peri-5 Me nucleus ($n = 3$) and the medial vestibular nucleus (MVe, $n = 1$).

Histology. The animals were deeply anesthetized and perfused through the ascending aorta, initially with 200 ml of Ringer's lactate solution with 0.1% heparine, followed by 1,000 ml of an ice-cold fixative in 0.1 M PB (pH 7.4) containing 4% paraformaldehyde, 0–0.25% glutaraldehyde and 0.2% picric acid. After removal from the skull, the brains were postfixed overnight at 4°C in 0.1 M PB containing 2% paraformaldehyde and 0.2% picric acid. The brains were then rinsed and cryoprotected by immersion in 0.1 M PB containing 30% sucrose for 48–72 h at 4°C. Afterwards, these specimens were rapidly frozen with CO_2 gas and coronal 20–25-μm-thick sections were cut on a cryostat. The free-floating sections were then incubated in CTb antiserum or stocked before staining in 0.1 M PB saline (NaCl, 0.9%) containing 0.3% Triton X-100 (PBST) and 0.1% sodium azide (PBST-Az, pH = 7.4).

Immunohistochemistry of cholera toxin B. Immunohistochemical detection of CTb was carried out by sequential incubations of free-floating sections according to Hsu *et al.*,[31] method slightly modified.[41] The sections were first submitted to a long incubation over three to four days at 4°C in PBST-Az with the "goat" CTb antiserum (List Biological Laboratories) at a 1:40,000 dilution, with gentle stirring. Then, they were rinsed 2 × 30 min in PBST and incubated for 90 min at room temperature or overnight at 4°C

Fig. 1. (A) Color photomicrograph illustrating a small CTb injection apparently limited to the ventral part of the LC (RLC16). The section has been counterstained with TH-immunohistochemistry (in brown) to help delineate the border of the LC. Note that the site did not substantially encroached on the lamina between the LC and the ventricle or the MVe region just lateral to the LC. Scale bar = 100 μm. (B) Color photomicrograph showing anterogradely labeled fibers in the nuclear core of the LC after the PHA-L injection in the preoptic region shown in Fig. 22E. The section has been counterstained with Neutral Red to help delineating the LC. Scale bar = 100 μm. (C) Color photomicrograph showing anterogradely labeled fibers in the LC and the periaqueductal gray medial to it after a CTb injection in the ventrolateral part of the periaqueductal gray. The section was counterstained with TH-immunohistochemistry in brown. Scale bar = 100 μm. (D) Color photomicrograph illustrating terminal-like dots in the LC after a CTb injection in the nucleus Kölliker–Fuse. The section was counterstained for TH-immunoreactivity which appears brown. Scale bar = 100 μm.

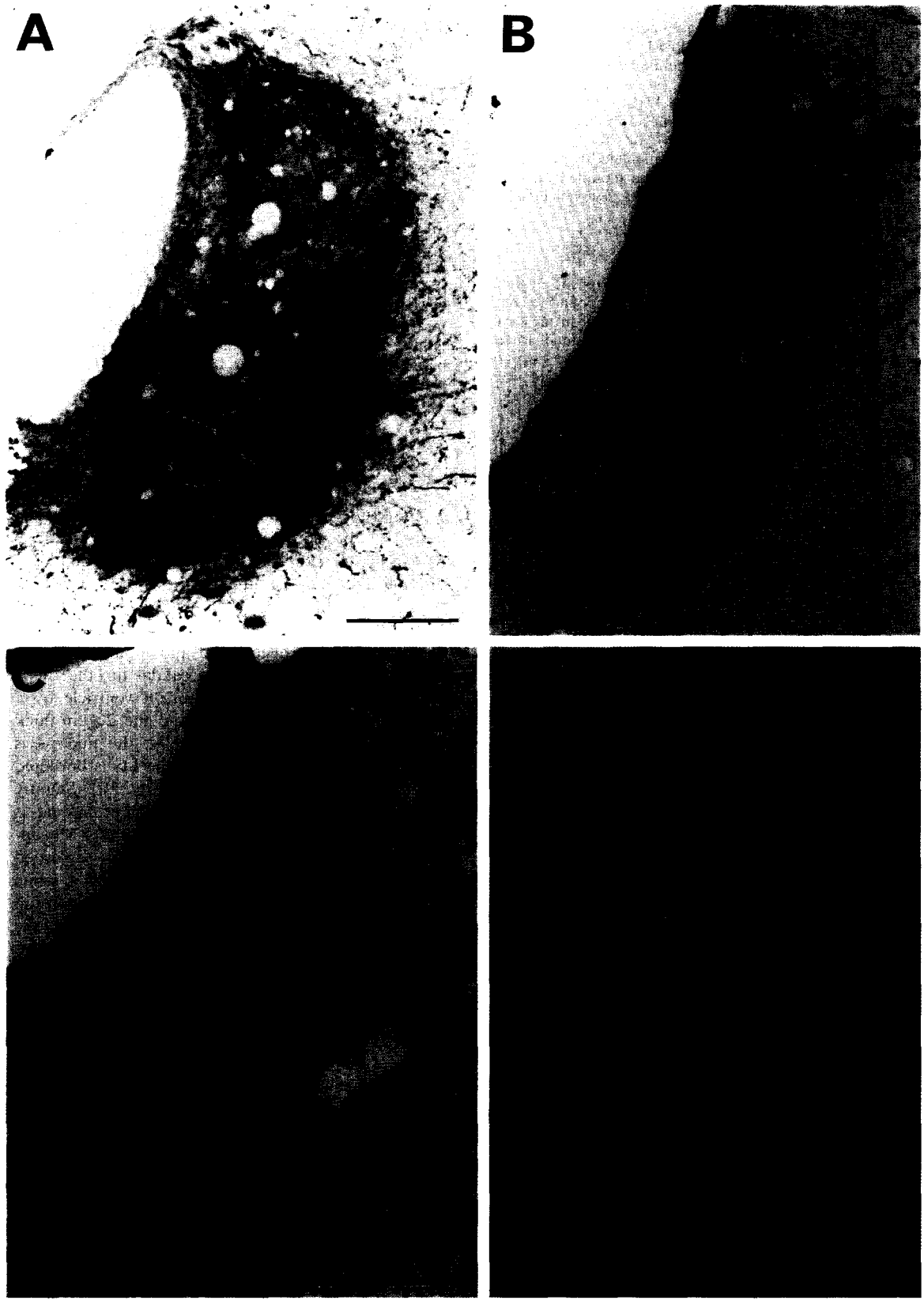

Fig. 1

in the biotinylated donkey anti-goat immunoglobulin (1:2,000 in PBST, Jackson Immunoresearch Lab) followed after 2 × 30 min rinses in PBST by streptavidin-HRP (1:40,000 in PBST, Jackson Immunoresearch Lab). Finally, after 2 × 30 min rinses in PBST, the sections were immersed in 0.02% 3,3′-diaminobenzidine-4 HCl (DAB, Sigma) containing 0.003% H_2O_2 and 0.6% nickel ammonium sulfate in 0.05 M Tris-HCl buffer (pH 7.6) for 10–15 min at room temperature. The reaction was terminated by two washes in PBST-Az. Finally, the sections were mounted on gelatin-coated glass slides, dried, dehydrated and coverslipped with Depex or Permount.

Anterograde tracing experiments

Injection protocol. Phaseolus vulgaris-leucoagglutinin (PHA-L) was injected in certain structures found to contain cells retrogradely labeled from the LC and, in most cases, CTb was also injected contralaterally in the same structure. A stereotaxic surgical method similar to the retrograde experiments was used, but the injections were made with a flat skull and the aid of brain surface landmarks for stereotaxic orientation. PHA-L (Vector Lab., 2.5% in 0.01 M PBS) was iontophoretically injected.[24] Cellular recordings through the injection pipette (10–20 μm tips) aided in localizing target sites. Injections were made with 5 μA of pulsed current (4 or 7 s on, 4 or 7 s off) for 30 min. For CTb, iontophoretic injections were made through 3–5 μm micropipettes using a 2 μA pulsed positive current for 15–30 min. Animals survived for seven to 15 days and were then deeply anesthetized and perfused. The brains were then postfixed and cut into frontal sections as described above for the retrograde experiments. Injections were made in the infralimbic cortex (PHA-L, $n = 1$), the area 1 of the frontal cortex and the adjacent hindlimb region of the primary somatosensory area (PHA-L, $n = 2$), the preoptic area located dorsal to the supraoptic nucleus (CTb, $n = 2$, PHA-L, $n = 2$), the dorsal hypothalamic area (CTb, $n = 2$, PHA-L, $n = 2$), the perifornical area (CTb, $n = 2$, PHA-L, $n = 2$), the lateral hypothalamic area latero-dorsal to the fornix (CTb, $n = 2$, PHA-L, $n = 2$), the lateral hypothalamic area dorso-medial to the subthalamic nucleus (CTb, $n = 1$, PHA-L, $n = 1$), the mesencephalic reticular formation (B9 serotoninergic group) (PHA-L, $n = 2$), the ventrolateral part of the periaqueductal gray (CTb, $n = 2$, PHA-L, $n = 3$), the dorsal raphe nucleus (CTb, $n = 3$), the latero-dorsal tegmental nucleus of Castaldi (CTb, $n = 3$), the nucleus Kölliker–Fuse (CTb, $n = 1$, PHA-L, $n = 1$), the nucleus raphe magnus (CTb, $n = 5$) and the lateral paragigantocellular nucleus (CTb, $n = 1$, PHA-L, $n = 4$).

Immunohistochemical procedures. The immunohistochemical detection of CTb was carried out as described above for the retrograde experiments. For PHA-L immunohistochemistry, the sections were first submitted to a long incubation over three to four days at 4°C in PBST-Az with a "rabbit" PHA-L antiserum (DAKO) at a 1:5000 dilution, with gentle stirring. Then, they were rinsed 2 × 30 min in PBST and incubated for 90 min at room temperature or overnight at 4°C in the biotinylated "donkey" anti-rabbit immunoglobulin (1:2000, Jackson Immunoresearch Lab.) followed after 2 × 30 min rinses in PBST by streptavidin-HRP (1:40,000, Jackson Immunoresearch Lab.). Finally, as for CTb staining, after 2 × 30 min rinses in PBST, the sections were immersed in 0.02% 3,3′-diaminobenzidine-4 HCl (DAB, Sigma) containing 0.003% H_2O_2 and 0.6% nickel ammonium sulfate in 0.05 M Tris-HCl buffer (pH 7.6) for 10–15 min at room temperature. The reaction was terminated by extensive washes in PBST-Az.

For double labeled sections, CTb-stained sections were incubated for four days at 4°C in rabbit antiserum to tyrosine hydroxylase (TH, 1:10,000, Institut Jacques Boy). After washes, the sections were placed sequentially for 90 min at room temperature in donkey anti-rabbit IgG (1:400, DAKO) and rabbit peroxidase-antiperoxidase (PAP, 1:400, DAKO). Sections were then reacted with 0.025% DAB containing 0.006% H_2O_2 in Tris-HCl buffer for 15–30 min. Following this procedure, the CTb anterogradely labeled fibers were blue-black, whereas the cytoplasm of noradrenergic neurons were brown (Fig. 1). All sections were then mounted on gelatin coated glass slides, dried, dehydrated and coverslipped with Depex.

RESULTS

Cytoarchitecture of the locus coeruleus area

The cytoarchitecture of the LC area has been described previously.[25,53,60,66] Nevertheless, in the course of our study of LC afferents, we found additional undefined landmarks in this area. To study the organization of the LC area, 20 μm frontal LC sections taken every 100 μm from control rat brains were stained with neutral red and mounted in rostro–caudal order. At its more caudal tip, the LC is separated medially from the fourth ventricle by a 30-μm-thick cell poor lamina and the 20-μm-thick ependyma. Laterally and ventrally, the nucleus is bordered by the MVe. Dorsally, the LC is bordered by the brachium conjunctivum (Fig. 2F). Slightly rostrally, the medially located cell poor lamina is thicker (approximately 100 μm) and the 5 Me appears laterally. At this level, the 5 Me is separated from the LC by an area containing few cells in white matter (Fig. 2B) that appears to be a rostral extension of the MVe. Slightly more rostrally, at the level of the maximum extension of the LC, this region becomes thinner and the 5 Me is very close to the lateral border of the LC. Medially, the LC is separated from the ventricle by a large undefined area that appears to be part of the pontine periaqueductal gray. At this level and more rostrally, the LC is bordered dorsally by the medial parabrachial nucleus (Fig. 3C).

Abbreviations used in the figures

3	oculomotor nucleus
3V	third ventricle
4	trochlear nucleus
7	facial nucleus
8n	vestibulocochlear nerve
10	dorsal motor nucleus of vagus
12	hypoglossal nucleus
ac	anterior commissure
aca	anterior commissure, anterior
AHC	anterior hypothalamic area, central part
AHP	anterior hypothalamic area, posterior part
Amb	ambiguus nucleus
AP	area postrema
Aq	aqueduct (Sylvius)
Arc	arcuate hypothalamic nucleus
ATg	anterior tegmental nucleus
B9	B9 5-hydroxytryptamine cells
Bar	Barrington's nucleus
BST	bed nucleus of the stria terminalis
BSTL	bed nucleus of the stria terminalis, lateral division

BSTM	bed nucleus of the stria terminalis, medial division
BSTV	bed nucleus of the stria terminalis, ventral division
Ce	central amygdaloid nucleus
CG	central (periaqueductal) gray
Cl	claustrum
CLI	caudal linear nucleus of the raphe
CNF	cuneiform nucleus
cp	cerebral peduncle, basal part
Cu	cuneate nucleus
CVL	caudoventrolateral reticular nucleus
DA	dorsal hypothalamic area
Dk	nucleus of Darkschewitsch
DLL	dorsal nucleus of the lateral lemniscus
DM	dorsomedial hypothalamic nucleus
DMC	dorsomedial hypothalamic nucleus, compact part
DMD	dorsomedial hypothalamic nucleus, diffuse part
DPGi	dorsal paragigantocellular nucleus
DR	dorsal raphe nucleus
DTg	dorsal tegmental nucleus
EP	entopeduncular nucleus
EW	Edinger–Westphal nucleus
f	fornix
F	nucleus of the fields of Forel
FF	fields of Forel
fmi	forceps minor corpus callosum
fr	fasciculus retroflexus
Fr1	frontal cortex, area 1
g7	genu of the facial nerve
Gi	gigantocellular reticular nucleus
GiA	gigantocellular reticular nucleus, alpha part
GiV	gigantocellular reticular nucleus, ventral part
Gr	gracile nucleus
HDB	nucleus of the horizontal limb of the diagonal band
ic	internal capsule
IL	infralimbic cortex
IO	inferior olive
IP	interpeduncular nucleus
IPA	interpeduncular nucleus, apical subnucleus
KF	Kölliker–Fuse nucleus
LC	locus coeruleus
LDT	laterodorsal tegmental nucleus
lfp	longitudinal fasciculus of the pons
LH	lateral hypothalamic area
LHb	lateral habenular nucleus
Li	linear nucleus of the medulla
ll	lateral lemniscus
LM	lateral mammillary nucleus
LPB	lateral parabrachial nucleus
LPGi	lateral paragigantocellular nucleus
LPO	lateral preoptic area
LRt	lateral reticular nucleus
LSO	lateral superior olive
LV	lateral ventricle
LVe	lateral vestibular nucleus
lvs	lateral vestibulospinal tract
MCLH	magnocellular nucleus of the lateral hypothalamus
MCPO	magnocellular preoptic nucleus
MdD	medullary reticular nucleus, dorsal part
MdV	medullary reticular nucleus, ventral part
Me5	mesencephalic trigeminal nucleus
me5	mesencephalic trigeminal tract
ml	medial lemniscus
mlf	medial longitudinal fasciculus
Mn	medial mamillary nucleus
MP	medial mamillary nucleus, posterior
MnPO	median preoptic nucleus
MnR	median raphe nucleus
Mo5	motor trigeminal nucleus
MPA	medial preoptic area
MPB	medial parabrachial nucleus
MPO	medial preoptic nucleus
MPOC	medial preoptic nucleus, central part
mt	mammillothalamic tract
MTu	medial tuberal nucleus
MVe	medial vestibular nucleus
opt	optic tract
ox	optic chiasm
Pa	paraventricular hypothalamic nucleus
PBG	parabigeminal nucleus
PCRt	parvocellular reticular nucleus
PDTg	posterodorsal tegmental nucleus
PeF	perifornical nucleus
PH	posterior hypothalamic area
PMD	premammillary nucleus, dorsal part
PMR	paramedian raphe
PMV	premammillary nucleus, ventral part
Pn	pontine nuclei
PnC	pontine reticular nucleus, caudal part
PnO	pontine reticular nucleus, oral part
PnV	pontine reticular nucleus, ventral part
PPT	pedunculopontine tegmental nucleus
Pr5	principal sensory trigeminal nucleus
PrH	prepositus hypoglossi nucleus
PVA	paraventricular thalamic nucleus, anterior part
py	pyramidal tract
R	red nucleus
RCh	retrochiasmatic area
RMC	red nucleus, magnocellular part
RMg	raphe magnus nucleus
ROb	raphe obscurus nucleus
RPa	raphe pallidus (postpyramidal raphe) nucleus
RPC	red nucleus, parvocellular part
RPn	raphe pontis nucleus
RPO	rostral periolivary region
RR	retrorubral nucleus
RRF	retrorubral field
rs	rubrospinal tract
RtT	reticulotegmental nucleus of the pons
s5	sensory root trigeminal nerve
SC	superior colliculus
SCh	suprachiasmatic nucleus
scp	superior cerebellar peduncle (brachium conjunctivum)
SHy	septohypothalamic nucleus
SI	substantia innominata
sm	stria medullaris of the thalamus
SN	substantia nigra
SNC	substantia nigra, compact part
SNR	substantia nigra, reticular part
SO	supraoptic nucleus
Sol	nucleus of the solitary tract
sol	solitary tract
SOR	supraoptic nucleus, retrochiasmatic (diffuse) part
sox	supraoptic decussation
sp5	spinal trigeminal tract
Sp5C	spinal trigeminal nucleus, caudal part
SPO	superior paraolivary nucleus
SpVe	spinal vestibular nucleus
st	stria terminalis
STH	subthalamic nucleus
TM	tuberomammillary nucleus
ts	tectospinal tract
Tz	nucleus of the trapezoid body
VLL	ventral nucleus of the lateral lemniscus
VMH	ventromedial hypothalamic nucleus
VMHC	ventromedial hypothalamic nucleus, central part
VP	ventral pallidum
VTA	ventral tegmental area (Tsai)
VTg	ventral tegmental nucleus (Gudden)
xscp	decussation of the superior cerebellar peduncle
ZI	zona incerta

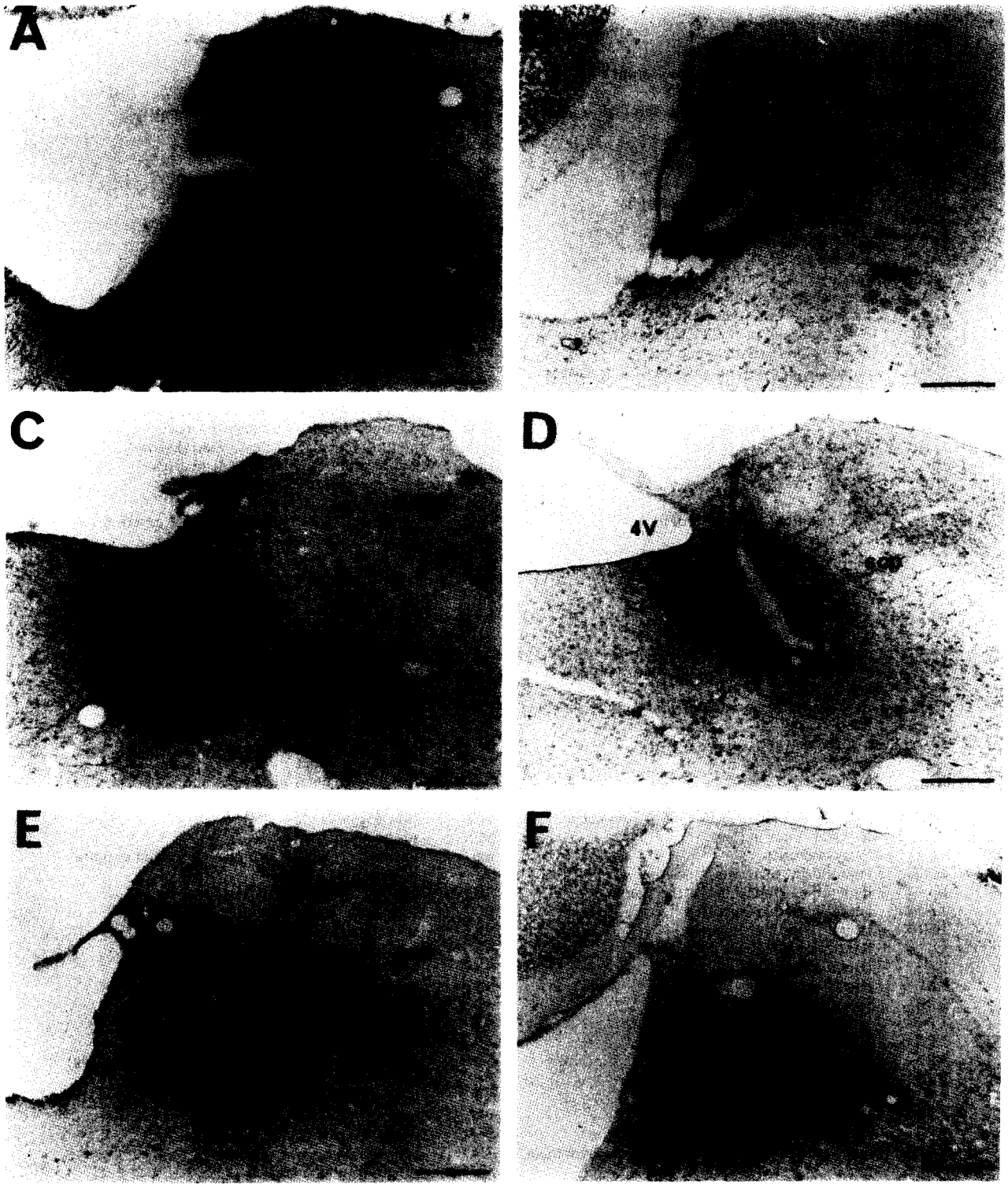

Fig. 2. (A) Illustration of a CTb injection site in the rat LC + peri-LC (RLC2, ~600 μm in diameter). Note that this site covered the entire LC and also involved the lamina and the periaqueductal gray between the LC and the fourth ventricle and part of the MVe area just lateral to the LC. (B) Illustration of a CTb injection site in the rat LC (RLC15, ~180 × 350 μm). Note that this site was localized in the caudal LC and did not substantially appear to involve the lamina and the periaqueductal gray medial to the LC. The MVe region lateral to the LC did not appear to be involved. (C) Illustration of a control CTb injection site in Barrington's nucleus (~400 μm in diameter). Note that this site involved also the periaqueductal gray surrounding the Bar but did not appear to involve the LC or the peri-5 Me nucleus. (D) Illustration of a CTb injection site in the peri-5 Me nucleus (~200 μm in diameter). Note that this site is apparently limited to this nucleus with only a small extension in the LC region dorsal to it. The Bar seems to be not involved. (E) Illustration of a control injection site of CTb in the mesencephalic trigeminal nucleus (Me5) (~300 μm in diameter). Note that this site did not appear to substantially involve the LC. The medial parabrachial nucleus is slightly involved in this site. (F) Illustration of a control CTb injection site in the MVe region just lateral to the caudal part of the LC (~300 μm in diameter). Note that this site did not appear to substantially involve the LC or the 5 Me. Scale bars = 200 μm (A–F).

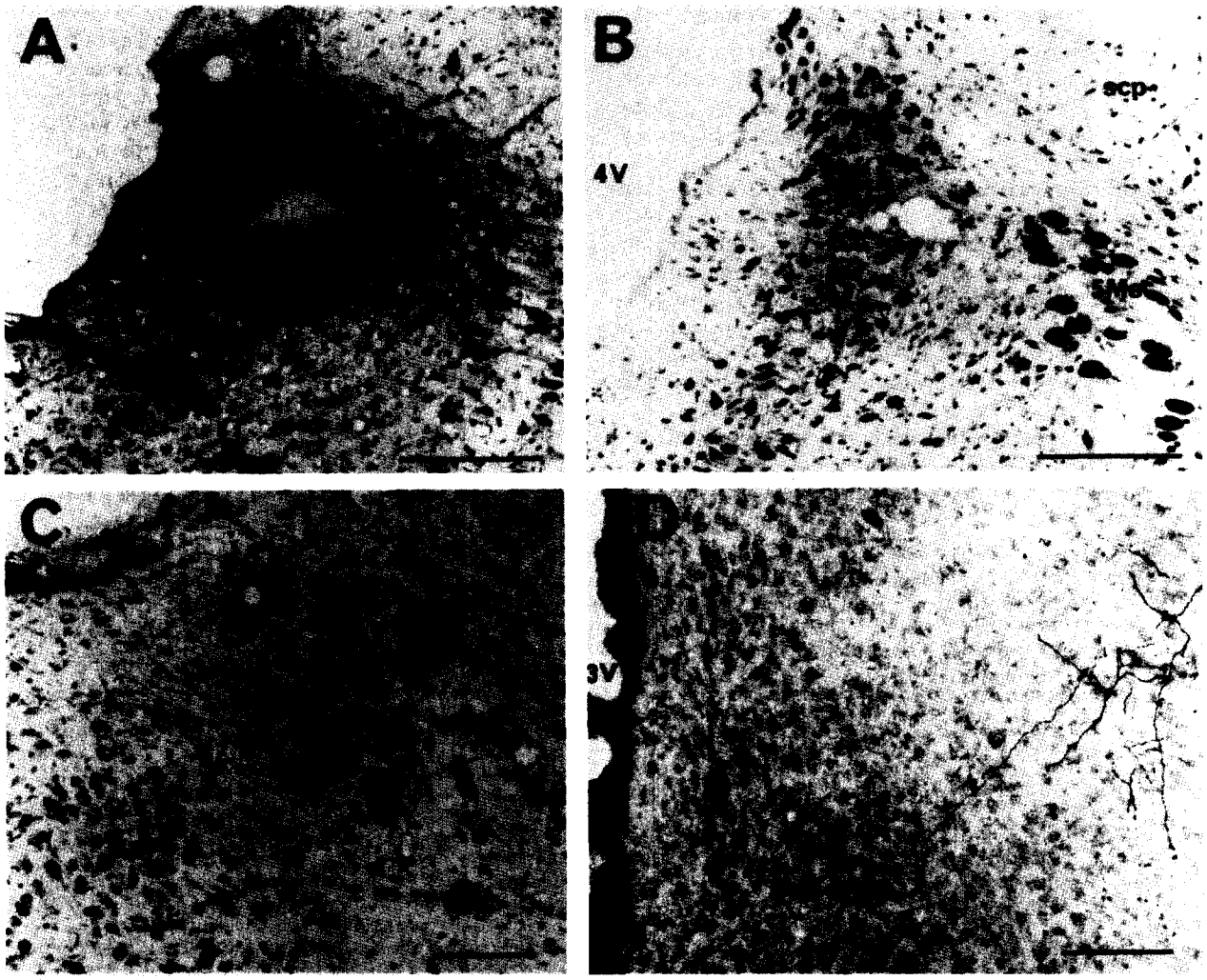

Fig. 3. (A) Illustration of a small CTb injection site in the LC (RLC6). The site also slightly involved the MVe area located between the LC and the Me5. Note that a crack is visible in the center of the site. Scale bar = 200 μm. (B) Photomicrograph of a section only counterstained with neutral red adjacent to that shown in A. Note that there is no trace of tissue necrosis in the center of the injection site, although a blood vessel is localized at this site. Scale bar = 200 μm. (C) Photomicrograph of a frontal section counterstained with neutral red at the level of the Bar and the peri-5 Me just medial to the Me5. Numerous retrogradely labeled cells are clustered in the peri-5 Me. These neurons were stained after a CTb injection in the dorsomedial nucleus of the hypothalamus. Scale bar = 100 μm. (D) Photomicrograph showing anterogradely labeled fibers in the dorsomedial nucleus of the hypothalamus after a CTb injection in the peri-5 Me nucleus. Scale bar = 100 μm.

More rostrally, the ventral part of the LC progressively becomes less compact and then disappears and only a dorsal collection of LC cells remains (Fig. 3C). Ventral to them, two groups of cells appear with a morphology distinct from the adjacent periaqueductal gray. One is located just ventral to the few LC cells and medial to the 5 Me and is composed of small ovoid cells. The second is located more medially and ventrally and is composed of slightly larger ovoid cells. The first group has not been previously defined. Therefore, because of its localization just medial to the 5 Me, we denote it as the Peri-5 Me nucleus (Fig. 3C). The second group of cells corresponds to the previously defined Barrington's nucleus (Bar).[8,59] With regard to the LC noradrenergic neurons, it is noteworthy that a large number of processes (apparently dendrites) were found outside the nuclear core of the LC in select peri-LC regions, particularly in the lamina between the LC and the fourth ventricle and also in the areas rostromedial and caudodorsal to the LC nucleus proper. Note that LC dendrites do not appear to be extensive lateral to the LC nucleus proper. This topographically specific distribution of presumed LC dendrites is similar to that previously reported in a more extensive analysis.[22,61]

Afferent projections to the locus coeruleus

Retrograde tracing experiments: injection sites. As illustrated in Figs 1A, 2, 3A and 4C, CTb iontophoretic injection sites were characterized by a dense central area surrounded by a peripheral zone containing diffuse tracer and stained fibers. Usually, the histochemical reaction produced a crack at the center of the site. This crack did not correspond to necrosis of the tissue as determined on sections that were only counter stained with Neutral Red adjacent to those immunostained with CTb (Fig. 3A, B) as we previously observed in the cat.[41] Indeed, on such sections, the tissue and the morphology of the LC cells localized in the injection site appeared normal (Fig. 3B).

We calculated that the homogeneous nuclear core of the LC is 170–230-μm-mediolaterally, 700-μm-dorsoventrally and 400–500-μm-long in the rostrocaudal direction. We obtained eight small CTb injection sites in the LC which appeared to have no or only limited extensions into surrounding areas. These sites had 200–350-μm-diameters and were round or ovoid (Figs 1A, 2B, 3A). Three sites were localized in the middle part of the LC (Fig. 2B), four in its ventral part (Fig. 1A) and one in its dorsal part. Three of them appeared to be restricted to the nuclear core of the LC (Figs 1A, 2B). Five of them slightly involved the MVe area just lateral to the LC (Fig. 3A). None of them appeared to involve the periaqueductal gray and the lamina medial to the LC, the Bar, the 5 Me and the peri-5 Me. We also obtained three large injection sites centered in the LC with 400–600-μm-diameters involving areas adjacent to the LC (peri-LC areas). These sites, which we termed LC + peri-LC injections, involved (1) the MVe areas just lateral and caudal to the LC and (2)

Fig. 4. (A) Photomicrograph illustrating the contralateral LC after a CTb injection in the LC + peri-LC. Note the presence of a few retrogradely labeled cells and anterogradely stained fibers in the LC. Scale bar = 100 μm. (B, D) Photomicrograph showing retrogradely labeled neurons in the nucleus prepositus hypoglossi (B) and the lateral paragigantocellular nucleus (D) after a CTb injection in the LC + peri-LC. Scale bars = 200 μm. (C) Photomicrograph of a CTb injection site in the LPGi. Scale bar = 500 μm. (E, F) Photomicrograph showing anterogradely labeled fibers in Barrington's nucleus (E) and the LC (F) after the CTb injection in the PGi shown in C. Note the presence of retrogradely labeled cells in the Bar nucleus (E). Scale bars = 200 μm.

Fig. 5. (A) Photomicrograph of a frontal section showing retrogradely labeled cells in the nucleus Kölliker–Fuse after a large CTb injection in the LC + peri-LC. Note also the anterograde labeling of the dorsal noradrenergic bundle at the upper left of the figure. Scale bar = 500 μm. (B) Photomicrograph illustrating a PHA-L injection site centered in the nucleus Kölliker–Fuse. Scale bar = 500 μm. (C) Enlargement of A showing at higher magnification the morphology of the retrogradely labeled cells in the nucleus Kölliker–Fuse. Scale bar = 50 μm. (D) Photomicrograph of a frontal section showing retrogradely labeled cells in the lateral parabrachial nucleus after a LC + peri-LC injection. Note also the anterograde labeling of the dorsal noradrenergic bundle ventrally to the mesencephalic trigeminal nucleus. Scale bar = 500 μm. (E) Photomicrograph showing anterogradely labeled fibers in the LC after the PHA-L injection in the nucleus Kölliker–Fuse shown in B. Note also the presence of a large number of fibers in the MVe area just lateral to the LC and in the lamina between the LC and the fourth ventricle. Scale bar = 200 μm.

Fig. 6. (A) Photomicrograph showing retrogradely labeled neurons in the lateral part of the periaqueductal gray at the level of the oculomotor nucleus after a large CTb injection site in the rat LC + peri-LC. Note the anterograde labeling of the dorsal noradrenergic bundle situated ventrolaterally to the periaqueductal gray. Scale bar = 500 μm. (B) Photomicrograph showing anterogradely labeled fibers in the nuclear core of the rat LC after the PHA-L injection in the lateral part of the periaqueductal gray shown in D. Only occasional fibers are localized in the MVe region lateral to the LC. Note that the dorsal LC is partly obscured by artefactual labeling in a tear in the tissue. Scale bar = 100 μm. (C) Enlargement of A showing at high magnification the morphology of the retrogradely labeled neurons in the periaqueductal gray after a LC + peri-LC injection. Scale bar = 50 μm. (D) Photomicrograph illustrating a PHA-L injection in the lateral part of the periaqueductal gray. Scale bar = 500 μm. (E) Photomicrograph illustrating anterogradely labeled fibers in the nuclear core of the LC after a CTb injection in the ventrolateral part of the periaqueductal gray. Note that the lamina between the LC and the fourth ventricle (on the left of the figure) contained more fibers that the nuclear core of the LC. Scale bar = 100 μm.

Fig. 7. (A) Photomicrograph illustrating the distribution of retrogradely labeled cells in the posterior hypothalamic areas after a CTb injection in the LC + peri-LC. Note that the cells are diffusely distributed in the posterior hypothalamic areas. Anterogradely labeled fibers belonging to the dorsal noradrenergic bundle are visible in the medial forebrain bundle (upper right of the figure). Scale bar = 200 μm. (B) Photomicrograph of a frontal section at the level of a PHA-L injection site localized just laterally to the dorsomedial hypothalamic nucleus. Scale bar = 500 μm. (C) Photomicrograph showing terminal-like dot labeling in the nuclear core of the LC after a CTb injection in the perifornical nucleus dorsal to the fornix at the level of the dorsomedial hypothalamic nucleus. Note the presence of numerous retrogradely labeled cells localized just medially to the LC. A few cells are localized in the LC proper. Scale bar = 100 μm. (D) Photomicrograph illustrating the dense plexus of fibers localized in the Barrington's nucleus after the PHA-L injection shown in B. A large number of fibers are also labeled in the surrounding periaqueductal gray and the peri-5 Me. Scale bar = 200 μm. (E) Photomicrograph showing anterogradely labeled fibers in the nuclear core of the LC and the lamina between the LC and the fourth ventricle after the PHA-L injection in the posterior hypothalamic area shown in B. Scale bar = 100 μm.

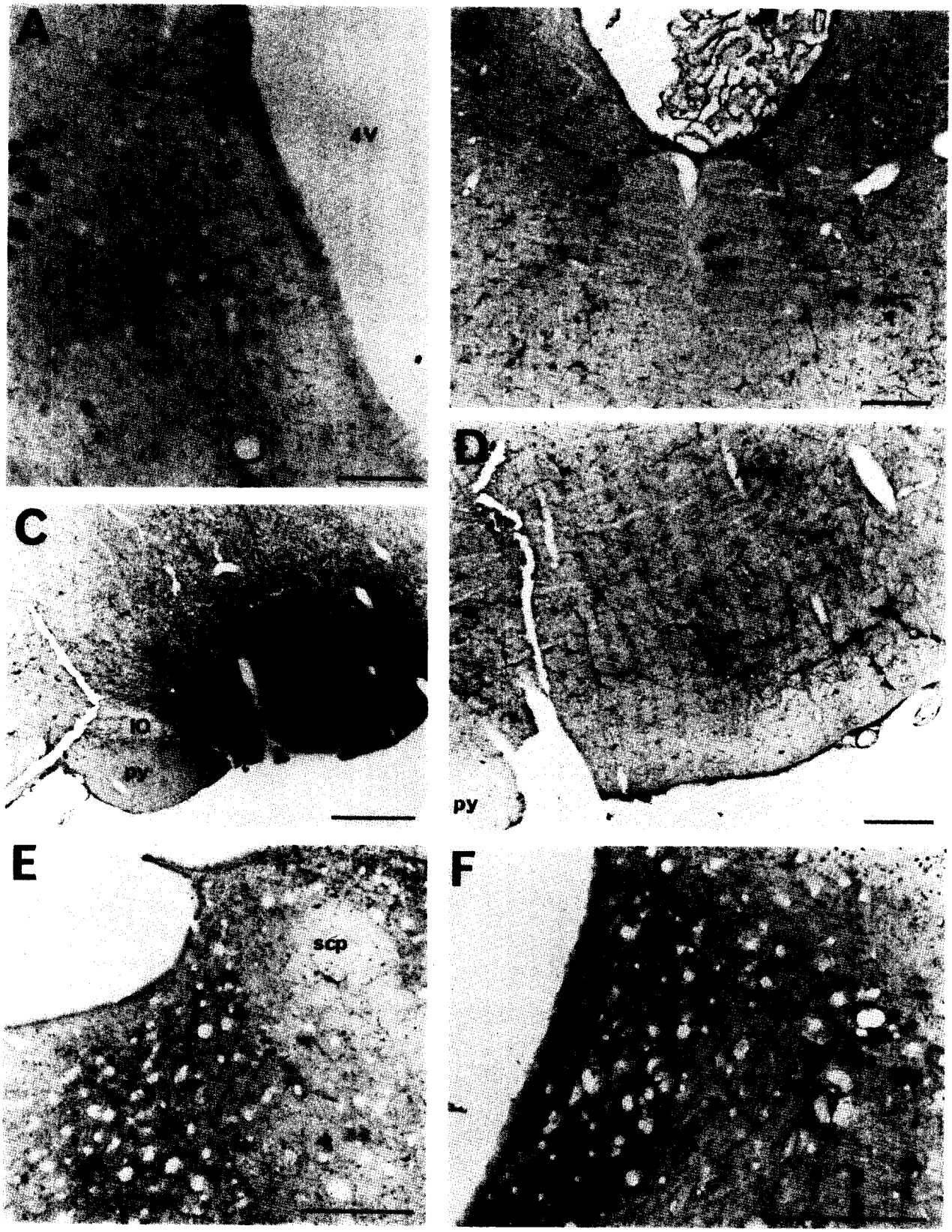

Fig. 4. (*Caption opposite*)

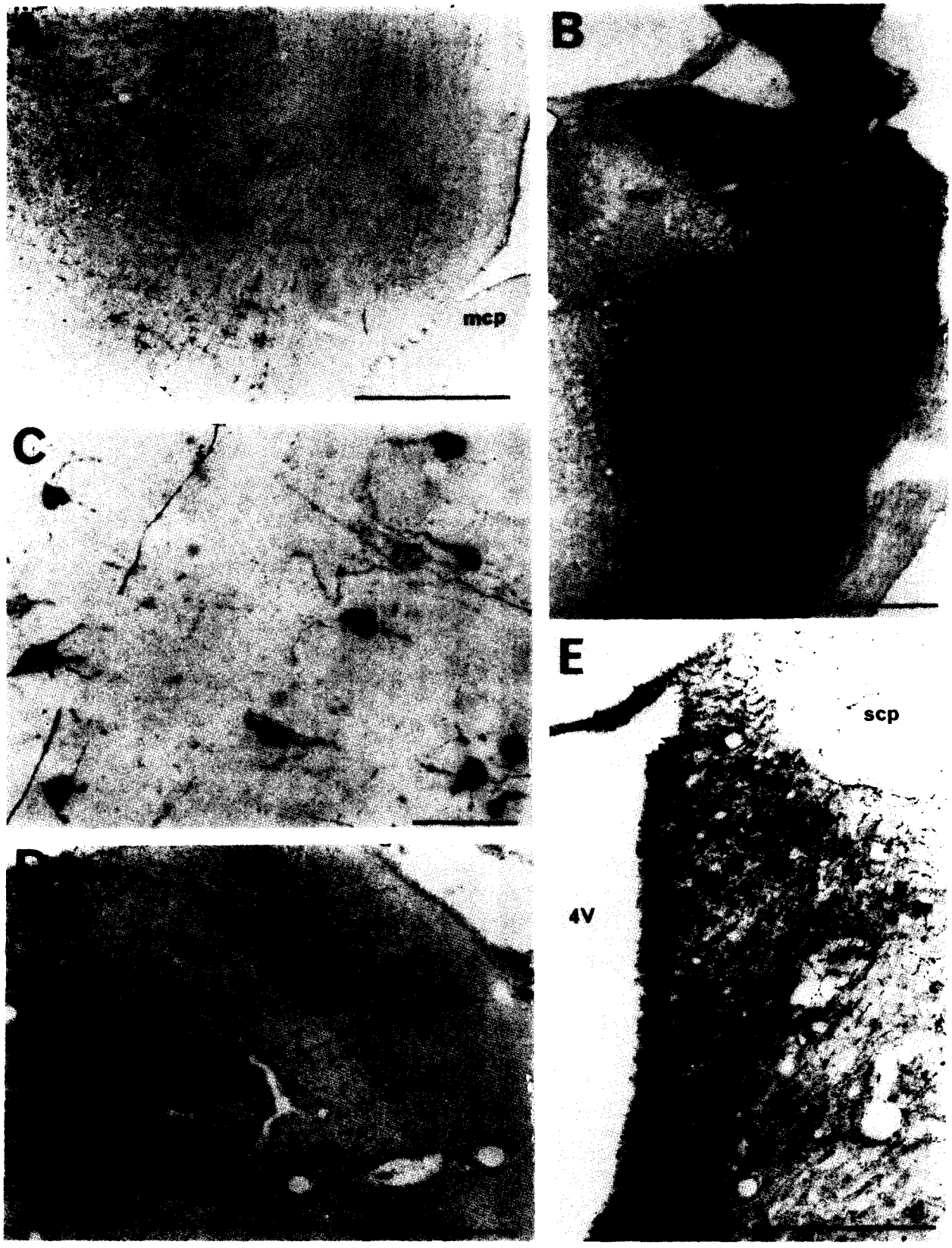

Fig. 5. (*Caption on page* 126)

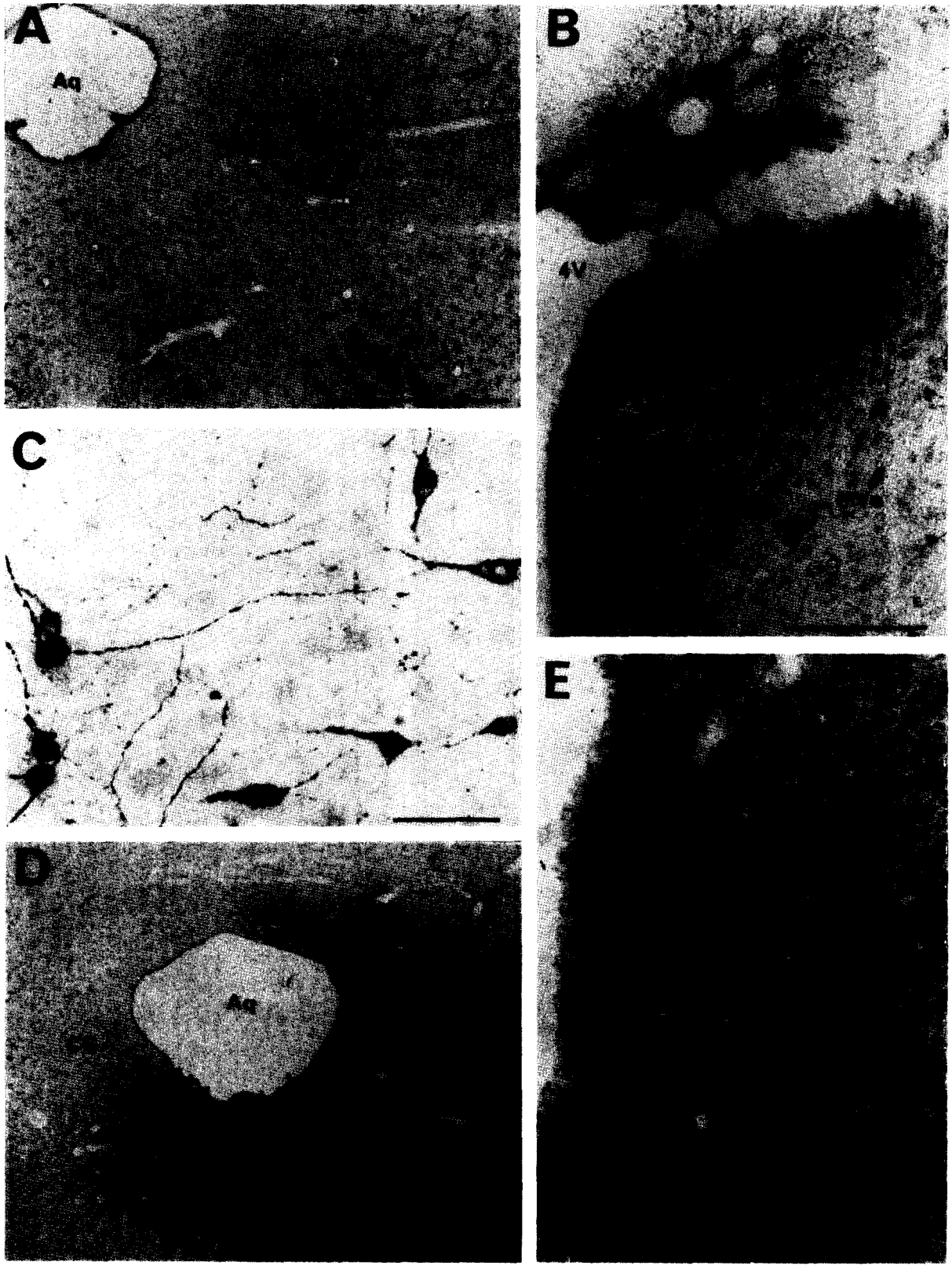

Fig. 6. (*Caption on page* 126)

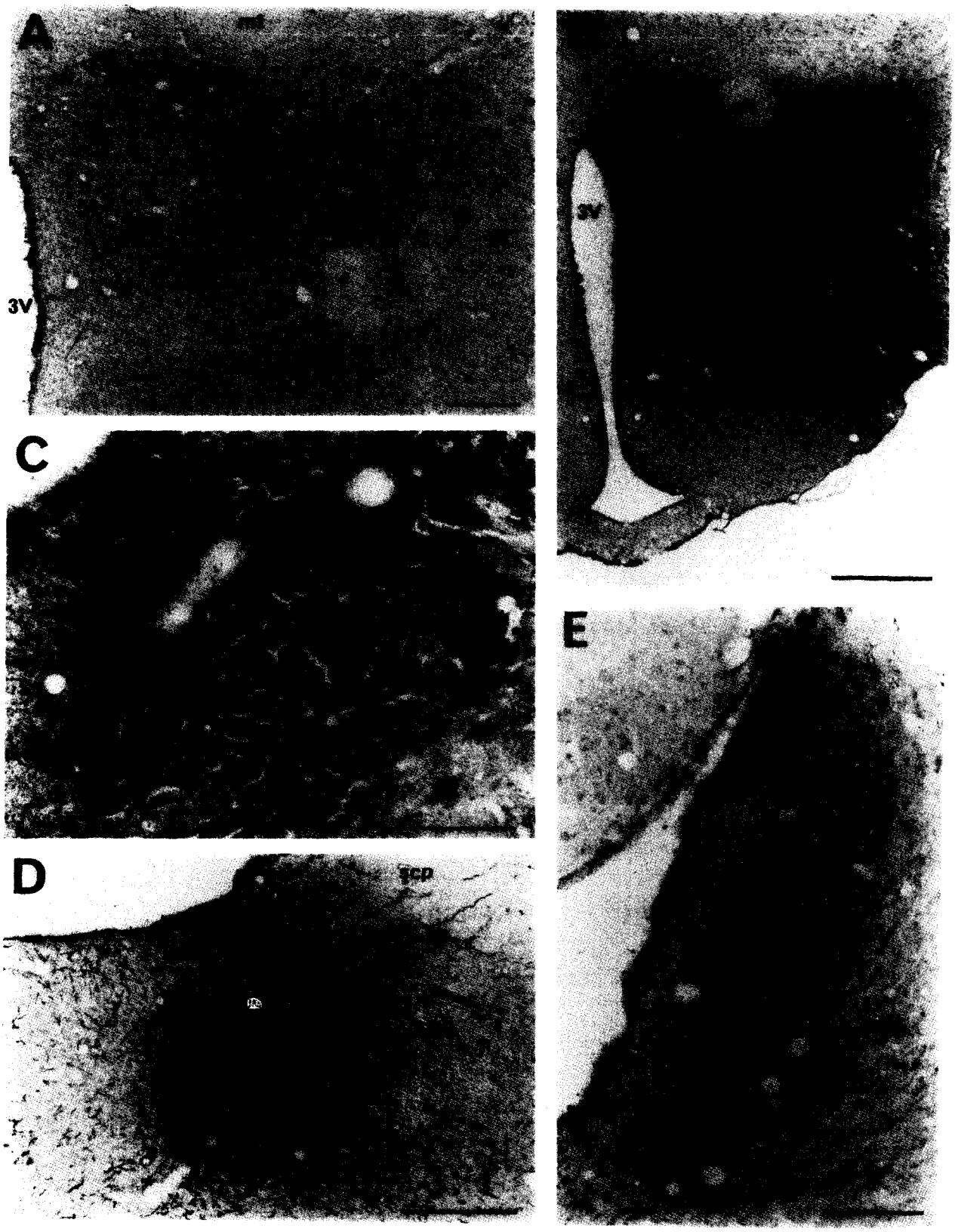

Fig. 7. (*Caption on page* 126)

the poor cell lamina and the periaqueductal gray medial to the LC (Fig. 2A). Three other large injections sites centered in the LC involved the same peri-LC areas but also partly the Bar, peri-5 Me and surrounding periaqueductal gray.

Nine control injection sites 300–400 μm in diameter were made in structures surrounding the LC. Three were centered in the Bar with only a moderate extension in the surrounding periaqueductal gray (Fig. 2C). Three other injections sites were centered in the peri-5 Me with two of them slightly involving either the Bar or the rostral part of the LC. One of these sites was smaller and appeared to be restricted to the peri-5 Me (Fig. 2D). Two other control injection sites were localized in the 5 Me lateral to the LC with no apparent involvement of the LC, the Bar, the peri-5 Me or the MVe (Fig. 2E). The lateral extension of these two sites slightly involved the medial parabrachial nucleus. One control injection site was localized in the MVe region just lateral to the caudal part of the LC (Fig. 2F). This site did not appear to involve the 5 Me.

Efferents from the locus coeruleus and surrounding areas

As previously described,[41] after CTb injections, in addition to the retrograde labeling, we also observed anterograde labeling of the efferents of the nuclei injected. This anterograde labeling helped to corroborate the apparent specificity of the injection sites.

After LC or LC + peri-LC injections, we observed a large number of fibers localized in the lamina and the periaqueductal gray between the LC and the ventricle as well as in the MVe region close to the ventricle just caudal to the LC. In addition, many coarse fibers exited the site rostrally and caudally. One population of fibers was ventral to the 5 Me forming a bundle at the location of the ascending noradrenergic bundle (Fig. 5D). In the rostral pons and the mesencephalon these fibers were localized ventrally to the periaqueductal gray (Fig. 6A). Rostrally in the forebrain, these fibers took a lateral position in the medial forebrain bundle (Fig. 7A). Scattered coarse fibers were visualized over the entire cerebral cortex (Figs 21C, D).

A second bundle of fibers excited ventrally and caudally from the injection site descending vertically medially to the trigeminal motor nucleus at the location of the descending noradrenergic bundle, and then in the dorsal part of the parvocellular reticular nucleus in the medulla. Excepting the labeling of these ascending and descending bundles, only a few fibers were visible in other areas including the pontine and mesencephalic ventrolateral part of the periaqueductal gray.

In contrast, after all control injections around the LC, no or only a few anterogradely labeled fibers were visible in the two bundles labeled after LC injections. Instead, for each nucleus, a specific pattern of anterograde labeling appeared. After Bar or peri-5 Me injections, a bundle of anterogradely labeled fibers was localized in the ventrolateral part of the pontine periaqueductal gray dorsal to the laterodorsal tegmental nucleus of Castaldi and proceeded close to the ventricle in the lateral part of the mesencephalic periaqueductal gray.

Only after Bar injections did we also see a descending bundle of fibers first medial to the trigeminal motor nucleus and then in the nucleus gigantocellularis up to the caudal medulla. Terminal like labeling was also visible in the lateral paragigantocellular nucleus.

Specifically after CTb injections in the peri-5 Me, anterogradely labeled varicose fibers were visible bilaterally in all posterior hypothalamic areas. The largest number of terminal-like fibers was clustered in the compact zone of the dorsomedial nucleus of the hypothalamus (Fig. 3D). Confirming this strong hypothalamic projection of the peri-5 Me, we observed a cluster of retrogradely labeled cells specifically in the peri-5 Me after CTb injections in the posterior hypothalamus, particularly those in the dorsomedial hypothalamic nucleus (Fig. 3C).

After the control MVe injection, specific anterograde labeling was visible bilaterally in the other vestibular nuclei as well as ipsilaterally in the oculomotor and trochlear nuclei and the interstitial nucleus of Cajal in the mesencephalon.

After 5 Me injections, anterogradely labeled fibers were specifically observed in the motor trigeminal nucleus and the medullary parvocellular reticular nucleus.

After large injections centered in the LC, we observed anterograde labeling not only in the ascending and descending noradrenergic bundles but also additional anterograde labeling with a localization depending on the nucleus surrounding the LC included in the site.

Retrograde labeling

In the following part of the results, we describe the distribution of retrogradely labeled cells from rostral to caudal structures. To illustrate results of retrograde labeling, we made camera lucida drawings of 20-μm-sections from brains with representative LC, LC + peri-LC and Bar, injections (Figs 8–20). A semiquantitative analysis of the retrograde labeling is also represented in Table 1.

The injection in the LC + peri-LC illustrated in Fig. 2A (rat RLC2) covered the entire LC and involved the periaqueductal gray and the cell poor lamina medial to it as well as part of the MVe region lateral to the LC. This site did not substantially encroach on the Bar, 5 Me and peri-5 Me. Strong anterograde labeling was present in the ascending and descending noradrenergic bundles and the terminal cortical field of the LC but also in the ventrolateral parts of the pontine and mesencephalic periaqueductal gray.

The representative LC injection illustrated in Fig. 2B (rat RLC15) was apparently restricted to the caudal and dorsal part of the LC. It did not appear to involve the lamina medial to the LC and the MVe region just lateral to the LC. After this injection, anterogradely labeled fibers were found only in the ascending and descending noradrenergic bundles.

The control site in Bar illustrated in Fig. 2C did not apparently involve the adjacent LC and peri-5 Me. No fibers were present in the noradrenergic bundles. Instead, we saw a bundle of anterogradely labeled fibers in the ventrolateral part of the pontine periaqueductal gray. A descending bundle of fibers medial to the trigeminal motor nucleus and then in the nucleus gigantocellularis up to the caudal medulla was also present.

Examples of 250–400-μm-diameter control injection sites localized in the peri-5 Me, and 5 Me, and the MVe are shown in Fig. 2D–F.

The cell counts given in the text for each area were made from one frontal section unilaterally only with the largest number of retrogradely labeled cells in the

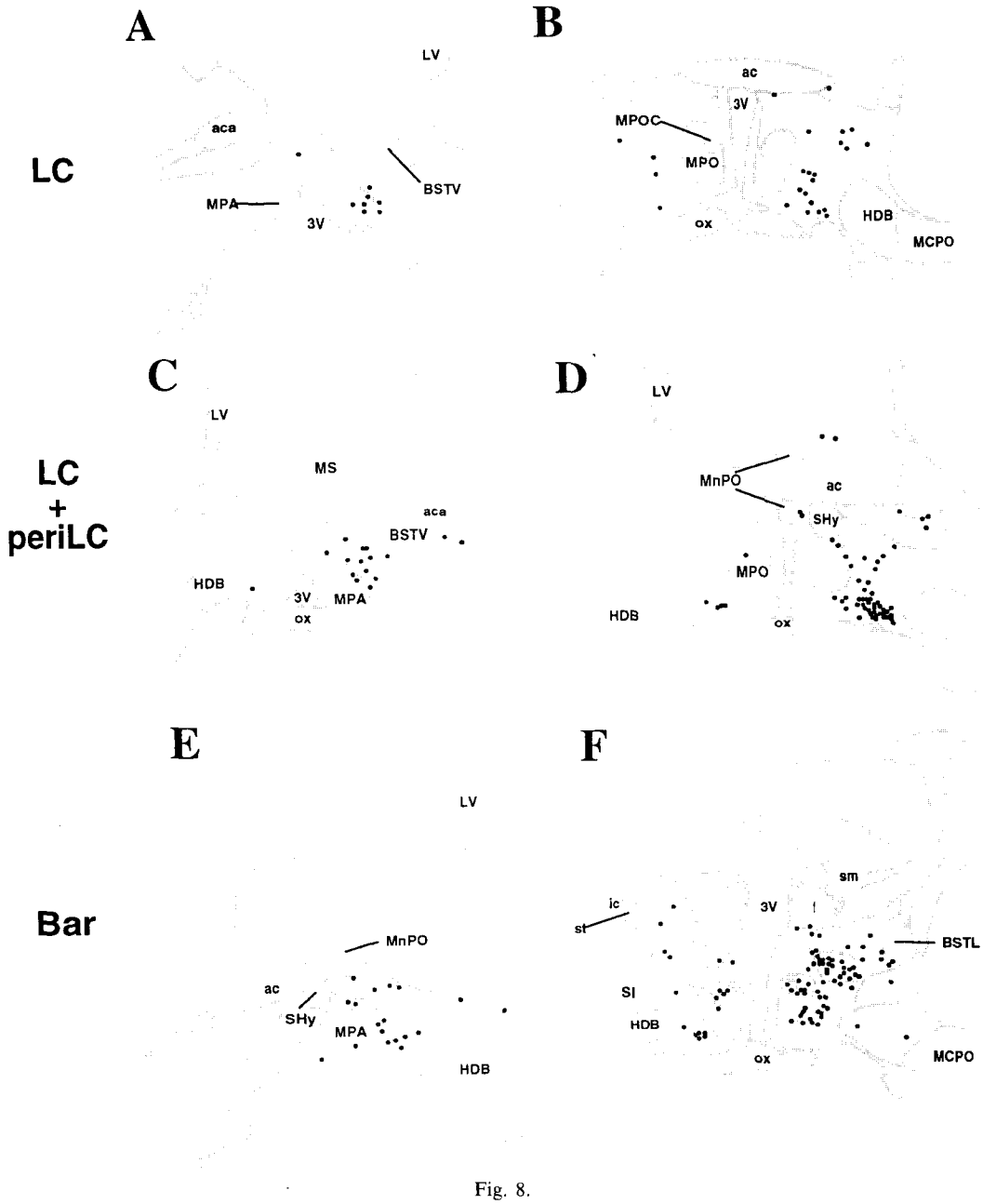

Fig. 8.

Figs 8–20. Camera lucida drawings of 20-μm-sections (from rostral to caudal levels) after an LC injections (A, B) (RLC15), an LC + peri-LC injection (C, D) (RLC2) or an injection in the Bar (E, F). Every dot represents one retrogradely labeled neuron.

representative injections drawn in Figs 8–20. Therefore, note that the total number of cells labeled for each area depends upon the laterality and rostrocaudal extension of labeling in that area.

The CTb labeling produced with the DAB-nickel histochemical procedure consisted of black punctate granules in the cell soma and dendrites of retrogradely labeled neurons (Figs 5C, 6C, 21, 22C). Importantly, after LC or LC + peri-LC injections we observed that the intensity of the retrograde labeling was stronger in the lateral paragigantocellular, prepositus hypoglossi and hypothalamic paraventricular nuclei than in the other nuclei. This difference in intensity was most visible with shorter incubations in primary antibody (overnight, room temperature) or higher dilutions of the antibodies yielding relatively weak immunostaining of CTb. After the normal immunostaining procedure, retrogradely labeled cells were darkly stained in all structures.

Cortical areas

After LC + peri-LC injections, a substantial number of retrogradely labeled pyramidal cells were observed mainly ipsilaterally in the infralimbic cortex (IF) close to the tenia tecta (11–18 cells/section) (Fig. 21D), the caudal part of the area 1 of the frontal cortex (Fr) (Fig. 21A, B) and the adjacent primary somatosensory area, particularly its lower limb

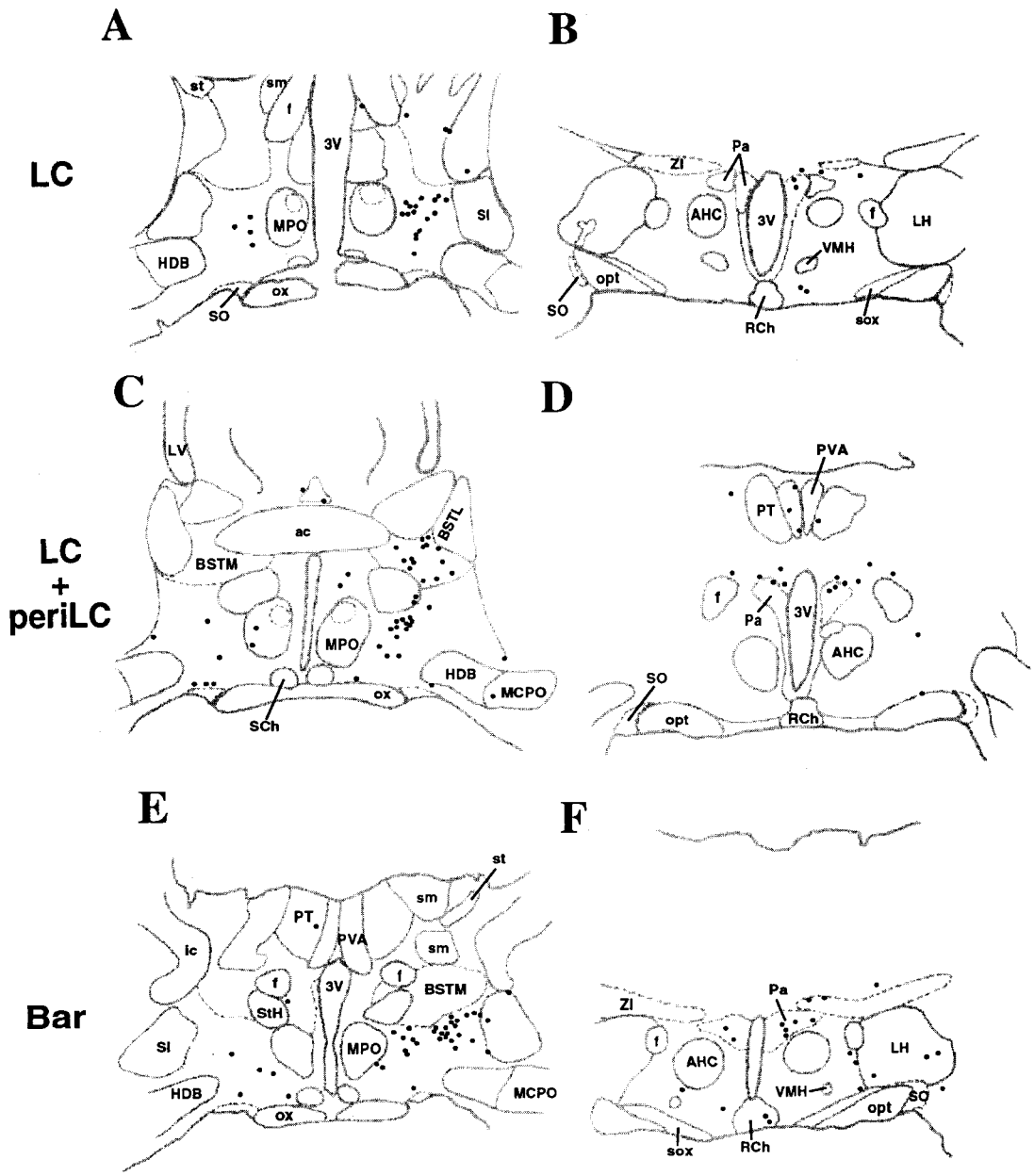

Fig. 9 (*caption opposite*).

region (4–12 cells/section). Smaller multipolar cells were also observed in the claustrum (Cl) (6–8 cells/section) (Fig. 21C). After LC or Bar injections, a much smaller number of retrogradely labeled cells were observed in these structures (1–2 cells/section). More cells were found in the frontal and infralimbic cortices after LC injection sites involving the MVe region lateral to the LC and the control injection in the MVe region lateral to the LC. After this restricted MVe injection, no or only occasional cells were visible in the insular cortex and the claustrum. After 5 Me injections, a large number of cells were localized in the claustrum and the insular cortex. Fewer appeared in the infralimbic cortex. The frontal cortex contained only occasional cells. After injections in the peri-5 Me, a substantial number of cells were observed in the infralimbic and insular cortex, and the claustrum. Only a few cells were visible in the frontal cortex.

Preoptic level

After LC + peri-LC injections, a dense collection of small cells (37–42 cells/section) was distributed with an ipsilateral predominance in the preoptic area localized dorsally to the supraoptic nucleus just rostral to and at the level of the rostral part of the suprachiasmatic nucleus (Figs 8D, 9C, 22A, C). This group extended rostrally up to the rostral end of the third ventricle (Fig. 8C). After LC injections, a substantial number of neurons was still specifically found in this region of the preoptic area (8–12 cells/section) (Figs 8A, B, 9A).

After LC + peri-LC injections, additional small cells were demonstrated ipsilaterally in the medial part of the bed nucleus of the stria terminalis (BSTM) (Fig. 9C).

After LC or LC + peri-LC injections, no or only a few cells were observed in the medial preoptic nucleus (MPO) and the lateral part of the bed nucleus of the stria terminalis (BSTL) (Figs 8B, D, 9A, C).

After Bar injections, many cells were localized in the preoptic area dorsal to the supraoptic nucleus and the medial part of the bed nucleus of the stria terminalis (Figs 8F, 9E, 22B). However, additional cell groups appeared in (1) the medial preoptic nucleus (Figs 8F, 22B), (2) the lateral preoptic area dorsal to the horizontal limb of the diagonal band of Broca (Fig. 9E) and (3) the magnocellular subdivision of the medial part of the bed nucleus of the stria terminalis (Fig. 8F, 22B).

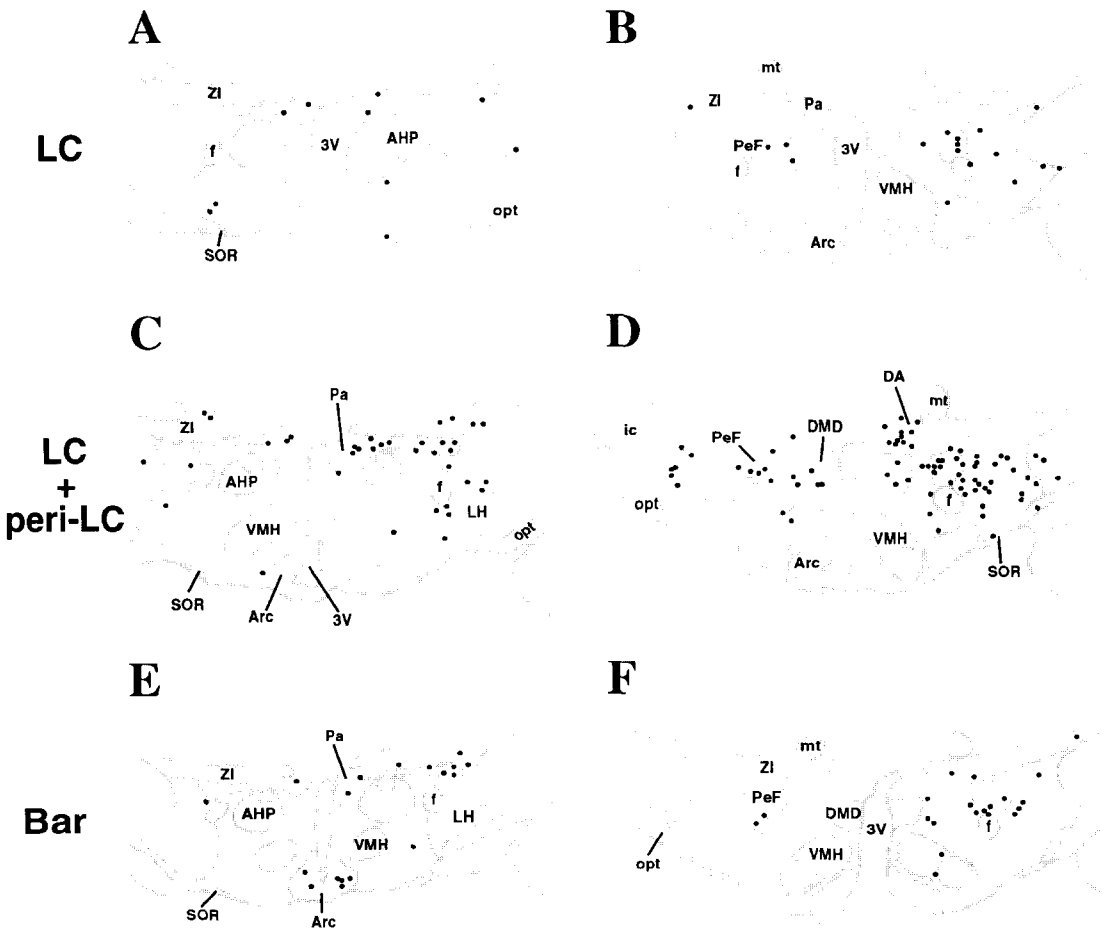

Fig. 10 (*caption on page* 132).

After injections in the 5 Me or peri-5 Me, a large number of small cells were clustered ipsilaterally in the lateral part of the bed nucleus of the stria terminalis (21–24 cells/section). Only a moderate number of cells were observed in the medial part of the bed nucleus of the stria terminalis and the preoptic areas.

After the specific MVe injection, no cells were identified in these rostral forebrain areas.

Midhypothalamic level

At the level of the midhypothalamus, after LC, LC + peri-LC, Bar, 5 Me or peri-5 Me injections, a moderate number of small cells were localized mainly ipsilaterally in the parvocellular parts of the hypothalamic paraventricular nucleus and its lateral extension dorsal to the fornix (Figs 9B, D, F, 10A, C, E). After LC or LC + peri-LC injections, cells were distributed in the dorsal cap of the nucleus (Figs 9B, D, 10A, C) while they were mainly localized in its medioventral part after Bar, 5 Me or peri-5 Me injections (Fig. 9F). Interestingly, the number of retrogradely labeled cells in this nucleus differed little after LC + peri-LC (5–7 cells/section) or LC (2–4 cells/sections) injections. At the same level, after any injection, only occasional cells were observed in the rostral part of the lateral hypothalamic area.

After 5 Me or peri-5 Me injections, a large number of small cells were seen with an ipsilateral predominance in the central nucleus of the amygdala (25–72 cells/sections). In the case of LC, LC + peri-LC, Bar or MVe injections, no or only occasional cells were distributed in this nucleus or anywhere in the amygdala.

Posterior hypothalamus

After LC or LC + peri-LC injections, small retrogradely labeled cells were observed in the dorsal hypothalamic area located dorsal to the dorsomedial hypothalamic nucleus (Figs 7A, 11A–D). Intermingled small and medium-sized neurons were also found in the rostral part of the perifornical nucleus and the lateral hypothalamic area at all levels of the posterior hypothalamus (Figs 7A, 10–12A, D). In these posterior hypothalamic areas, there was a substantial difference in number of cells between LC + peri-LC injections (50–60 cells/section) and LC injections (13–21 cells/section).

After injections into the Bar, although neurons were found in the same areas as after LC or

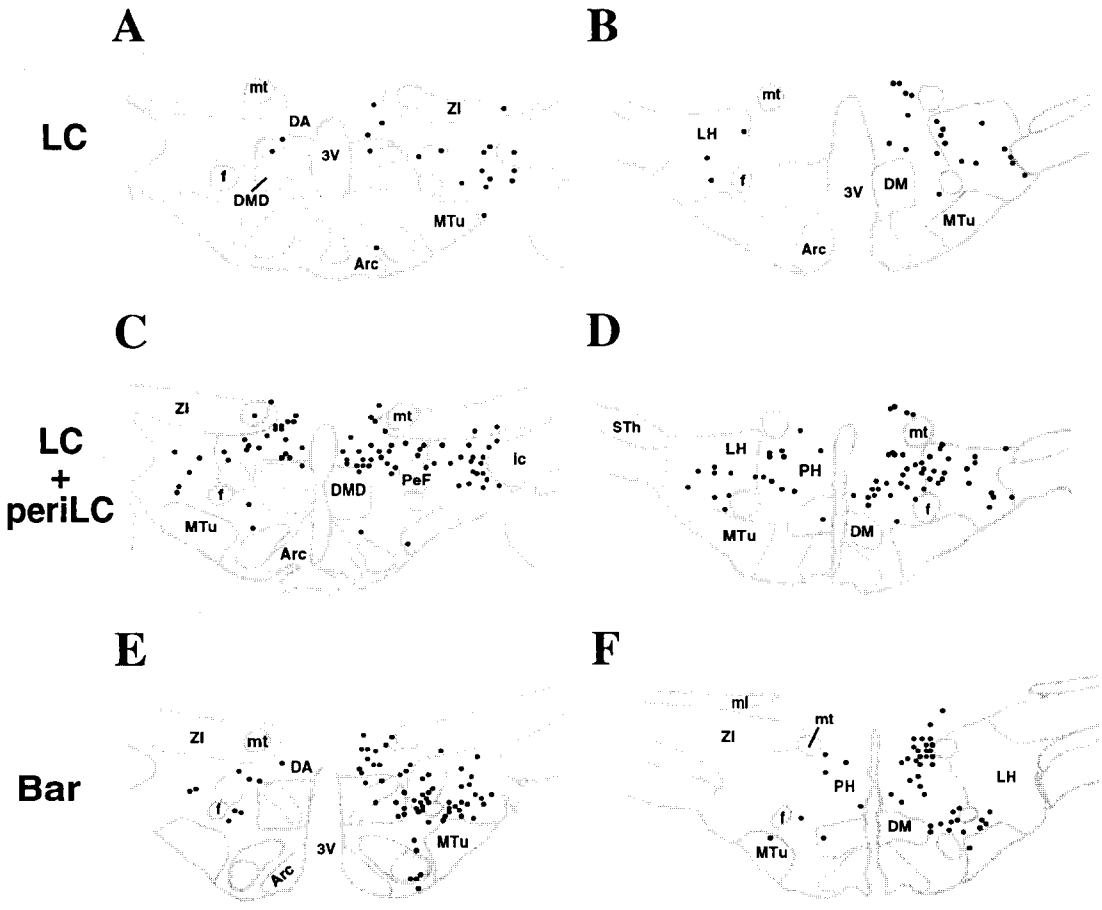

Fig. 11 (*caption on page* 132).

LC + peri-LC injections, additional groups of small cells appeared (1) in the caudal part of the dorsal hypothalamic area (Fig. 11F), and (2) around the fornix and ventromedial to it (Fig. 11E). In contrast to LC or LC + peri-LC injections, only a few cells appeared in the lateral hypothalamic area immediately medial to the internal capsule (Fig. 11E, F).

After 5 Me or peri-5 Me injections, the overall distribution of cells in the posterior hypothalamic areas was again different. A large number of small to medium-sized cells was found only in the lateral and caudal part of the lateral hypothalamic area located just medial to the internal capsule and the subthalamic nucleus. Fewer neurons were present in the perifornical nucleus and the dorsal hypothalamic area compared to LC, LC + peri-LC or Bar injections.

After the injection in the MVe, a substantial number of rather medium-sized neurons were diffusely distributed in the posterior hypothalamic areas with no clear topography.

After LC, LC + peri-LC, 5 Me or MVe injections, no or only occasional cells were observed in the arcuate nucleus of the hypothalamus (Figs 10, 11). After injections into the Bar (Fig. 10E) or peri-5 Me, slightly more cells were localized in this nucleus.

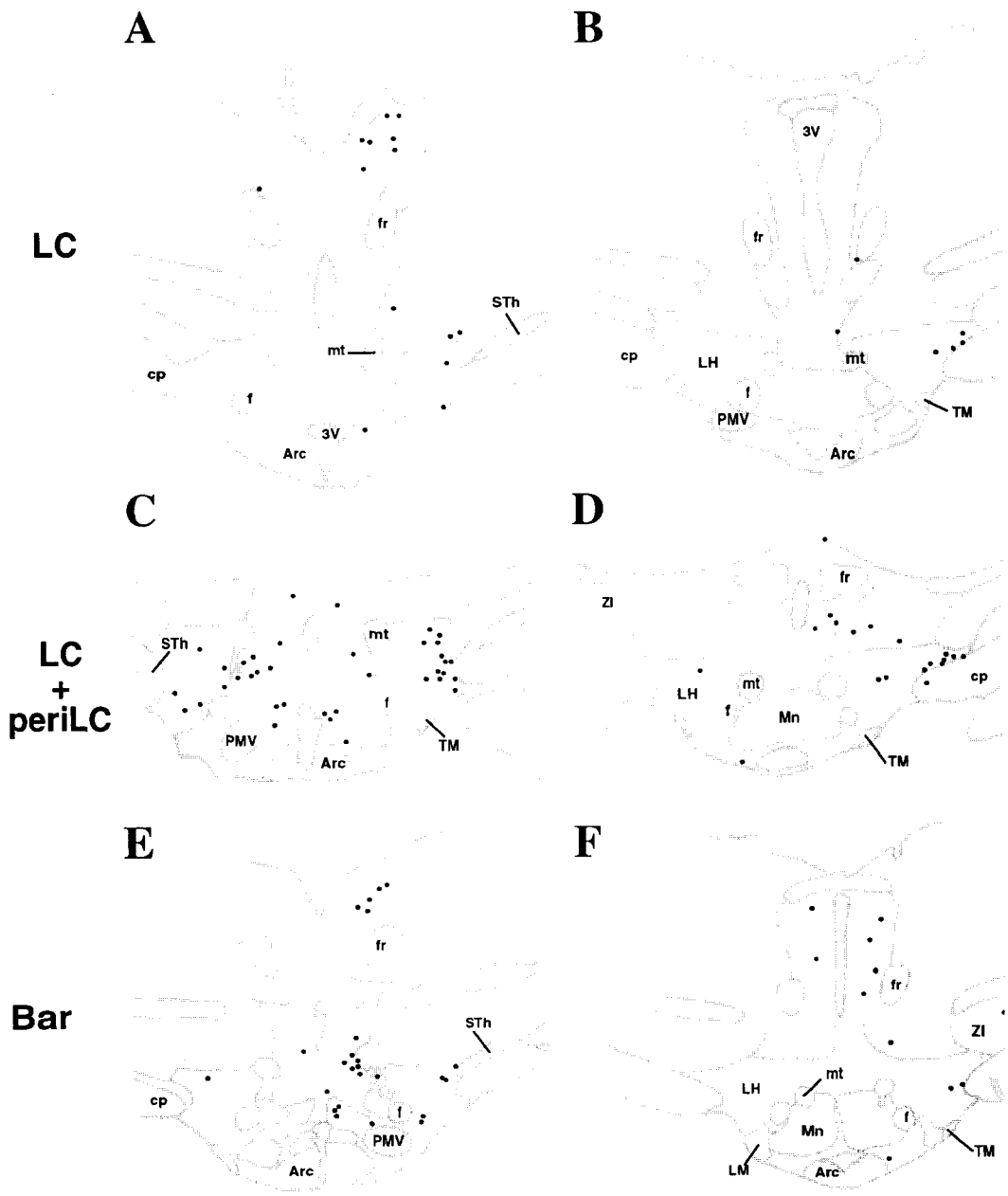

Fig. 12 (*caption on page* 132).

In all cases, no or only a few cells were distributed in other structures such as the ventromedial hypothalamic nucleus, the tuberomamillary nucleus and the lateral habenula (Figs 10–12).

After LC, LC + peri-LC or Bar injections, a small group of cells was consistently present in an undefined area located dorsal to the fasciculus retroflexus and ventral to the caudal tip of the lateral habenula (Fig. 12A).

Specifically after the MVe injection, cells were observed in the retrorubral field and the interstitial nucleus of Cajal.

Mesencephalon

After LC + peri-LC or Bar injections, a large number of small cells was labeled in the lateral and ventrolateral parts of the periaqueductal gray (Figs 6A,C, 13–16) (LC + peri-LC: 40–50 cells/section, Bar: 20–30 cells/section). After LC injections, a substantial number of cells were still observed in this area (Figs 13–16A, B) (10–15 cells/section). The distribution of the labeled cells appeared to be different for Bar and LC or LC + peri-LC injections. After Bar injections, the great majority of the CTb-positive cells were clustered in a medial area close to the ventricle (Figs 14F, 15E, F, 16E), whereas they were more diffusely distributed laterally and ventrolaterally after LC or LC + peri-LC injections (Figs 14–16A–D). After peri-5 Me injections, a large number of cells were also seen in the same regions as after LC injections. After 5 Me or MVe injections, only a few labeled cells were observed in the periaqueductal gray.

After LC + peri-LC injections, a large number of small cells also appeared in the dorsal part of the periaqueductal gray (13–23 cells per section) (Figs 13–15C, D). After LC injections, the number of cells was much lower in this area (1–5 cells/section)

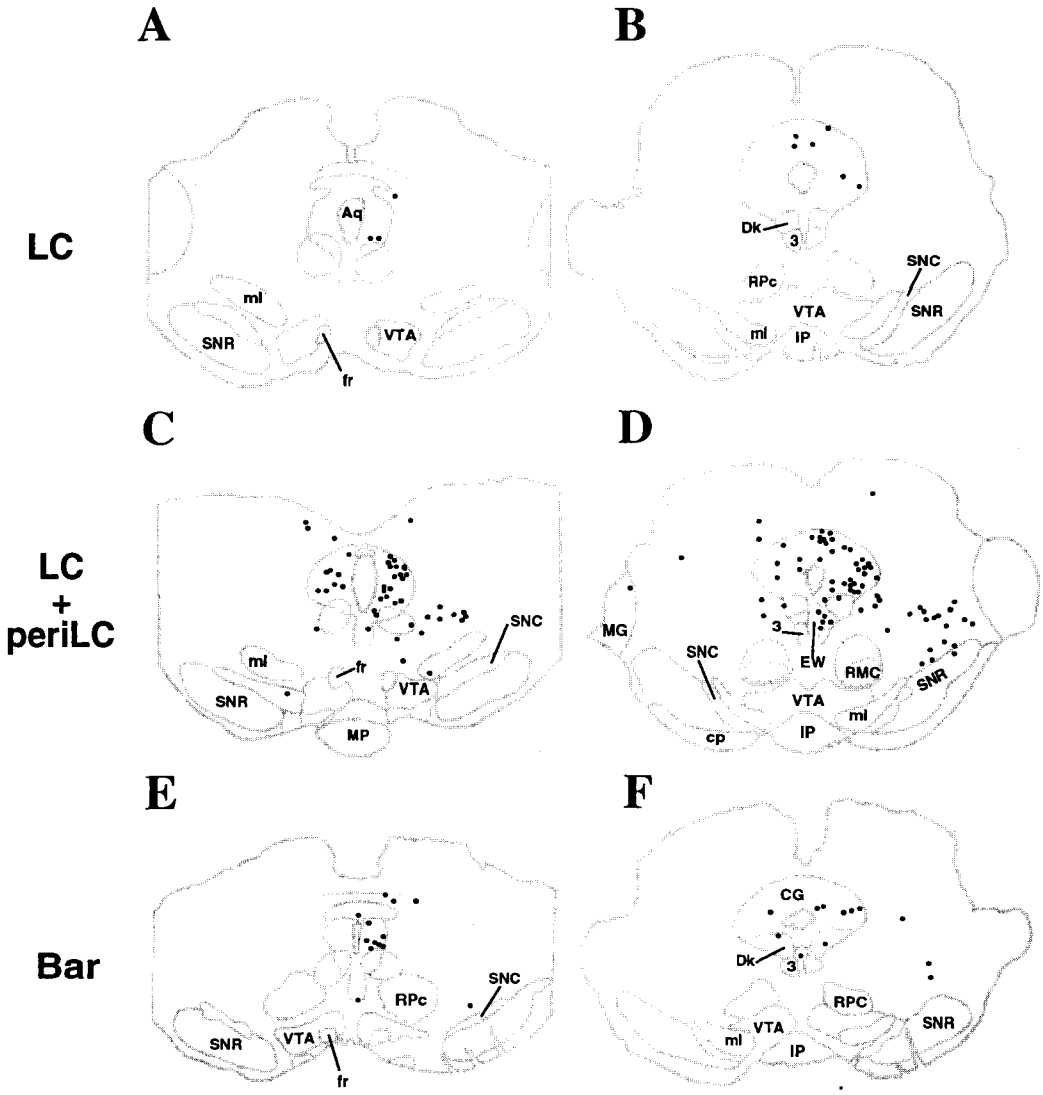

Fig. 13 (*caption on page* 132).

(Figs 13–15A, B). After Bar (Figs 13–15E, F), peri-5 Me, 5 Me or MVe injections, only a few cells were visible in the dorsal periaqueductal gray.

After LC + peri-LC injections, a large number of small and medium-sized cells was found with an ipsilateral predominance in the mesencephalic reticular formation, particularly (1) dorsal to the lateral part of the substantia nigra (Fig. 13D), (2) lateral to the periaqueductal gray (Fig. 14C, D), (3) lateral to the median raphe nucleus (Fig. 14C, D) and (4) in and just dorsal to the median lemniscus and lateral to the interpeduncular nucleus (Figs 14, 15A, D). Fewer labeled cells were observed in these areas after LC (Figs 13, 14A, B), Bar (Figs 13, 14E, F), 5 Me, peri-5 Me or MVe injections.

After LC or LC + peri-LC injections, a few medium-sized cells were seen with a slight ipsilateral predominance in the median raphe nucleus (Figs 15, 16A–D). Only occasional cells were observed in this structure after Bar (Figs 16, 17E, F), 5 Me, peri-5 Me or MVe injections.

After LC + peri-LC injections, a large number of small cells was localized mainly in the rostral, dorsal and dorsolateral parts of the dorsal raphe nucleus (Figs 15D). Fewer cells were visible in the caudal part of the nucleus (Fig. 16C, D). Although many fewer in number, neurons were also seen in the dorsal and dorsolateral parts of the nucleus raphe dorsalis after LC or Bar injections (Figs 15–17A, B, E, F). After 5 Me, peri-5 Me or MVe injections, a substantial

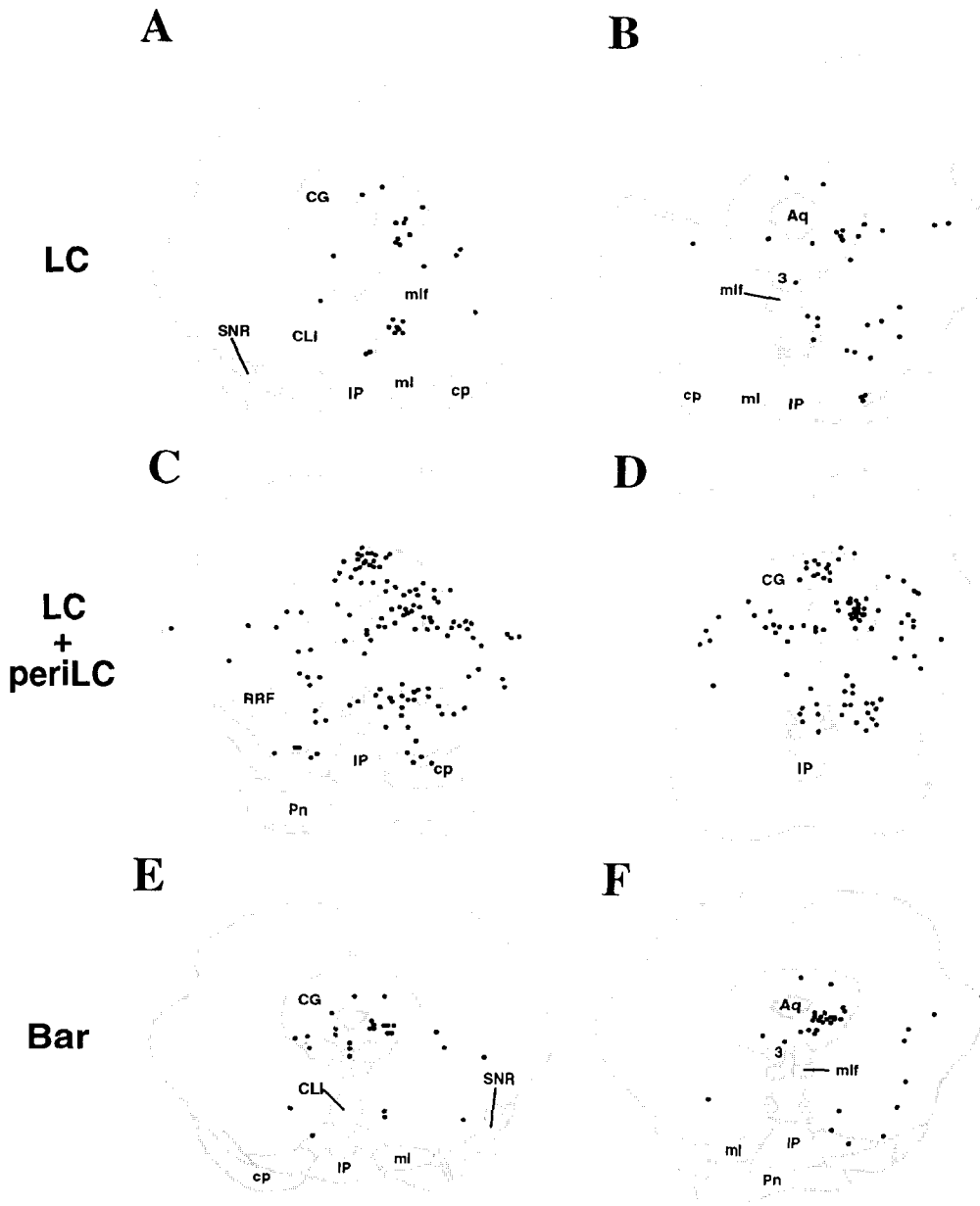

Fig. 14 (*caption on page* 132).

number of medium-sized cells was found in the medioventral part of the nucleus raphe dorsalis.

After LC + peri-LC injections, a few cells were also observed in the Edinger–Westphal nucleus (Figs 13D, 14C). No such cells were observed after LC injections. A large number of CTb-positive cells were localized in the Edinger–Westphal nucleus after the specific MVe injection.

Pons

After LC or LC + peri-LC injections, small cells (LC + peri-LC, 40 cells; LC, 13 cells per section) were observed, bilaterally with a slight ipsilateral predominance, in the Kölliker–Fuse nucleus (K–F) (Figs 16A–D, 17A, B). The neurons were localized just dorsally to the rubrospinal tract (rs) and ventral to the brachium conjunctivum at the caudal levels of the ventral tegmental nucleus of Gudden (VTg) (Figs 5A, C, 16, 17). After Bar or MVe injections, a limited number of cells were distributed in the Kölliker–Fuse nucleus (4–5 cells/section) (Fig. 11E, F). Only occasional cells were observed after 5 Me or peri-5 Me injections.

After LC + peri-LC injections, a large number of small cells was seen, with a large ipsilateral predominance, in the lateral parabrachial nucleus (LPB)

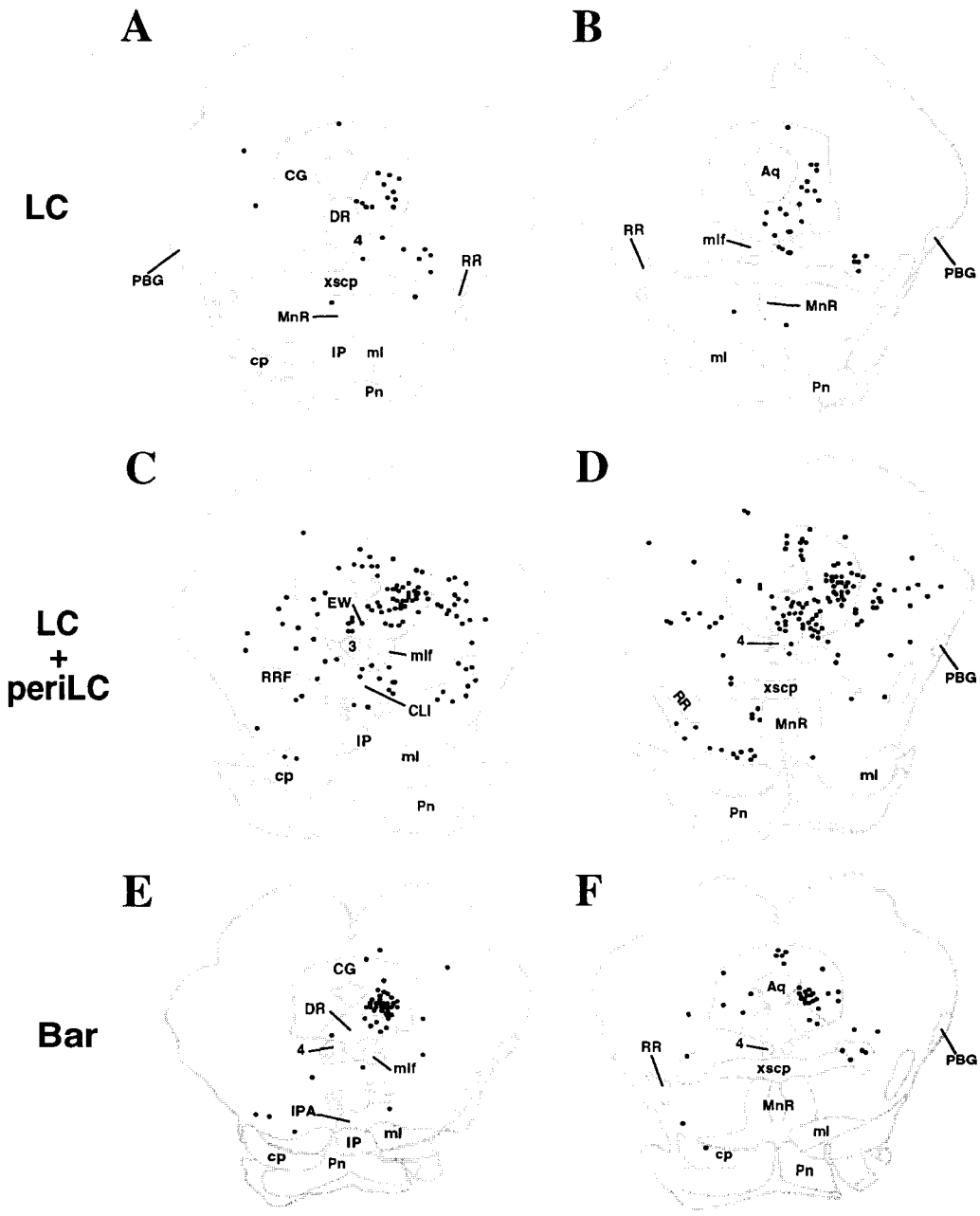

Fig. 15 (*caption on page* 132).

(Figs 17C, D, 5D). The number of cells was limited after LC (Fig. 17A, B), Bar (Fig. 17E, F) or 5 Me injections. Few cells appeared in this nucleus after peri-5 Me or MVe injections.

After LC + peri-LC injections, the laterodorsal tegmental nucleus of Castaldi (LDT) also contained mainly ipsilaterally a small number of medium-sized retrogradely labeled cells (Figs 16D, 17C, D). After LC (Figs 16B, 17A, B), Bar (Figs 16, 17E, F), 5 Me, peri-5 Me or MVe injections, only a few cells were found in this nucleus. After LC, LC + peri-LC or the control injections, only a few medium-sized cells were demonstrated ipsilaterally in the pedunculopontine nucleus (PPT) (Figs 15, 16).

At the caudal pontine level, after LC + peri-LC injections, medium-sized cells with an ipsilateral predominance were observed ventral to the facial nerve and laterodorsal to the superior olivary complex in the area of the A5 noradrenergic cell group[16] (Figs 17–18C, D). A few cells were still present in this area after LC injections (Fig. 18A, B). No or only occasional cells were seen there after Bar (Fig. 18E, F), 5 Me, peri-5 Me or MVe injections.

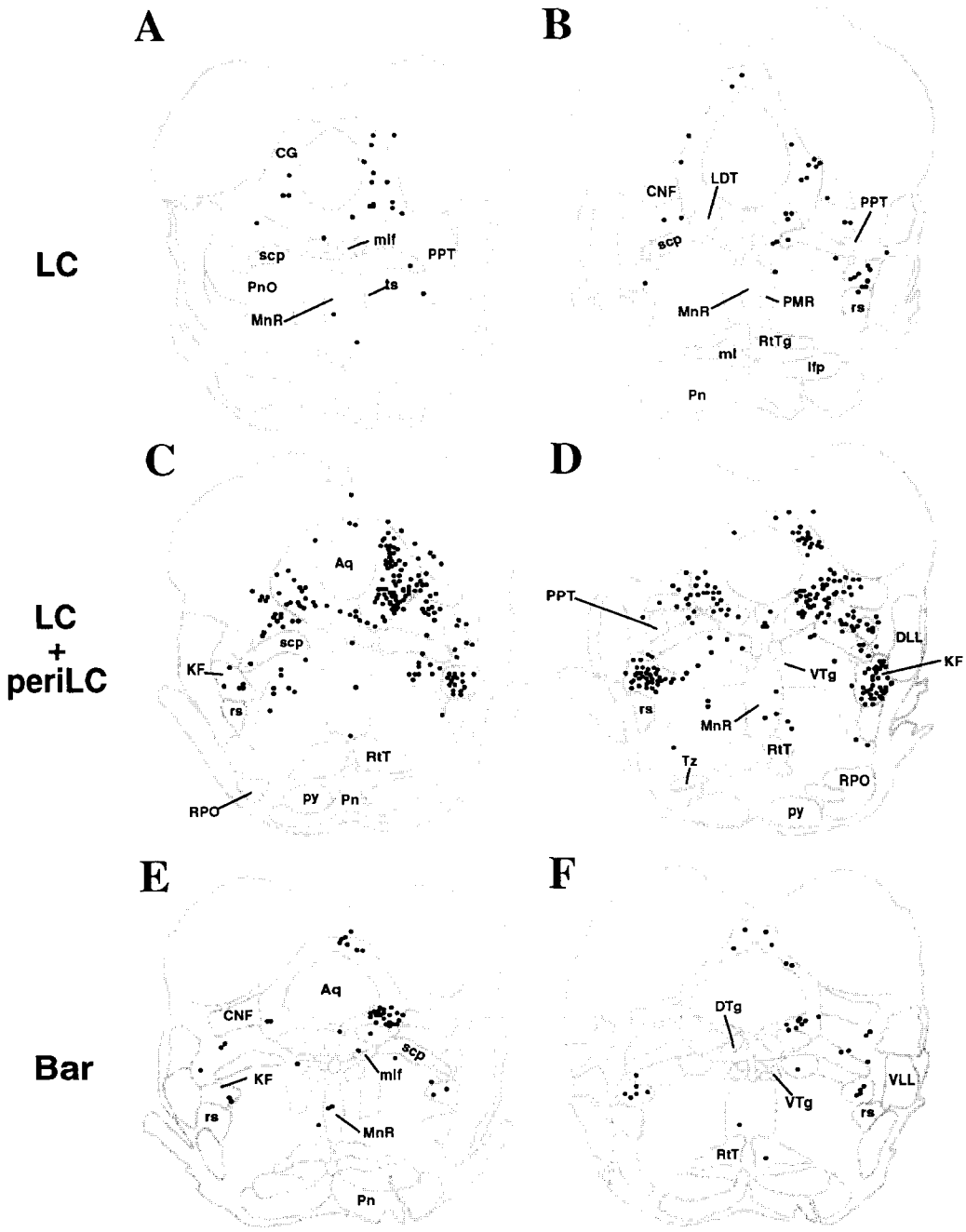

Fig. 16 (caption on page 132).

The nuclei raphe pontis and magnus contained only a small number of medium-sized cells after LC, LC + peri-LC or Bar injections (Figs 17–19). Nearly no cells were observed in these raphe nuclei after 5 Me, peri-5 Me or MVe injections. The pontine reticular formation contained small to medium-sized dispersed cells after LC + peri-LC (Figs 17, 18C, D), 5 Me or MVe injections. After LC (Figs 17, 18A, D), peri-5 Me or Bar injections (Figs 17, 18), only occasional cells were present in this area.

After LC or LC + peri-LC injections, only a small number (maximum 5 cells/section) of retrogradely labeled neurons were identified in the structures adjacent to the LC such as the Bar and the peri-5 Me. Only after LC + peri-LC injections were a few labeled cells present in the contralateral LC (Figs 4A, 18C, D). After Bar injections, darkly stained medium-sized

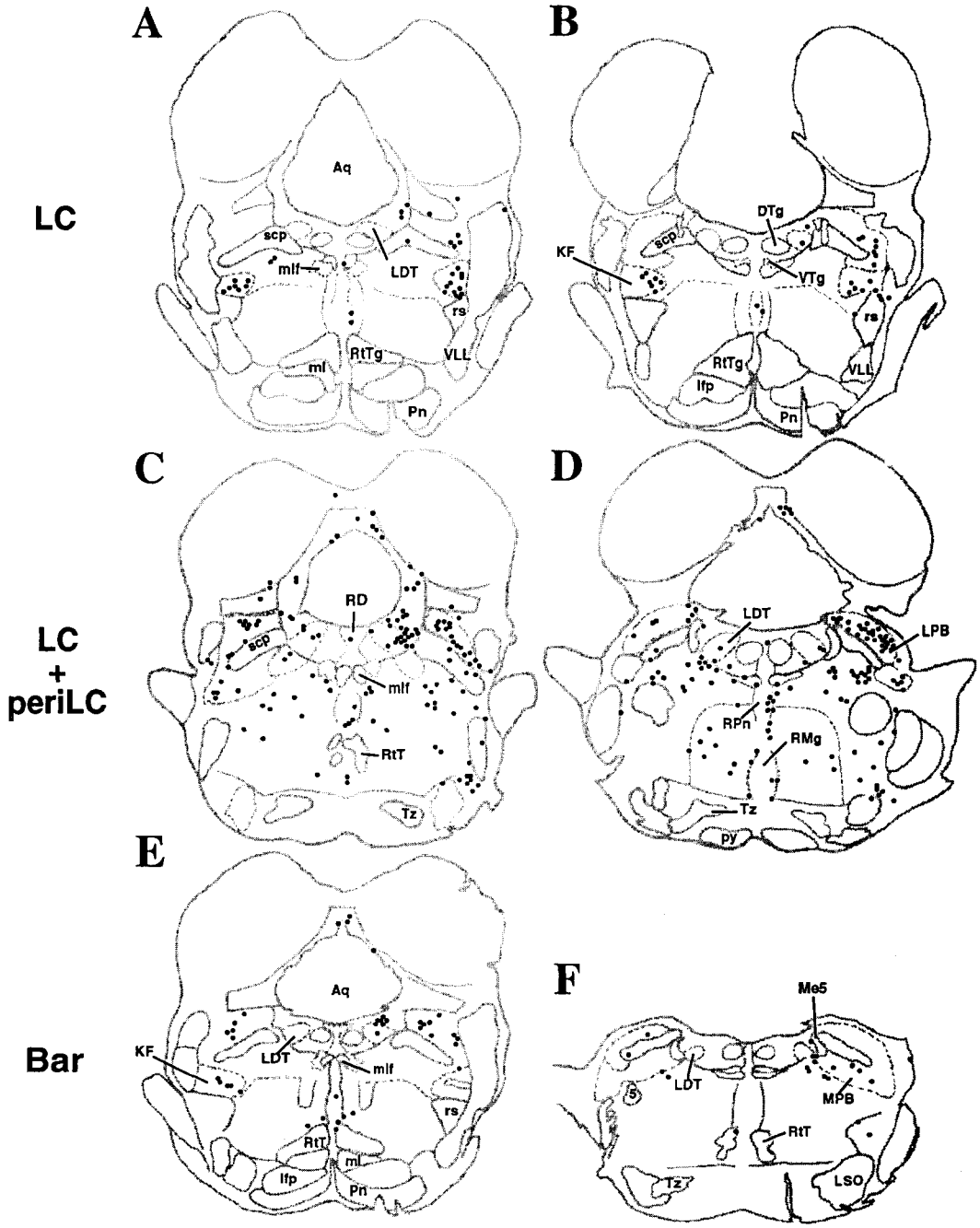

Fig. 17 (*caption on page* 132).

cells were found in the ipsilateral LC caudal to the injection site.

Medulla

After LC or LC + peri-LC injections involving the MVe area just lateral or caudal to the LC, a number of cells was distributed with a slight ipsilateral predominance in the vestibular nuclei (Fig. 19C, D). Only rare cells were observed in these nuclei after LC (Fig. 19A, B), Bar (Fig. 19E, F) or Peri-5 Me injections. In contrast, a large number of retrogradely labeled neurons were found bilaterally in the vestibular nuclei after the control injection in the MVe.

The lateral paragigantocellular nucleus (LPGi) contained a large number of small and medium-sized cells with a large ipsilateral predominance after LC + peri-LC injections (25–30 cells/section) (Figs 4D, 19D). A substantial number of cells was still observed in this nucleus after LC injections (10–14 cells/section) (Fig. 19B). After Bar injections, a small number of cells was localized in this area (5 cells/section) (Fig. 19F). Fewer cells were visible after 5 Me, peri-5 Me or MVe injections.

After LC or LC + peri-LC injections, the dorsomedial rostral medulla contained a substantial to large number of medium-sized retrogradely labeled cells (LC + peri-LC, 22 cells; LC, 7 cells/section) (Figs 4B, 19A, C). More precisely, these cells were located in the ventromedial part of the nucleus prepositus hypoglossi (PrH) and the reticular formation ventral to it [dorsal paragigantocellular nucleus (DPGi)].[49] Note that the number of cells are based on unilateral counts; cells in the dorsomedial rostral medulla were bilaterally located.

After the MVe control injection, a large number of cells was also distributed in the dorsomedial rostral medulla (ventromedial part of the nucleus prepositus hypoglossi and dorsal paragigantocellular nucleus) with a distribution similar to LC or LC + peri-LC injections but with a strong contralateral predominance. After Bar (Fig. 19E, F), 5 Me or peri-5 Me injections, only a few cells were observed in the same area.

After LC, LC + peri-LC or Bar injections, only a small number of cells were localized in the caudal part of the nucleus of the solitary tract (Fig. 20).

After 5 Me injections, a large number of small cells was seen with a small ipsilateral predominance in the rostral and caudal parts of the nucleus of the solitary tract (Sol). The caudal part of this nucleus also

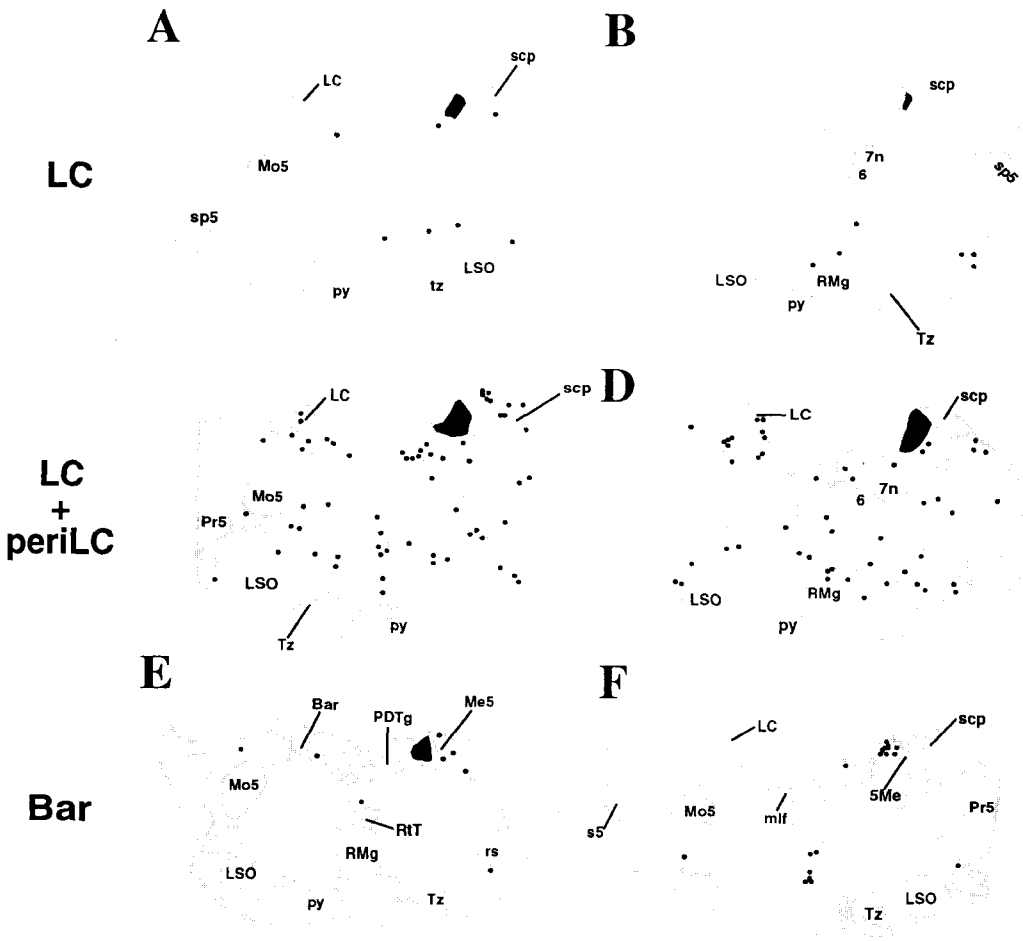

Fig. 18 (*caption on page* 132).

contained a large number of cells after Peri-5 Me injections.

After LC + peri-LC injections, small cells were observed mainly ipsilaterally in the caudoventrolateral reticular nucleus (Fig. 20D). This area also contained a few cells after LC injections (Fig. 20B) and occasional cells after Bar (Fig. 20F), 5 Me, peri-5 Me or MVe injections.

Only after 5 Me injections, a large number of small cells was seen with a small ipsilateral predominance in the parvocellular reticular nucleus (PCRt).

Spinal cord

Even after LC + peri-LC injections, we observed only a limited number of retrogradely labeled cells mainly ipsilaterally in the intermediate layers at all levels of the spinal cord. No cells were observed in the superficial layers. After LC injections, only occasional cells were observed in the intermediate layers of the cord. The spinal cord was not examined in control experiments.

Anterograde tracing experiments

General remarks. In most rats, PHA-L and CTb were iontophoretically deposited on opposite sides of the brain in the same structures and CTb or PHA-L immunohistochemistry was performed on alternate sections. This procedure allowed us to increase results obtained with each animal, and to directly compare the anterograde labeling visualized by two different tracers. The CTb injection sites (1 μA, 15–30 min) with a diameter of about 600 μm were darkly stained, round or ovoid and sharply delineated (Fig. 4C). In contrast, the delineation of the PHA-L injection sites was more difficult. Indeed, PHA-L sites (5 μA, 30 min) contained darkly labeled cells in the center of a light blue grey area about 1 mm in diameter (Figs 22E, 7B, 6D, 5B). Using PHA-L, the anterogradely labeled fibers were strongly and completely labeled (Figs 7E, 23A–D). The CTb anterogradely labeled fibers were in general less completely labeled and sometimes showed only punctate labeling particularly when using stronger fixation (Figs 1D, 23E). Moreover, in the case of CTb, in addition to the anterograde labeling of fibers, retrogradely labeled cells and dendrites were present in and around LC, in particular after CTb injections in the structures receiving an input from the LC or peri-LC such as the posterior hypothalamic areas (Fig. 7C), the preoptic area and the Kölliker–Fuse nucleus (Fig. 1D). Only a few retrogradely labeled cells were seen in the LC after CTb injections in the periaqueductal gray, the

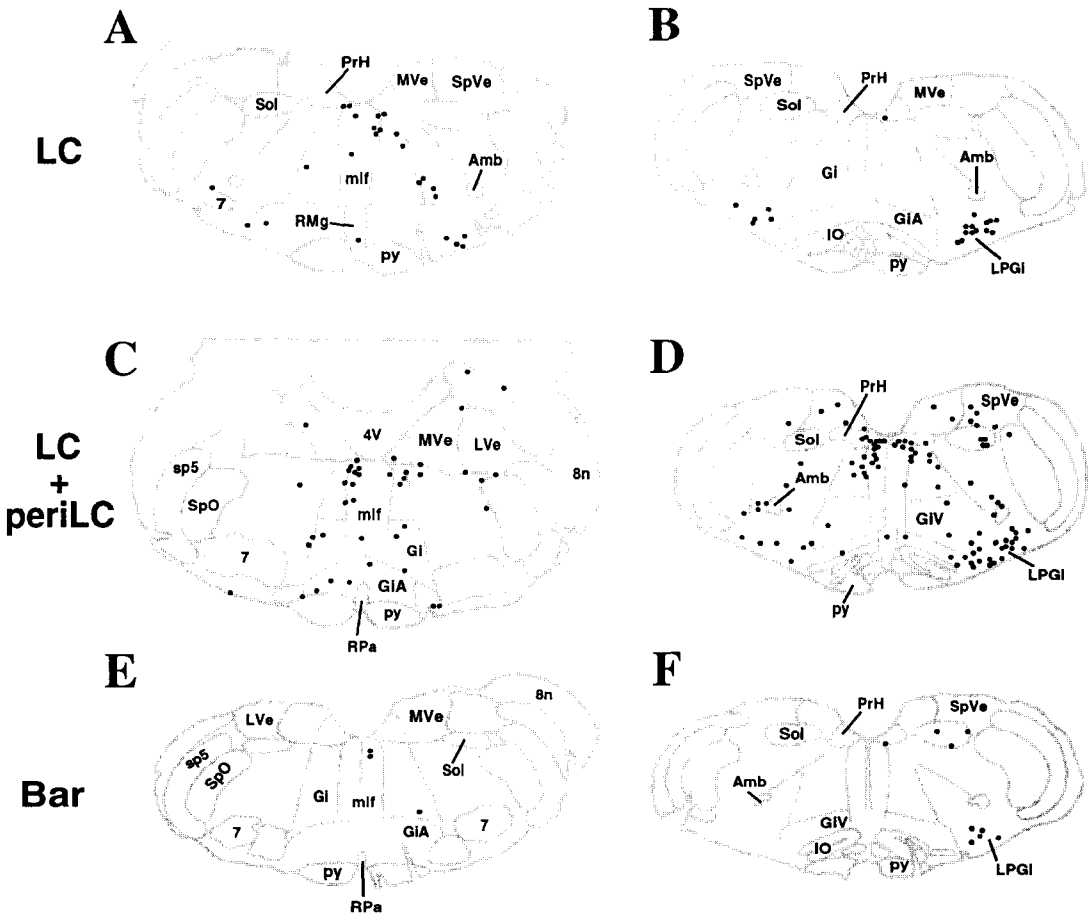

Fig. 19 (*caption on page* 132).

laterodorsal tegmental nucleus, or the dorsal raphe and magnus nuclei.

Despite the differences between the two tracers, after PHA-L and CTb injections in the same contralateral structures we found comparable amounts of anterogradely labeled fibers in the efferent nuclei of the structure injected.

Frontal cortex. After PHA-L injections involving area 1 of the frontal cortex and the adjacent lower limb region of the primary somatosensory area, only a few fibers were observed in the LC, Bar, Peri-5 Me, 5 Me, the lamina between the LC and the fourth ventricle and the periaqueductal gray region medial to the LC (Fig. 24C, D). In contrast, a large number of varicose fibers were clustered in the MVe regions located (1) between the LC and the 5 Me (Fig. 24D) and (2) just lateral to the caudal pole of the LC and (3) caudally to the LC close to the ventricle. Many fibers were also observed in the periaqueductal gray and the pontine reticular formation ventromedial to the LC (Fig. 24C, D).

Infralimbic cortex. After a PHA-L injection in the infralimbic cortex, only occasional fibers appeared in the nuclear core of the LC, the 5 Me and the Bar. More fibers were observed in the lamina located between the LC and the fourth ventricle, the periaqueductal gray ventromedial to the LC, the Peri-5 Me, the rostral part of the LC, the MVe regions (1) just lateral to the LC and (2) caudal to it close to the ventricle. The largest number of fibers was observed in the medial parabrachial nucleus.

Preoptic area dorsal to the supraoptic nucleus. After PHA-L (Fig. 22E) or CTb injections in the preoptic area dorsal to the supraoptic nucleus, many anterogradely labeled fibers were localized in the nuclear core of the LC (Figs 1B, 23B). A similar number of fibers was observed in the peri-5 Me (Fig. 23A). A larger number of fibers was found in (1) the periaqueductal gray medial or ventral to the LC, (2) the cell poor lamina and the ependyma separating the LC from the fourth ventricle (Figs 1B, 23B), (3) the MVe region and the ependyma next to the ventricle caudal to the LC (Fig. 22D). The greatest innervation in the LC area, however, was a very dense plexus of anterogradely labeled varicose fibers covering the Bar (Fig. 23A). A few or no fibers were found in the 5 Me (Fig. 23A) and the MVe (Fig. 22D), respectively.

Posterior hypothalamic areas. The distribution of anterogradely labeled fibers in the LC area considerably varied depending on the localization of the injection sites in posterior hypothalamic areas.

PHA-L or CTb injections in the dorsal hypothalamic area dorsal to the dorsomedial hypothalamic nucleus and caudal to it (CTb, $n = 2$, PHA-L, $n = 2$)

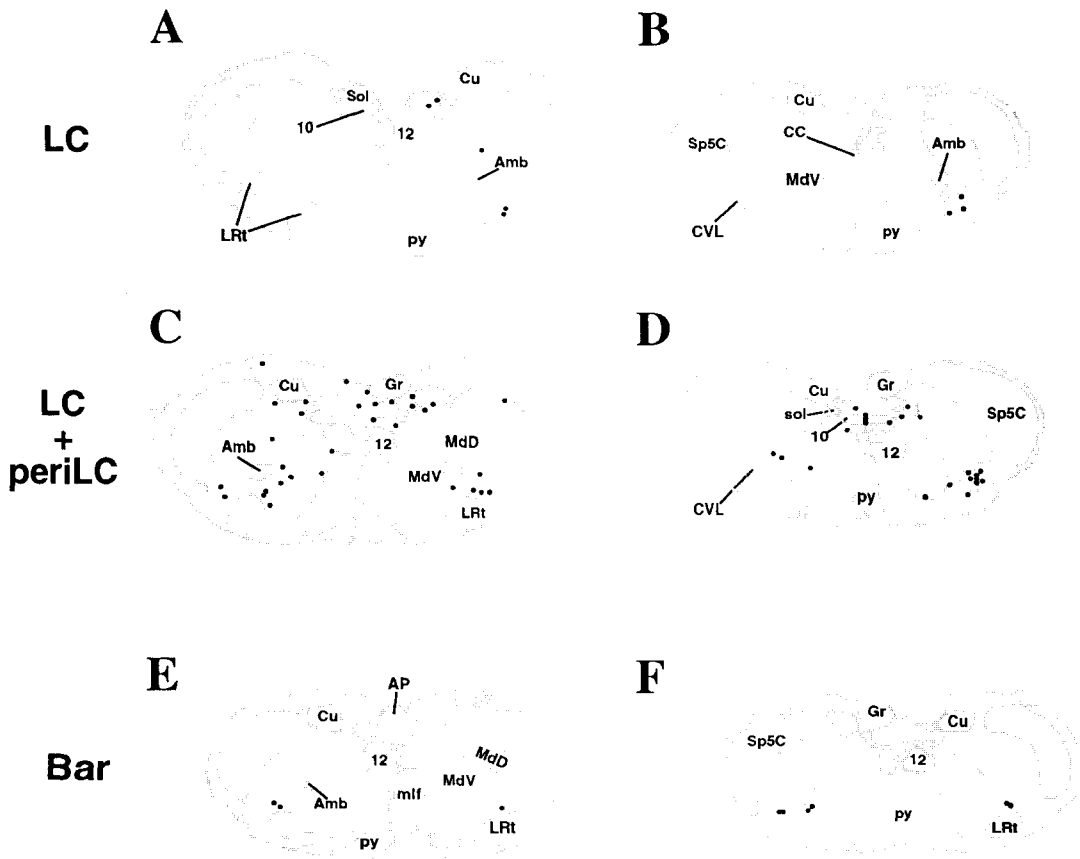

Fig. 20 (*caption on page* 132).

and in the perifornical area (CTb, $n = 2$, PHA-L, $n = 2$) (Fig. 7B) gave rise to dense anterogradely labeled fibers in Bar (Fig. 7D), a large number of fibers in the lamina and the ependyma between the LC and the fourth ventricle and the periaqueductal gray medial to the LC (Fig. 7E), a substantial number of fibers in the peri-5 Me (Fig. 7D), a small number of fibers in the LC (Fig. 7E), medial parabrachial nucleus, and 5 Me (Fig. 7D). Some fibers were also observed in the ependyma caudal to the LC and the adjacent MVe region.

After PHA-L or CTb injections in the lateral hypothalamic area just laterodorsal to the fornix at the level of the dorsomedial hypothalamic nucleus (CTb, $n = 2$, PHA-L, $n = 2$), we observed a moderate number of fibers in the LC and the 5 Me (Figs 7C, 23E). A much larger number of anterogradely labeled fibers was localized in the areas surrounding the LC, including Bar, peri-5 Me, medial parabrachial nucleus (Fig. 23E), the lamina and the ependyma between the LC and the fourth ventricle, the periaqueductal gray medial to the LC (Fig. 7C) and the MVe regions (1) just lateral to the LC and (2) caudal to the LC close to the ventricle including the ependyma. A few fibers were localized in the other parts of the MVe.

Table 1. Analysis of retrograde labeling following injections in locus coeruleus and surrounding structures[1]

Injection site	LC	LC+ peri-LC	Bar	5Me	peri-5Me	MVe
Cortex						
infralimbic cortex	+−	+++	+−	+	++	+
insular cortex		+−		+++	+	
claustrum	+−	++	+−	++	++	+−
frontal cortex	+−	++	+−	+−	+−	++
Hypothalamic level						
preoptic area	+++	++++	++++	++	+	
medial preoptic nucleus		+	+++	+−	+	
bed nucleus, lateral part		+−		++++	++++	
bed nucleus, medial part	+	+++	++++	+++	++	
paraventricular nucleus	+	+	++	+	++	+−
central nucleus of the amygdala		+−		++++	++++	+−
dorsal hypothalamic area	+	++++	+++	+−	+++	++
lateral hypothalamic area	++	++++	+	+++	+++	+++
perifornical nucleus	+	+++	++++	+	+−	++
ventromedial hypothalamic nucleus	+−	+−	+	+−	+−	+−
tuberomamillary nucleus	+−	+−	+−	+−	+−	+−
arcuate nucleus	+−	+−	+	+−	+−	
lateral habenula		+−	+−	+−	+	
Mesencephalon						
ventrolateral part of the periaqueductal grey	+++	++++	++++	+	+++	+
dorsomedial part of the periaqueductal grey	+	++++	+	+−	+−	+
mesencephalic reticular formation	+++	++++	++	+++	++	+
Raphe						
median raphe nucleus	+	++	+−		+−	+−
dorsal raphe nucleus	++	+++	+	++	++	+
nucleus raphe pontis	+−	++	+−			+−
nucleus raphe magnus	+	+	+	+−	+−	+−
Pons						
nucleus laterodorsal tegmental of Castaldi	+−	+	+−	+−	+−	+−
nucleus Kölliker-Füse	+++	++++	+	+−	+	+−
lateral parabrachial nucleus	+	++++	++	+++	+	+−
A5 noradrenergic group	+	+	+−		+−	
pontine reticular formation	+−	++		++	+−	+++
locus coeruleus		+c	++			+−
Medulla						
vestibular nuclei		++			+−	++++
lateral paragigantocellular nucleus	+++	++++	+	+−	+	+
dorsomedial rostral medulla	++	++++	+	+	+	+++
parvocellular reticular nucleus	+−	+		++++	+−	+
nucleus of the solitary tract, rostral part		++	+	+++	+	+−
nucleus of the solitary tract, caudal part	+−	+	+	++	++	+−
caudoventrolateral reticular nucleus	+	++	+−	+−	+−	+−

[1]Semiquantitative analysis of retrograde labeling following CTb injections in LC, LC + peri, LC, Bar, 5Me, peri-5Me or MVe. Cell counts were made from the frontal sections at each level containing the largest number of retrogradely labeled cells. Labeling is presented semi-quantitatively which reflects the relative density of labeled neurons per region on a scale of 1–2 labeled neurons, + −; 3–5, +; 6–10, + +; 11–20, + + +; 21–50, + + + +. Note that this table is based upon the number of cells at one level and in one hemisphere only for each area; the total number of cells labeled for each nucleus depends on the bilaterality and rostrocaudal extension of that area.

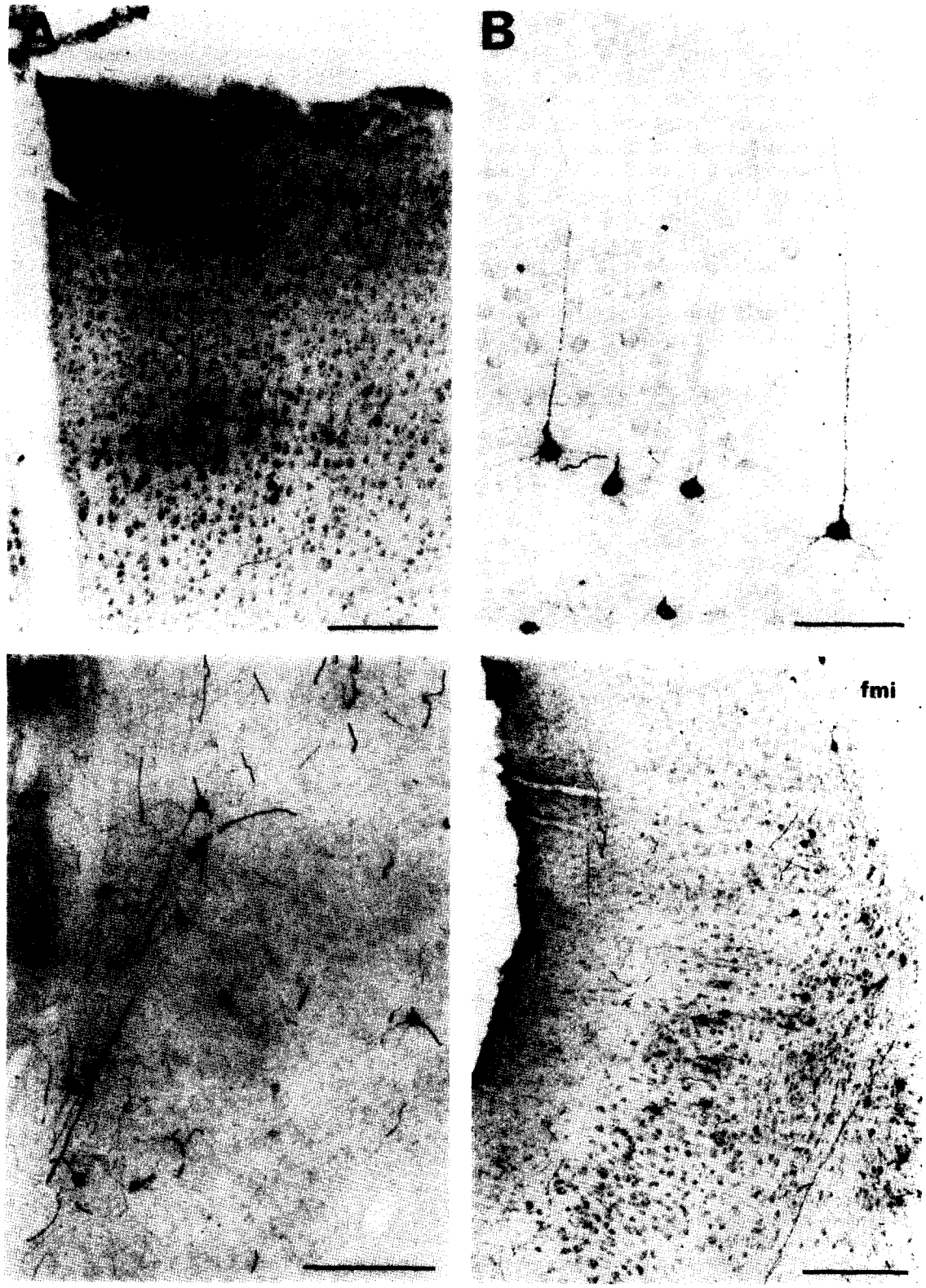

Fig. 21. (A, B) Photomicrographs showing retrogradely labeled pyramidal cells in the layer 4 of the frontal cortex after a LC + peri-LC injection of CTb. Note that the distal dendrites of these cells are labeled up to the superficial layers of the cortex. Scale bar = 200 μm (A) or 100 μm (B). (C) Photomicrograph illustrating retrogradely labeled cells in the claustrum after a CTb injection in the rat LC + peri-LC. Note the presence of anterogradely labeled fibers in the same area. Scale bar = 200 μm. (D) Photomicrograph of a frontal section showing retrogradely labeled cells in the infralimbic cortex after a CTb injection in the LC + peri-LC. Note also the presence of anterogradely labeled fibers in the same area. Medial is to the left and dorsal to the top. Scale bar = 200 μm.

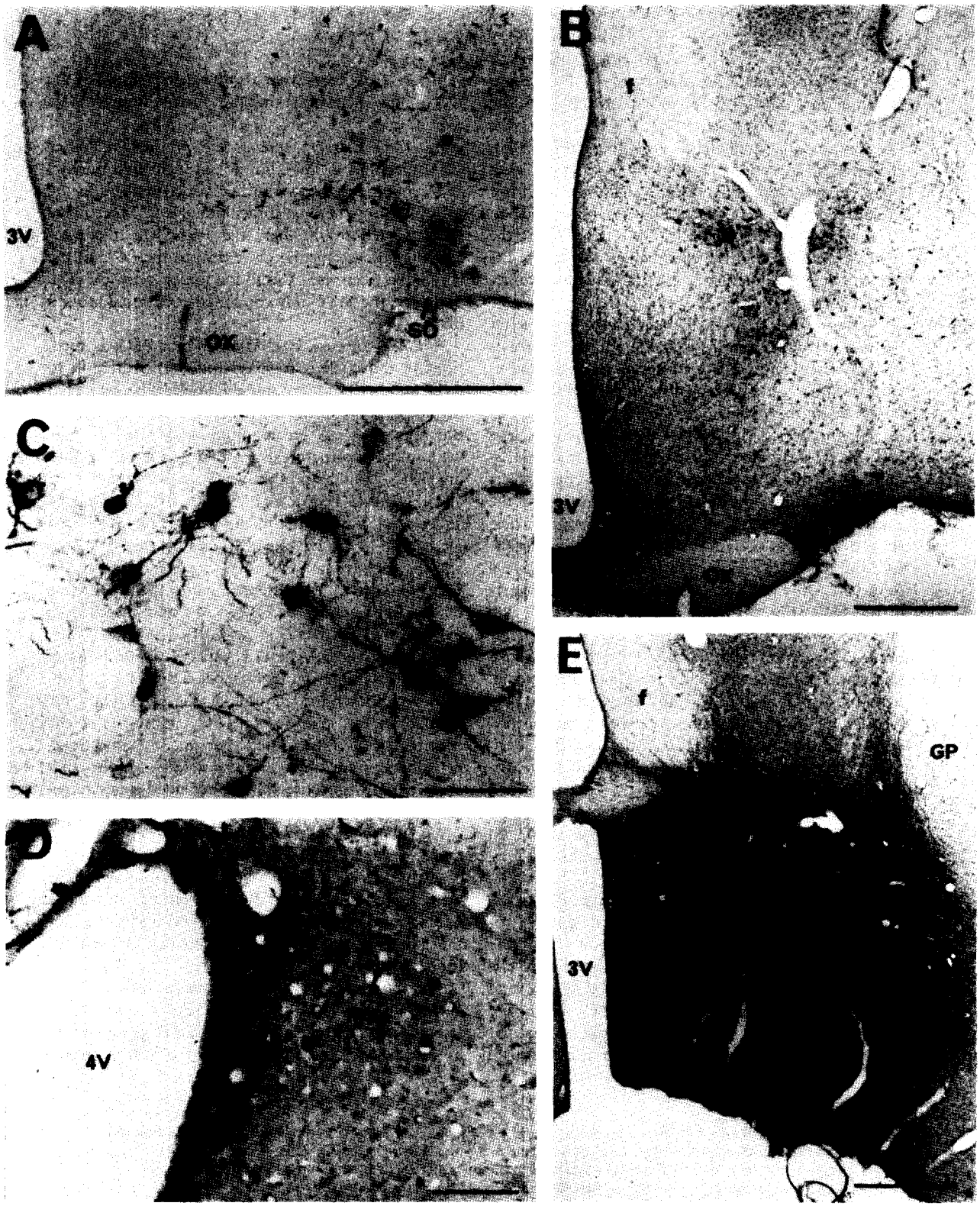

Fig. 22. (A) Photomicrograph showing numerous retrogradely labeled cells clustered in the preoptic region dorsal to the supraoptic nucleus after a CTb injection in the LC + peri-LC. Scale bar = 500 μm. (B) Photomicrograph showing the retrogradely labeled cells in the preoptic region after an injection in Barrington's nucleus. Note that the distribution of the retrogradely labeled cells is clearly different from that shown in A after the LC + peri-LC injection. In particular, a cluster of cells is specifically labeled in the magnocellular subdivision of the medial part of the bed nucleus of the stria terminals. Scale bar = 500 μm. (C) Enlargement of A showing the morphology of the retrogradely labeled cells localized in the preoptic region. Scale bar = 50 μm. (D) Photomicrograph illustrating anterogradely labeled fibers in the ependyma and the extreme caudal tip of the LC after the PHA-L injection in the preoptic region shown in E. Note that the MVe area lateral to the LC contained no labeled fibers. Scale bar = 100 μm. (E) Photomicrograph showing the location of the PHA-L injection in the preoptic region giving the staining shown in D and in Fig. 23A and B. Scale bar = 500 μm.

After PHA-L or CTb injections in the lateral hypothalamic area located dorso-medially to the subthalamic nucleus (CTb, $n = 1$, PHA-L, $n = 1$), the LC contained a small number of fibers (Fig. 23C). However, as found with other hypothalamic injections, many more fibers were seen in structures surrounding the LC, including the Bar, medial parabrachial nucleus, the Peri-5 Me (Fig. 23D), the 5 Me, the lamina and the ependyma between the LC and the fourth ventricle and the periaqueductal gray medial to the LC (Fig. 23C, D).

Ventrolateral part of the periaqueductal gray. After CTb or PHA-L injections in the lateral or ventrolateral part of the periaqueductal gray, a substantial to large number of anterogradely labeled fibers were observed in the nuclear core of the LC (Figs 1C, 6B, E), the Peri-5 Me, medial parabrachial nucleus and the rostral part of the 5 Me. A much large number of fibers were localized in peri-coerular regions, including the Bar, the lamina and the ependyma between the LC and the fourth ventricle (Fig. 6B, E), the periaqueductal gray medial to the LC, and the MVe region close to the ventricle caudal to the LC. Only few fibers were seen in the other parts of the MVe (Fig. 6B).

Area of the B9 serotoninergic cell group. After PHA-L injections in the area of the mesencephalic reticular formation in and dorsal to the medial lemniscus just caudal to the red nucleus at the location of the B9 serotoninergic cell group, a few scattered fibers were observed in the LC, Bar, Peri-5 Me and the lamina between the LC and the ventricle. Nearly no fibers were localized in the 5 Me and the median parabrachial nucleus. A large number of fibers were distributed in the laterodorsal tegmental nucleus of Castaldi and the periaqueductal gray medial to the Bar and the LC.

Nucleus raphe dorsalis. After CTb injections in the nucleus raphe dorsalis, a substantial number of fibers were observed in the Bar and Peri-5 Me as well as in the periaqueductal gray medial to the LC. Only a few anterogradely labeled fibers were observed in the nuclear core of the LC, the medial parabrachial nucleus, the 5 Me, and the lamina and the ependyma separating the LC from the fourth ventricle. Few fibers were also localized caudal to the LC in the ependyma and the periventricular MVe region.

Laterodorsal tegmental nucleus of Castaldi. After CTb injections in the laterodorsal tegmental nucleus of Castaldi, we observed a few varicose fibers in the LC and the median parabrachial nucleus. More fibers were located in the Bar, the Peri-5 Me, the periaqueductal gray medial or ventral to the LC and the lamina between the LC and the fourth ventricle. The 5 Me and the MVe only contained occasional labeled fibers.

Kölliker–Fuse nucleus. After CTb or PHA-L injections in the nucleus Kölliker-Fuse, a substantial to large number of anterogradely labeled fibers covered the nuclear core of the LC (Figs 1D, 5E, 24B) and the Bar (Fig. 24A). A greater number of labeled fibers were found in structures surrounding the LC, including (1) the lamina and the ependyma between the LC and the fourth ventricle (Figs 5E, 24B), (2) the periaqueductal gray medial to the LC, (3) the MVe area just lateral to the LC (Fig. 5E) and (4) the MVe area and the ependyma close to the ventricle caudal to the LC. Few labeled fibers were found in the other areas of the MVe, the 5 Me, Peri-5 Me and the median parabrachial nucleus (Fig. 24A, B).

Locus coeruleus. After LC + peri-LC injections of CTb, a few anterogradely labeled fibers were observed in the contralateral LC (Fig. 4A). Only occasional fibers were seen in the areas around the contralateral LC (Fig. 4A). After small LC injections, no fibers were seen contralaterally. Note that LC + peri-LC injections of CTb yielded a few retrogradely labeled contralateral LC neurons (Fig. 4A).

Nucleus raphe magnus. After CTb injections in the nucleus raphe magnus, a substantial number of varicose anterogradely labeled fibers were observed in the median parabrachial nucleus. In contrast, only a few fibers were visible in the LC, the Peri-5 Me, the Bar, the 5 Me and the lamina between the LC and the fourth ventricle.

Lateral paragigantocellular nucleus. After CTb or PHA-L injections in the retrofacial region of the lateral paragigantocellular nucleus, a large number of anterogradely labeled fibers were observed in the

Fig. 23. (A, B) Dark-field color photomicrographs showing anterogradely labeled fibers in the Bar (A) and the LC (B) after the PHA-L injection in the preoptic area shown in Fig. 22E. A dense plexus of fibers is covering the Bar in A. Fibers are localized in the nuclear core of the LC in B. Note that only few fibers are localized in the MVe region just lateral to the LC. Scale bars = 200 μm. (C, D) Dark-field color photomicrograph of frontal sections illustrating anterogradely labeled fibers in the LC in C and in the nuclei rostral to it in D after a PHA-L injection in the lateral hypothalamic area of the posterior hypothalamus. The injection site was localized dorsolaterally to the fornix at the rostral level of the subthalamic nucleus. Note in C the fibers localized in the nuclear core of the LC. More fibers are found in surrounding structures. In D, the anterogradely labeled fibers are diffusely distributed over the Bar, peri-5 Me, 5 Me, rostral pole of the LC, medial parabrachial nucleus and the periaqueductal gray surrounding these nuclei. Scale bars = 200 μm. (E) Dark-field color photomicrograph illustrating anterogradely labeled fibers in the LC and surrounding structures after a CTb injection in the perifornical nucleus dorsal to the fornix at the level of the dorsomedial hypothalamic nucleus. Note the terminal-like dots in the nuclear core of the LC. More terminal-like labeling is visible in the medial parabrachial nucleus and the lamina between the LC and the fourth ventricle. Scale bar = 200 μm.

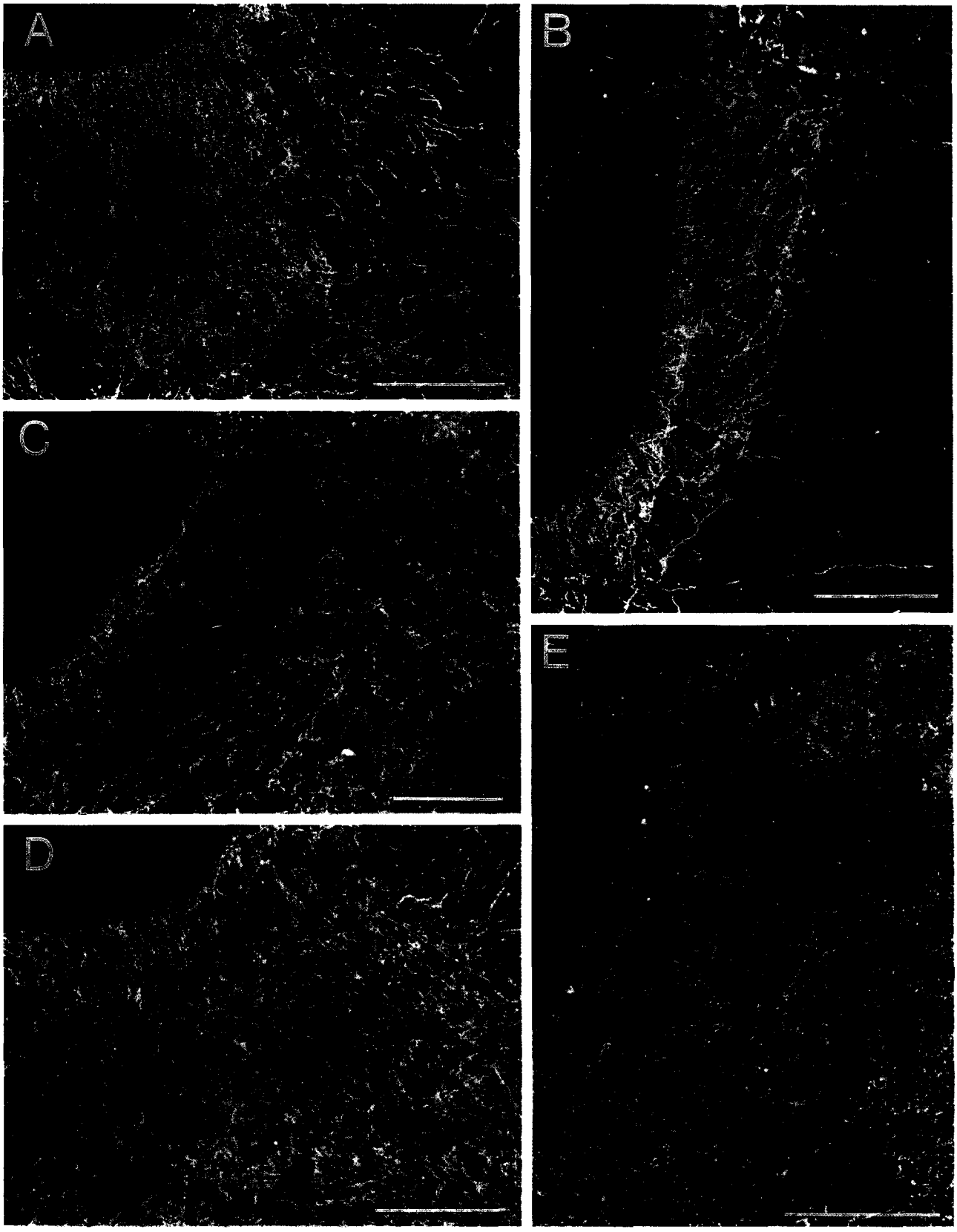

Fig. 23.

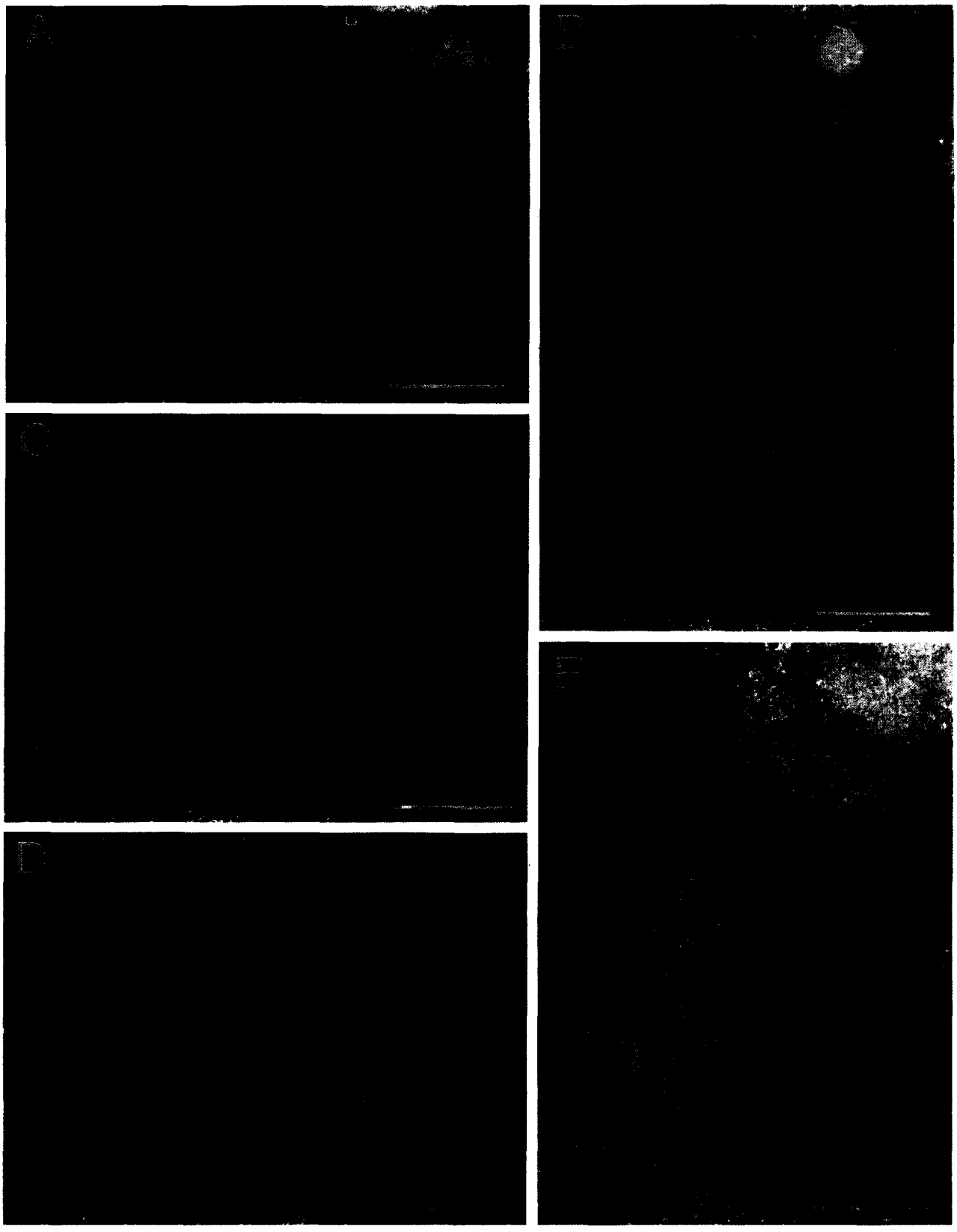

Fig. 24. (A, B) Color dark-field photomicrographs of frontal sections respectively at the level of Barrington's nucleus (A) and the LC (B) showing the presence of anterogradely labeled fibers in these nuclei after the PHA-L injection in the nucleus Kölliker–Fuse shown in Fig. 5. Scale bar = 200 μm. (C, D) Color dark-field photomicrographs of frontal sections showing the distribution of anterogradely labeled fibers at the level of Barrington's nucleus (C) and the LC (D) after a PHA-L injection in the area 1 of the frontal cortex. Note that only a few anterogradely labeled fibers are localized in the LC itself. Scale bars = 200 μm. (E) Color dark-field photomicrograph of a frontal section showing anterogradely labeled fibers in the LC after a PHA-L injection in the lateral paragigantocellular nucleus. Scale bar = 200 μm.

nuclear core of the LC (Figs 4F, 24E, 25B), the Bar, Peri-5 Me and the median parabrachial nucleus (Figs 4E, 25A). A similar number of fibers were also observed in the ependyma and the lamina separating the LC from the ventricle, the periaqueductal gray medial or ventral to the LC and the periventricular MVe region and the ependyma caudal to the LC. Only occasional fibers were localized in the other MVe regions and the 5 Me (Figs 4F, 25B). Overall, anterograde labeling from the retrofacial lateral paragigantocellular nucleus appeared to have a higher ratio of fibers in the core LC: peri-LC compared to other afferents studied.

DISCUSSION

In this report, introducing in rats a method of combining electrophysiological recordings followed by microiontophoretic injections of CTb through the same micropipette, we obtained evidence for specific afferents to the LC. We confirmed many of these afferents with control retrograde and anterograde tracing experiments. Afferents to the LC that contained a substantial number of retrogradely labeled neurons after injections that were apparently restricted to the LC, and that were confirmed with substantial to large fiber innervation of the LC using anterograde tract-tracing with PHA-L or CTb, included the lateral paragigantocellular and Kölliker–Fuse nuclei, the preoptic area, and the ventrolateral periaqueductal gray. We also found a substantial number of retrogradely labeled neurons in posterior hypothalamic areas after injections that were apparently restricted to the LC but we observed only a moderate to small fiber innervation of the LC using anterograde tract-tracing with PHA-L or CTb. The dorsomedial rostral medulla also contained many cells retrogradely labeled from the LC; anterograde tracing was not conducted as it was reported in a previous study.[6]

Technical considerations

The sensitivity of tract tracing molecules, and the methods for their use, have advanced considerably since the first studies were performed to examine inputs to the LC.[10,13] Moreover, the "microanatomy" of the LC region, with marked differences in inputs to closely neighboring small areas surrounding the LC vs the LC proper, has become apparent only recently with the advent of more sensitive tracers

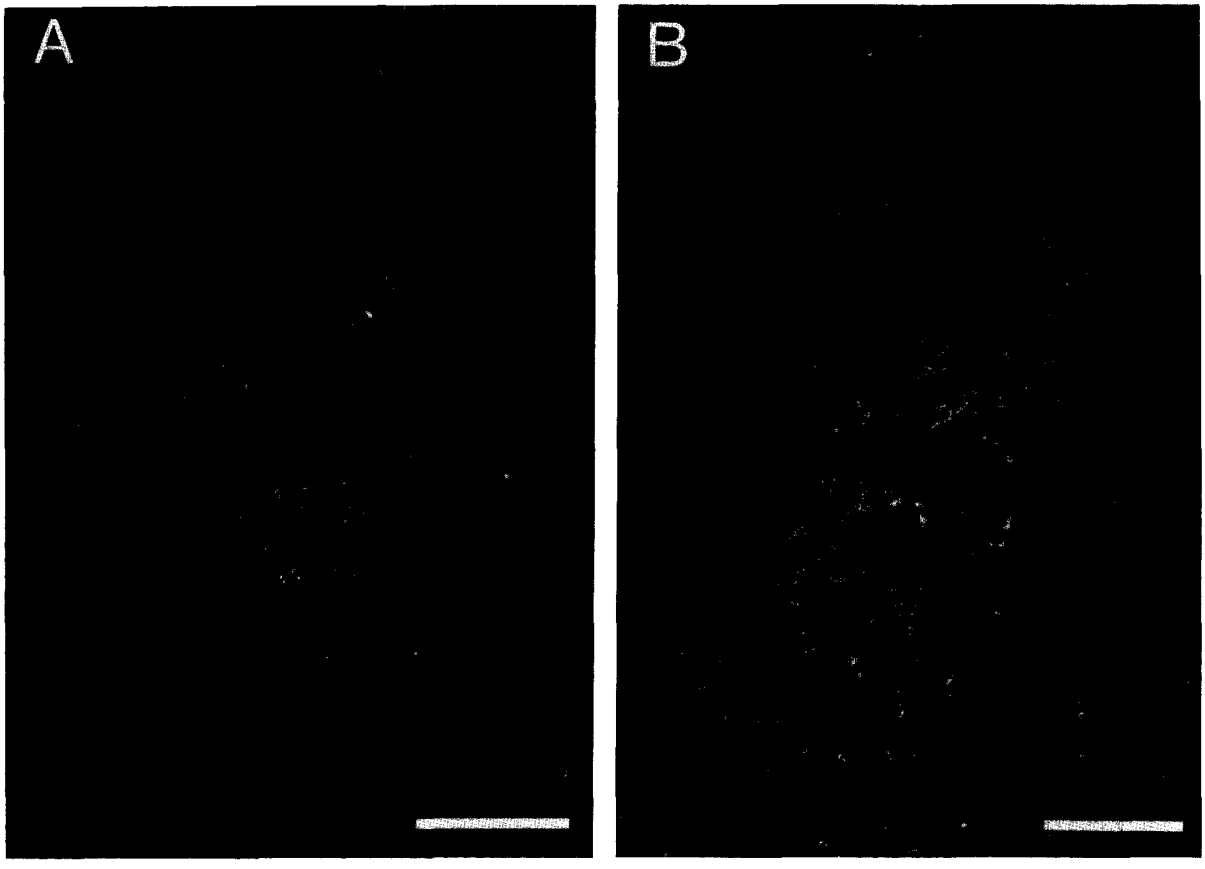

Fig. 25. (A, B) Darkfield photomicrographs of frontal sections respectively at the level of the Barrington's nucleus (A) and the LC (B) showing the presence of anterogradely labeled fibers in these nuclei after a PHA-L injection in the lateral paragigantocellular nucleus. Scale bar = 200 μm.

allowing tracing from small deposits and with the development of sensitive anterograde tract-tracers (e.g., PHA-L).[24] Our results differ from previous tract-tracing studies of afferents to LC in two major ways: (i) we found that several previously reported inputs to the LC project instead to areas surrounding the LC; and (ii) we observed afferents to the LC that were not reported in previous studies. Both of these differences between our results and those in previous studies can be attributed to increased sensitivity of tracers, and the increased awareness of the "microanatomy" of the dorsolateral pontine tegmentum.

Injections of unconjugated HRP yielded labeling in several structures that were not substantially retrogradely labeled in our study (e.g., amygdala, dorsal spinal horn, nucleus of the solitary tract).[10,13] Our results and those of Aston-Jones *et al.*[6,7] using anterograde tracing indicate that these inputs are directed to surrounding nuclei but not to the core LC nucleus (see detailed discussion below). Thus, it appears that injections of unconjugated HRP may have diffused out of the LC proper to label afferents not only to the LC, but also inputs that selectively innervate areas and nuclei around the LC but not the LC proper. This is a potential difficulty of retrograde studies of afferents to small brain nuclei, and indicates the importance of making focal injections of retrograde tracers restricted to the nuclear core of the LC. These findings also underscore the importance of confirming suspected afferents with anterograde tract tracing.

While the above analysis indicates the importance of making small injections of retrograde tracers restricted to the nuclear core of the LC, a potential problem with such small tracer deposits is that the sensitivity of the tracer may be too low to reveal all inputs to the area injected. Indeed, the present study as well as recent retrograde tracing experiments using pressure injections of WGA conjugated to inactivated (apo) HRP and coupled to colloidal gold (WGA-apoHRP-Au) in the LC (Aston-Jones and Zhu, unpublished observations) reveal certain inputs that were not apparent in previous experiments that used WGA-HRP or Fluoro-Gold as retrograde tracers. This analysis indicates that CTb (and WGA-apoHRP-Au) may be more sensitive tract-tracers than WGA-HRP and Fluoro-Gold when employed in very small deposits.

There is another advantage of the smaller injections made possible by the increased sensitivity of CTb and WGA-apoHRP-Au compared to previous tracers: It becomes more feasible to analyse possible inputs from neurons in the areas surrounding the injection site. For example, previous studies with WGA-HRP injections into the LC were inconclusive regarding possible inputs from the periaqueductal gray due (at least in part) to the close proximity of this area to the LC injection site.[6]

It is noteworthy that CTb may have its own limitations as a retrograde tracer as well. For example, although we and others found no evidence for trans-synaptic transport in the central and peripheral nervous system,[41,54] detailed studies remain to be done to completely exclude such a possibility. In addition, the size of the injection site in the first hours after CTb injections is unknown. It is possible that the site in these early hours is larger than after 1–7 days, and that apparently small injections in animals with long survival times may actually have been considerably larger during the earlier periods of uptake and transport. In addition, it is possible that CTb (or any other tracer) is selectively taken up and transported by certain fibers and not by others. If this is true, there may be additional inputs to the LC or the surrounding area that are not revealed in the present set of experiments. Of interest in this regard, we observed only a limited number of labeled cells in the LDT and the peri-LC area after CTb injections in the LC. In contrast, after small WGA-apoHRP-Au injections into the LC, a considerable number of labeled neurons were seen in certain nuclei immediately surrounding LC, e.g. Bar (Aston-Jones *et al.*, unpublished observations). One explanation for such a difference in local labeling obtained with these two tracers might be that WGA-apoHRP-Au, but not CTb, is taken up and transported by dendrites of neurons that may invade the LC. Another possibility is that CTb excludes axonal inputs to the LC from surrounding regions based upon some other selective uptake or transport property of this compound. These considerations underscore the importance of confirming results of retrograde labeling with anterograde tracing.

Although we found that CTb is a good anterograde tracer, it also has some limitations (see anterograde section in Results), the most serious being that this compound strongly retrogradely labels neurons and their processes. Retrogradely labeled neuronal processes could be mistaken for anterogradely labeled fiber inputs. Therefore, injections into areas that are efferent targets of the LC may lead to erroneous conclusions regarding sources of anterograde fiber labeling in the LC. This is a particularly common problem with studies of afferents to the LC because of the uniquely widespread projections of LC neurons. Therefore, while negative results with anterograde labeling of CTb may be very informative (assuming effective transport from the cells of interest is demonstrated), positive fiber labeling in the LC after injections of CTb into most CNS areas should be taken as only tentative evidence of afferent innervation. For this reason, we confirmed many of our results by an alternative method that do not generate robust retrograde labeling (e.g., PHAL).

Neurons and dendrites of the peri-coerulear region

Anatomical studies have shown that the region surrounding the LC is complex and contains neurons as well as neuropil. Locus coeruleus neurons are multipolar and have long dendrites that extend into surrounding regions.[26,60,66] Recent studies[22,61] have

confirmed that LC dendrites extend for considerable distances into peri-LC regions, but are polarized being particularly densely located in two peri-LC zones, the rostromedial and caudal juxtaependymal zones. In our study, after PHA-L or CTb injections in some areas (preoptic area, posterior hypothalamic areas, periaqueductal gray, Kölliker–Fuse), we observed generally more anterogradely labeled fibers in these peri-LC areas than in the nuclear core of the LC. These results suggest that LC noradrenergic cells might receive considerable inputs on their dendrites outside the nuclear core of the LC. Peri-LC areas also receive a great deal of input from regions that do not, or only minimally, innervate the LC (e.g., nucleus of the solitary tract, prefrontal and infralimbic cortex, amygdala, dorsal raphe), raising the possibility that LC dendrites may receive innervation from areas that do not innervate the LC proper. One way to examine this possibility is use of electrophysiological methods to measure the functional influence of afferents to such peri-LC regions on LC impulse activity. This has been done for some possible afferents, including the central nucleus of the amygdala,[6] nucleus of the solitary tract[19] and prefrontal cortex.[12] In each case, little or no effect was found in LC activity of stimulating the test afferent with single electrical pulses. However, similar tests needed to be conducted for other possible afferents as well. Moreover, it is possible that stimulation paradigms may not reveal modulatory effects of inputs to distal dendrites of LC neurons. Therefore, ultrastructural studies of the peri-LC region employing anterograde tracing and dopamine-beta-hydroxylase staining are also needed to evaluate the possible status of peri-LC afferents as inputs to LC dendrites. It is also noteworthy that LC dendrites do not extent laterally into the 5 Me, nucleus parabrachialis or similar areas, nor caudally into the vestibular nucleus, so that afferents to these regions (e.g., frontal cortex, amygdala, spinal cord) are unlikely to contact LC neurons or dendrites.

Conversely, examination of the LC region using NADPH or cholinacetyltransferase staining has revealed that cholinergic neurons of the LDT region possess extensive dendrites, some of which innervate the LC nucleus or peri-LC dendritic zone.[33,53] This raises issues of interest to the study of afferents to the LC: (i) do dendrites of these LDT neurons act presynaptically on LC neurons via a cholinergic mechanism? and (ii) do dendrites of LDT neurons located within the LC receive inputs from neurons that project into the LC? The latter possibility raises especially important issues that have not been addressed in studies to date, e.g. do some inputs to the LC preferentially innervate non-LC elements located within the LC? This possibility seems most reasonable for those projections that: (i) are not particularly dense within the LC proper and; (ii) densely innervate the area of source neurons in the region around LC that give rise to the non-LC dendrites located in the LC nucleus (e.g., dorsal raphe, lateral hypothalamus, preoptic area, periaqueductal gray and nucleus of the solitary tract, among others). These various data illustrate the complexity of connectivity studies in small deep brain nuclei, and point out the need for functional (electrophysiological) and ultrastructural studies to test possible inputs.

Cortical areas

After LC injections, Cedarbaum and Aghajanian[10] and Clavier[13] observed some labeled cells in the insular cortex. In agreement with anterograde tracing studies with PHA-L or WGA-HRP showing that the insular cortex projects densely to areas corresponding to the Peri-5 Me and the 5 Me[44,72] rather than to the LC, we observed labeled cells in the insular cortex only after 5 Me or Peri-5 Me injections.

We observed a few labeled cells in the frontal and infralimbic cortex and the claustrum after LC injections. However, the frontal and infralimbic cortices contained many more cells after a specific MVe injection or Peri-5 Me injections. Moreover, after PHA-L injections in the frontal or infralimbic cortices, we found only occasional anterogradely labeled fibers in the LC and many more fibers in the MVe and the Peri-5 Me. These results are in agreement with previous anterograde tracing studies with PHA-L or WGA-HRP showing that the infralimbic cortex projects to an area corresponding to the Peri-5 Me rather than to the LC proper.[12,32,68]

Together, these results suggest that the infralimbic, insular and frontal cortices and the claustrum provide only a very limited input to the nuclear core of the LC and rather strongly project to the peri-LC areas and the surrounding nuclei. As noted above, such limited fiber labeling in the LC could reflect inputs to LC neurons or to non-LC elements located within the LC. Also, it remains to be determined whether cortical projections to peri-LC areas that densely contain LC dendrites (ventromedial and caudodorsal to the LC[42,65]) are directed to the dendrites of noradrenergic neurons or to non-noradrenergic cells and dendrites also present in these areas.

Preoptic level

After LC injections, previous reports showed either a limited number[10,13] or only occasional labeled cells in some animals[6] in the preoptic area. In contrast, after LC injections we observed a substantial number of cells in the preoptic area dorsal to the supraoptic nucleus. By means of anterograde tracing with PHA-L and CTb, we confirmed that the preoptic area dorsal to the supraoptic nucleus substantially innervates the nuclear core of the LC itself. Recent studies[53] using WGA-apoHRP-Au and PHA-L have also confirmed that the preoptic area sends direct projections to the LC, although projections were much denser to areas surrounding the LC. It is noteworthy that, as found for several inputs to the LC (described above), anterograde tracing revealed a denser innervation

from the preoptic area in peri-LC areas than in the LC proper. It remains to be determined with electron microscopic observations whether this projection to the peri-LC is directed to the dendrites of noradrenergic neurons or to non-adrenergic cells and dendrites also present in these areas.

After injections of CTb in the Bar, we observed a large number of cells in the same area but also in the medial preoptic nucleus and the lateral preoptic area. By means of anterograde tracing with PHA-L and CTb, we confirmed that the preoptic area dorsal to the supraoptic nucleus very densely innervates the Bar. Recent studies[53,68a] using WGA-apoHRP-Au and PHA-L have also confirmed that the preoptic area sends dense projections to areas surrounding the LC in particular the Bar. In agreement with these results, Swanson[67] using autoradiography demonstrated a projection from the lateral preoptic area to an area corresponding to the area of the Bar and rostral LC. Conrad and Pfaff[15] using autoradiography, and Simerly and Swanson[63] with PHA-L injections in the medial preoptic nucleus or area, also demonstrated anterogradely labeled fibers in a region corresponding to Bar.

We also saw a large number of labeled cells in the medial part of the bed nucleus of the stria terminalis after Bar injections. Fewer cells were found after LC + peri-LC, 5 Me or Peri-5 Me injections. Moga *et al.*[44] reported anterogradely labeled fibers in the Bar after WGA-HRP injections in the medial part of the bed nucleus of the stria terminalis confirming that this nucleus is mainly projecting to the Bar.

Cedarbaum and Aghajanian[10] observed a relatively large number of cells in the lateral part of the bed nucleus of the stria terminalis after HRP injections into the LC. We saw a large number of cells in this area only after 5 Me or Peri-5 Me injections. In agreement with our results, Moga *et al.*[44] saw anterogradely labeled fibers in the peri-5 Me and Me5 after WGA-HRP injections in the lateral part of the bed nucleus of the stria terminalis. These data indicate that the lateral part of the bed nucleus of the stria terminalis project to the 5 Me and peri-5 Me but not to the LC.

Midhypothalamic level

We and other previous authors[6,10] excepting Clavier[13] found a small number of retrogradely labeled neurons in the dorsal cap of the hypothalamic paraventricular nucleus after LC injections. Such a weak projection has also been observed in anterograde tracing experiments using tritiated amino acids and PHA-L.[15,38] We further found that the surrounding nuclei, particularly the Peri-5 Me and the Bar, also received a projection from the paraventricular nucleus but from the medioventral parvocellular aspect.

At the same level, Cedarbaum and Aghajanian[10] and Clavier[13] described a large number of retrogradely labeled cells in the central nucleus of the amygdala after HRP injections into the LC. In contrast, we and Aston-Jones *et al.*[6] saw no or only occasional labeled cells in this nucleus. We observed a large number of labeled cells in the central nucleus of the amygdala only after CTb injections in the 5 Me or Peri-5 Me. After injections of the anterograde tracer WGA-HRP in the central nucleus of the amygdala, no fibers were observed in the LC while the 5 Me, Peri-5 Me and the median parabrachial nucleus contained a great number of anterogradely labeled fibers.[6,44] Stimulation of the central nucleus of the amygdala yielded little or no response in LC but markedly excited nearby parabrachial neurons.[6] Taken together, these results indicate that the central nucleus of the amygdala does not project to the LC but rather to the adjacent 5 Me, Peri-5 Me and median parabrachial nucleus.

Posterior hypothalamus

After LC injections, Aston-Jones *et al.*[6] saw occasional cells in some animals in the posterior hypothalamus. Cedarbaum and Aghajanian[10] and Clavier,[13] after large LC injections very likely encroaching upon neighboring areas, reported the presence of cells in posterior hypothalamic areas. We observed a substantial number of small and medium-sized retrogradely labeled cells in the lateral and dorsal hypothalamic areas and the rostral perifornical nucleus after LC injections. We determined that these regions also project with a topographic organization for each nucleus to the Bar, 5 Me, Peri-5 Me and MVe. After Bar injections, labeled neurons were clustered (1) in the caudal part of the dorsal hypothalamic area and (2) around and ventromedial to the fornix. After 5 Me and Peri-5 Me injections, they were mostly located in the lateral hypothalamic area just medial to the internal capsule and the subthalamic nucleus. Finally after MVe injections, medium-sized cells were diffusely distributed over the posterior hypothalamic areas and the perifornical nucleus. We confirmed these results for peri-LC injections with anterograde tracing with CTb and PHA-L; note, however, that the LC only contained a small number of fibers following such anterograde tracing. Studies using anterograde tracers such as tritiated amino acids, WGA-HRP and PHA-L have reported a projection from the posterior hypothalamic areas to the region of the LC.[30,69,70] However, for most of them, the distribution of the terminals was not precise enough to draw a comparison with our study. Only Allen and Cechetto[1] recently reported a strong specific projection from the perifornical region to the Bar and from the lateral hypothalamic area to a region corresponding to the Peri-5 Me and 5 Me. On the other hand, Shirokawa and Nakamura[62] reported antidromic activation of dorsal hypothalamic area neurons from the area of the LC. These data taken together indicate that the dorsal and lateral posterior hypothalamic areas and the perifornical nucleus may provide inputs to the LC and surrounding nuclei with

a very specific topographic organization. It is noteworthy that, as found for several of the inputs to the LC, anterograde tracing revealed that these hypothalamic regions innervate the peri-LC region more strongly than the LC itself (discussed above in "Neurons and Dendrites in Peri-LC"). Further experiments are necessary to determine the neurotransmitter content of these pathways as well as their physiological roles.

We also observed occasional cells in the hypothalamic ventromedial nucleus after LC + peri-LC injections. Although sparse anterograde labeling has been reported in the LC after tritiated amino acid and PHA-L injections in this hypothalamic nucleus,[36,38,58] more precise studies seem to be necessary to define the exact terminal field of this projection.

In contrast with previous studies, we consistently found a few retrogradely labeled cells in the tuberomammillary nucleus after LC but also Bar, Peri-5 Me, 5 Me and MVe injections. This nucleus contains only histamine neurons.[48] A significant number of histamine immunostained fibers has been observed in the area of the LC.[47] These data indicate that histamine neurons of the tuberomamillary nucleus may provide a weak diffuse innervation of the LC and surrounding nuclei. Additional studies with anterograde transport from the tuberomammillary nucleus or histamine immunohistochemistry are needed to test this possibility.

Mesencephalon

Cedarbaum and Aghajanian[10] and Clavier[13] reported large numbers of retrogradely labeled neurons in the ventrolateral periaqueductal gray following injections of HRP into the LC. However, as discussed above, injections in these studies very likely encroached upon neighboring areas, so that these retrograde labelings may have reflected inputs to peri-LC areas. Aston-Jones *et al.*[6] found that periaqueductal gray cells were not consistently labeled following injections of WGA-HRP into the LC; periaqueductal gray cells were often labeled near the LC injection site in that study, but as they were near the halo of the injection it was concluded that additional studies would be necessary to determine the status of the periaqueductal gray as a possible afferent to the LC. Retrograde and anterograde labeling in our study confirm that the ventrolateral part of the periaqueductal gray directly innervates the LC. These findings are also consistent with recent studies using retrograde transport of WGA-apoHRP-Au (which allows very small injections but is none the less very sensitive) (Aston-Jones *et al.*, unpublished observations). However, as noted above for other afferents (and discussed above under "Neurons and Dendrites in the Peri-LC Area"), the innervation of the peri-LC region by the periaqueductal gray was much greater than to the LC proper. In general, our results agree with those of a more recent study of periaqueductal gray inputs to the LC region.[21] These authors found only a modest number of cells retrogradely labeled in the ventrolateral periaqueductal gray after apparently restricted injections of WGA-HRP into the LC. Moreover, PHA-L anterograde labeling in that study revealed strong inputs to the Bar and other peri-LC regions, but more moderate input to the LC proper. These anatomical results were consistent with physiological studies in that paper, which indicated a modest connection (via antidromic activation) and synaptic influence from the periaqueductal gray on LC neurons but a much greater functional connection from the periaqueductal gray to nearby peri-LC regions.

No anterograde data is available for the projection from the dorsal part of the periaqueductal gray to the LC. Suggesting the specificity of this afferent, we found only a few retrogradely labeled cells in the dorsal periaqueductal gray after control injections in the nuclei surrounding the LC. However, neurons were not observed in the dorsal part of the periaqueductal gray in previous reports.[6,10,13]

We and Cedarbaum and Aghajanian[10] found a large number of neurons in the mesencephalic reticular formation after large LC + peri-LC injections. We observed a substantial number of cells even after LC injections apparently not involving peri-LC areas. The cells were localized lateral to the median raphe nucleus and in a region inside and just dorsal to the medial lemniscus, in the area of the B9 serotonin cell group.[16] This area does not correspond to the ventral tegmental area previously reported to project to the LC using anterograde tracing methods.[28,64] Indeed, Aston-Jones *et al.*[6] using WGA-HRP as a anterograde tracer, have demonstrated that the ventral tegmental area projects to the medial parabrachial nucleus and a region located rostral to the Peri-5 Me but not to the LC itself. On the contrary, after injections of PHA-L in the B9 region, we observed a few anterogradely labeled fibers in the nuclear core of the LC. Together, these data suggest that the LC receives a small projection from the B9 region and no input from the ventral tegmental area. Further anterograde studies are necessary to confirm projections to the LC from the other parts of the mesencephalic reticular formation.

Raphe nuclei

In agreement with Cedarbaum and Aghajanian[10] and Clavier,[13] we observed a substantial number of rather small retrogradely labeled cells in the dorsal raphe nucleus particularly its rostral and dorsolateral extensions after LC + peri-LC injections. We and Cedarbaum and Aghajanian[10] observed also fewer cells in the median raphe nucleus after such injections. After LC or Bar injections, we observed fewer cells in these raphe nuclei. Aston-Jones *et al.*[6] saw a few weakly labeled cells in some animals in the dorsal and median raphe nuclei with LC injections of WGA-HRP. After CTb injections in the Peri-5 Me, 5 Me and MVe, we observed mainly medium-sized

retrogradely labeled neurons in the medioventral part of the dorsal raphe nucleus and occasional cells in the median raphe nucleus. In agreement with these results, after tritiated proline injections in the dorsal and median raphe nuclei, weak projections to the area of the LC have been reported.[14] Furthermore, after CTb injections in the medioventral part of the dorsal raphe nucleus, we found a substantial number of fibers in the nuclei surrounding the LC and only a few in the LC proper. This is consistent with previous results obtained with PHA-L.[7]

Using radioautographic detection of serotonin, Leger *et al.*[37] found only a partial decrease in the number of serotonin terminals in the LC after lesions of the dorsal, median or pontis raphe nuclei. In addition, recent studies by Pieribone *et al.*[52] found no discernable decrease in the density of 5-HT-immunoreactive fibers in the LC after lesions of the dorsal raphe nucleus. Furthermore, in our preliminary experiments combining CTb retrograde staining with 5-HT immunohistochemistry after even large LC injections of CTb, we found only a few double-stained neurons in the dorsal raphe nucleus. In contrast, many 5-HT- and CTb-immunoreactive cells were observed in the median raphe nucleus and the B9 serotoninergic cell group.[9] Together, these results suggest that the serotonin innervation of the LC arises primarily from the median raphe nucleus and the B9 serotonin cell group and only to a minor extent from the dorsal raphe nucleus. Additional double-labeling and anterograde tracing experiments are necessary to confirm these preliminary results.

Pons

In the pons, after LC or LC + peri-LC injections, a large number of retrogradely labeled neurons was present bilaterally in the Kölliker–Fuse nucleus. Few or only occasional retrogradely labeled cells were localized in this nucleus after control injections in the Bar, the MVe, peri-5 Me or 5 Me. Clavier[13] also described a contralateral projection from the Kölliker–Fuse nucleus to the LC. In contrast, Cedarbaum and Aghajanian[10] and Aston-Jones *et al.*[6] reported a few or no cells in this nucleus. However, we confirmed the strong bilateral input from the Kölliker–Fuse nucleus to the LC using PHA-L and CTb as anterograde tracers and this projection has also been observed recently with retrograde transport of WGA-apoHRP-Au from small pressure injections into the LC (Aston-Jones and Zhu, unpublished observations). Such discrepancies between ours and previous results might be due to the weaker sensitivity of the tracers previously used compared with that of CTb and WGA-apoHRP-Au (as discussed above; see "Technical Considerations").

We observed a large number of cells in the lateral parabrachial nucleus after LC + peri-LC injections. A small number of cells was also present in this nucleus after LC, Bar or 5 Me injections. Cedarbaum and Aghajanian[10] and Clavier[13] reported cells in this region only contralaterally. Aston-Jones *et al.*[6] often saw cells located within the halo of their LC injection sites in this region. Further anterograde experiments are necessary to determine whether the retrograde labeling in the present study reflects afferents to areas neighboring the LC, or to the LC itself.

After LC or LC + peri-LC injections, we consistently observed a small number of cells lying dorsal and lateral to the superior olive, medial to the exiting fibers of the facial nerve at the location of the A5 noradrenergic cell group.[16] We observed only a few or no cells in this area after control injections in surrounding nuclei suggesting the specificity of this input to the LC. Cedarbaum and Aghajanian[10] and Clavier[13] also observed labeled cells in this area, but Aston-Jones *et al.*[6] did not consistently obtain such labeling with focal WGA-HRP injections in the LC. Anterograde and immunohistochemical experiments are necessary to test this possible projection and to determine if it consists of noradrenergic A5 neurons.

After LC, Bar, Peri-5 Me, 5 Me or MVe injections, we observed only a few retrogradely labeled cells in the pedunculopontine and laterodorsal tegmental nuclei where most of the pontine cholinergic cells are located. We also saw only few anterogradely labeled fibers in the LC after CTb injections in the laterodorsal tegmental nucleus. In agreement with these results, only a few scattered cholinergic axons were observed in the LC after choline-acetyltransferase immunohistochemistry.[33,55]

After LC + peri-LC injections, we, Cedarbaum and Aghajanian[10] and Clavier[13] observed a few labeled cells in the contralateral LC. However, Aston-Jones *et al.*[6] observed no contralateral labeling after WGA-HRP injections into the LC. Consistent with this result, we saw no cells after CTb injections apparently restricted to the LC or with control injections in surrounding nuclei. After LC + peri-LC injections, we also observed a few anterogradely labeled fibers in the contralateral LC but not in adjacent nuclei. Taken together, these results suggest only a weak, if any, contralateral projection of the LC.

Medulla

After LC injections, Cedarbaum and Aghajanian,[10] Clavier[13] and Fung *et al.*[23] reported a large number of labeled cells in the vestibular nuclei. Aston-Jones *et al.*[6] noted that the vestibular nuclei often contained labeled cells but only within the halo of their injection sites. We saw labeled cells in the vestibular nuclei only after LC + peri-LC injections involving the adjacent MVe. After a control injection restricted to the MVe area located just lateral to the LC, we observed a large number of cells and anterogradely labeled fibers bilaterally in the vestibular nuclei. These results indicate that the MVe region close to the LC, but not the LC itself, may be reciprocally innervated by the other vestibular nuclei.

Cedarbaum and Aghajanian[10] and Clavier[13] observed a large number of cells in the ventrolateral part of the medullary reticular formation after LC injections, which they ascribed to the lateral reticular nucleus. Aston-Jones *et al.*[6] described a large number of cells specifically in the lateral paragigantocellular nucleus (LPGi) localized in the rostral ventrolateral medulla, but not extending more caudally into the lateral reticular nucleus. After either LC or LC + peri-LC injections, we also saw a large number of cells specifically in the LPGi. We found fewer retrogradely labeled cells in the LPGi after Bar, 5 Me, Peri-5 Me or MVe injections. Confirming these data, we and Aston-Jones *et al.*[6] found a large number of anterogradely labeled fibers in the LC after PHA-L, CTb or WGA-HRP injections in the LPGi.

Cedarbaum and Aghajanian[10] and Clavier[13] reported a few and no cells, respectively, in the dorsomedial rostral medulla (ventromedial nucleus prepositus hypoglossi and dorsal paragigantocellular nucleus) after LC injections. Aston-Jones *et al.*[6] found a large number of retrogradely labeled neurons bilaterally in the dorsomedial rostral medulla after WGA-HRP injections in the LC. We also found bilaterally a large number of cells in this region after LC or LC + peri-LC injections of CTb. Note that the counts given in the Results here were for the ipsilateral dorsomedial rostral medulla only; this projection is strongly bilateral, so that many contralateral cells also innervate the LC. Also, the main collection of LC-projecting neurons in the dorsomedial rostral medulla is a rostrocaudally oriented narrow column of neurons, so that counts in one frontal section may not fully represent the labeled neurons. It is noteworthy that in the Aston-Jones *et al.*[6] study and the present investigation, the neurons labeled retrogradely from the LC in the nucleus prepositus hypoglossi were specifically located in its ventromedial aspect; the bulk of the nucleus did not contain labeled cells.

We also observed a large number of cells in the dorsomedial rostral medulla with a similar distribution but with a strong contralateral predominance after a control injection in the adjacent MVe area just lateral to the LC. As for LC injections, the neurons in the nucleus prepositus hypoglossi were specifically located in its ventromedial aspect; the bulk of the nucleus did not contain labeled cells.

Only a few cells were localized in the dorsomedial medulla after CTb injections in the Bar, 5 Me and Peri-5 Me.

After WGA-HRP injections in the dorsomedial rostral medulla, Aston-Jones *et al.*[6] further reported the presence of a large number of anterogradely labeled fibers in the LC. Also, Ennis and Aston-Jones[20] obtained frequent antidromic activation of neurons in the dorsomedial rostral medulla after focal LC stimulation, and potent synaptically mediated inhibition of LC activity after stimulation of the dorsomedial rostral medulla. Taken together, these results suggest that the dorsomedial rostral medulla strongly projects to the LC and the adjacent MVe area.

Cedarbaum and Aghajanian[10] and Clavier[13] found a large number of cells in all subdivisions of the nucleus of the solitary tract. In contrast, after small LC injections, we and Aston-Jones *et al.*[6] respectively found a few or no cells in this nucleus. We observed numerous cells in the rostral or caudal parts of the nucleus of the solitary tract only after 5 Me or Peri-5 Me injections, respectively. After WGA-HRP or PHA-L injections in the nucleus of the solitary tract, Aston-Jones *et al.*[6] and Herbert *et al.*[27] reported sparse scattered fibers in the LC and Bar and a large number of fibers in the Peri-5 Me and Me5. These and additional electrophysiological data[19] suggest that the nucleus of the solitary tract strongly projects to the peri-5 Me and Me5 and provides only a weak, if any, input to the LC itself.

In agreement with Cedarbaum and Aghajanian,[10] we observed a small number of cells in the caudoventrolateral medullary reticular formation in the region of the A1 noradrenergic cell group[16] after LC or LC + peri-LC injections. In support of the specificity of this afferent, we found only a few cells in this area after our control injections in nuclei surrounding the LC. Nevertheless, additional anterograde experiments are necessary to confirm these results.

Physiological significance

Inactivation of locus coeruleus noradrenergic neurons during paradoxical sleep. Although it is well accepted that the noradrenergic neurons of the LC cease firing during paradoxical sleep (PS-off cells),[4,29] the mechanisms responsible for this inactivation have not been elucidated. Nevertheless, as first proposed by Aston-Jones and Bloom,[4] evidence suggests that these cells might be tonically inhibited by extrinsic afferents rather than defacilitated during PS. These investigators reported spontaneous and sensory-evoked field potentials without unit activity in the LC during paradoxical sleep.[4] These potentials were proposed to reflect concerted excitatory postsynaptic responses in the presence of strong tonic inhibition preventing discharge. Consistent with this view, LC cells display a tonic pacemaker activity in brain slices,[71] in the absence of possible facilitatory inputs. The neurons responsible for such tonic inhibition of the LC might be located in the brainstem. Indeed, pontile cats with sections at the level of the superior colliculus display periods of PS alternating with wakefulness[34] suggesting that the neurons responsible for the inhibition of the monoaminergic neurons including the locus coeruleus neurons are localized in the brainstem. In its reciprocal interaction model, Sakai[56] has proposed that during PS, the PS-off noradrenergic cells of the LC might be under a monosynaptic inhibition provided by the PS executive neurons (PS-on cells) located in the medial or mediodorsal pontine reticular formation. Our results

do not support the existence of a monosynaptic projection from such neurons. Indeed, we found no or only a weak projection from the medial or mediodorsal pontine reticular formation to the LC. The only strong pontine input to LC identified in the present study was from the Kölliker–Fuse nucleus localized in the lateral part of the pontine reticular formation. Of interest regarding this result, Data *et al.*[17] recently reported that injection of carbachol in the peribrachial area just caudal to the Kölliker–Fuse nucleus induces a long-term enhancement of PS. Additional experiments are necessary to determine whether the Kölliker–Fuse nucleus might participate in this effect.

It has also been proposed that the GABAergic neurons recently observed in the region of the pedunculopontine nucleus and the nuclei surrounding the LC such as the Bar, the peri-5 Me and the laterodorsal tegmental nucleus[33] might be, in the reciprocal interaction model, the missing inhibitory link between the presumed cholinergic PS-on cells in these nuclei and the noradrenergic PS-off cells of the LC. Although we cannot rule out possible dendrodendritic interactions not revealed using CTb as a retrograde tracer (see above "Neurons and dendrites of the peri-coerulear region"), our results do not support the existence of short inhibitory projections to the LC from interneurons located in the vicinity of the LC nor from the pedunculopontine nucleus. Indeed, we observed only a few CTb labeled cells in the pedunculopontine nucleus and the nuclei surrounding the LC after CTb injections in the LC.

Together, these data suggest that the neurons inhibiting the LC during PS might be rather located in one of the three strong brainstem afferents we report here namely the Kölliker–Fuse nucleus, the LPGi or the dorsomedial rostral medulla. Among these, the projection from the dorsomedial rostral medulla to the LC seems to be a good candidate for such inhibition. Indeed, Ennis and Aston-Jones[19,20] have shown that this pathway is inhibitory and uses GABA as a neurotransmitter.

We have recently demonstrated that in addition to GABA, the LC is strongly inhibited by glycine.[40] It has also been shown that during PS the motoneurons are tonically hyperpolarized by glycine.[11] In view of these results, we hypothesized that during PS, the LC noradrenergic cells are tonically inhibited by the glycinergic neurons responsible for the inhibition of the somatic motoneurons. LC cells might also be hyperpolarized by other types of neurotransmitters found to inhibit LC cells such as noradrenaline or enkephalin.[7] In this regard it is also noteworthy that Aston-Jones *et al.*[3] have recently found potent alpha2 adrenoceptor-mediated inhibition of LC neurons from the LPGi, presumably reflecting the strong input from C1 neurons located within the PGi.[2,35,50,51] Moreover, the PGi and the dorsomedial medulla provide a dense enkephalinergic input to the LC,[18] and enkephalin strongly inhibits LC neurons.[46] Thus, it is also possible that inhibition of LC during PS reflects PGi input to these neurons.

Also of great interest regarding the sleep–waking cycle, we found evidence for inputs from the preoptic area dorsal to the supraoptic nucleus and the posterior hypothalamic areas. Indeed, a large body of evidence indicates that these two regions play crucial roles respectively in the onset of sleep and in wakefulness. In this regard, it would be of great interest to determine if these projections participate in the regulation of the activity of the noradrenergic cells of the LC across the sleep–waking cycle.

CONCLUSION

In conclusion, our results indicate that a number of structures project to the LC and might therefore play a role in the modulation of the activity of the noradrenergic neurons across the sleep–waking cycle. Further experiments are necessary to determine the specific role of each of these afferents.

Acknowledgements—This work was supported by INSERM, CNRS, Region Rhône-Alpes, USPHS Grant NS 24698, the DRET 91-130. We wish to thank Yan Zhu, Paul Charléty, Jean-Marie Petit, Christelle Peyron, Béatrice Humbert and Bernard Roussel for their help. We also thank Patrice Fort for his helpful comments.

This article is dedicated to the memory of our colleague and friend Michel Buda, director of the INSERM U 171, who tragically died in August of 1993. This collaborative work on the locus coeruleus, a nucleus he had been studying for many years with his recognized neurochemical skills, was made possible by his constant support and scientific advice as well as his amicable personality marked by a sense of humour and humanism. We wish to thank him.

REFERENCES

1. Allen G. V. and Cechetto D. F. (1992) Functional and anatomical organization of cardiovascular pressor and depressor sites in the lateral hypothalamic area: I. Descending projections. *J. comp. Neurol.* **315,** 313–332.
2. Astier B., Kitahama K., Denoroy L., Jouvet M. and Renaud B. (1987) Immunohistochemical evidence for the adrenergic medullary longitudinal bundle as a major ascending pathway to the locus coeruleus. *Neurosci. Lett.* **74,** 132–138.
3. Aston-Jones G., Astier B. and Ennis M. (1992) Inhibition of locus coeruleus noradrenergic neurons by C1 adrenergic cells in the rostral ventral medulla. *Neuroscience* **48,** 371–382.
4. Aston-Jones G. and Bloom F. E. (1981) Activity of norepinephrine-containing locus coeruleus neurons in behaving rats anticipates fluctuations in the sleep–waking cycle. *J. Neurosci.* **1,** 876–886.
5. Aston-Jones G. and Bloom F. E. (1981) Norepinephrine containing locus coeruleus neurons in behaving rats exhibit pronounced responses to non-noxious environmental stimuli. *J. Neurosci.* **8,** 887–900.

6. Aston-Jones G., Ennis M., Pieribone V. A., Nickell W. T. and Shipley M. T. (1986) The brain nucleus locus coeruleus: restricted afferent control of a broad efferent network. *Science* **234,** 734–737.
7. Aston-Jones G., Shipley M. T., Chouvet G. (1991) Afferent regulation of locus coeruleus neurons: anatomy, physiology and pharmacology. In: *Progress in Brain Research, Vol.* 88 (eds Barnes C. D. and Pompeiano O.), pp. 47–75. Elsevier, Amsterdam.
8. Barrington F. J. F. (1925) The effect of lesions of the hind- and midbrain on micturition in the cat. *Quart. J. Exp. Physiol.* **15,** 81–102.
9. Buda M., Akaoka H., Aston-Jones G. (1993) Modulation of locus coeruleus activity by serotoninergic afferents. In: *Serotonin, the Cerebellum and Ataxia* (eds Trouillas P. and Fuxe K.), pp. 237–253. Raven Press, New York.
10. Cedarbaum J. M. and Aghajanian G. K. (1978) Afferent projections to the rat locus coeruleus as determined by a retrograde tracing technique. *J. comp. Neurol.* **178,** 1–16.
11. Chase M. H., Soja P. J. and Morales F. R. (1989) Evidence that glycine mediates the postsynaptic potentials that inhibit lumbar motoneurons during the atonia of active sleep. *J. Neurosci.* **9,** 743–751.
12. Chiang C., Ennis M., Pieribone V. A. and Aston-Jones G. (1987) Effects of prefrontal cortex stimulation on locus coeruleus discharge. *Abstr. Soc. Neurosci.* **13,** 9–12.
13. Clavier R. M. (1979) Afferent projections to the self-stimulation regions of the dorsal pons, including the locus coeruleus, in the rat as demonstrated by the horseradish peroxidase technique. *Brain Res. Bull.* **4,** 497–504.
14. Conrad L. C. A., Leonard C. M. and Pfaff D. W. (1974) Connections of the median and dorsal raphe nuclei in the rat: an autoradiographic and degeneration study. *J. comp. Neurol.* **156,** 179–206.
15. Conrad L. C. A. and Pfaff D. W. (1976) Efferents from medial basal forebrain and hypothalamus in the rat. I. An autoradiographic study of the medial preoptic area. *J. comp. Neurol.* **169,** 185–220.
16. Dahlström A. and Fuxe K. (1964) Evidence for the existence of monoamine neurons in the central nervous system. I. Demonstration of monoamines in the cell bodies of brain stem neurons. *Acta physiol. scand.*, Suppl. 232, **62,** 1–55.
17. Datta S., Calvo J. M., Quattrochi J. and Hobson J. A. (1991) Long-term enhancement of REM sleep following cholinergic stimulation. *NeuroReport* **2,** 619–622.
18. Drolet G., Van Bockstaele E. J. and Aston-Jones G. (1992) Robust enkephalin innervation of the locus coeruleus from the rostral medulla. *J. Neurosci.* **12,** 3162–3174.
19. Ennis M. and Aston-Jones G. (1989) Potent inhibitory input to locus coeruleus from the nucleus prepositus hypoglossi. *Brain Res. Bull.* **22,** 793–803.
20. Ennis M. and Aston-Jones G. (1989) GABA-mediated inhibition of locus coeruleus from the dorsomedial rostral medulla. *J. Neurosci.* **9,** 2973–2981.
21. Ennis M., Behbehani M., Shipley M. T., Van Bockstaele E. J. and Aston-Jones G. (1991) Projections from the periaqueductal gray to the rostromedial pericoerulear region and nucleus locus coeruleus: anatomic and physiologic studies. *J. comp. Neurol.* **306,** 480–494.
22. Fu L., Shipley M. T. and Aston-Jones G. (1989) Dendrites of rat locus coeruleus are asymmetrically distributed: Immunocytochemical LM and EM studies. *Abstr. Soc. Neurosci.* **15,** 1013.
23. Fung S. J., Reddy V. K., Bowker R. M. and Barnes C. D. (1987) Differential labeling of the vestibular complex following unilateral injections of horseradish peroxidase into the cat and rat locus coeruleus. *Brain Res.* **401,** 347–352.
24. Gerfen C. R. and Sawchenko P. E. (1984) An anterograde neuroanatomical tracing method that shows the detailed morphology of neurons, their axons and terminals: immunohistochemical localization of an axonally transported plant lectin, Phaseolus vulgaris leucoagglutinin (PHA-L). *Brain Res.* **290,** 219–238.
25. Groves P. M. and Wilson C. J. (1980) Fine structure of rat locus coeruleus. *J. comp. Neurol.* **193,** 841–852.
26. Grzanna R. and Molliver M. E. (1980) The locus coeruleus in the rat: an immunohistochemical delineation. *Neuroscience* **5,** 21–40.
27. Herbert H., Moga M. M. and Saper C. B. (1990) Connections of the parabrachialis nucleus with the nucleus of the solitary tract and the medullary reticular formation. *J. comp. Neurol.* **293,** 540–580.
28. Herkenham M. and Nauta W. J. (1979) Efferent connections of the habenular nuclei in the rat. *J. comp. Neurol.* **187,** 19–47.
29. Hobson J. A., McCarley R. W. and Wyzinski P. W. (1975) Sleep cycle oscillation: reciprocal discharge by two brainstem neuronal groups. *Science* **189,** 55–58.
30. Hosoya Y. and Matsushita M. (1981) Brainstem projections from the lateral hypothalamic area in the rat, as studied with autoradiography. *Neurosci. Lett.* **24,** 111–116.
31. Hsu S., Raine L. and Fanger H. (1981) A comparative study of the peroxydase-antiperoxydase method and an avidin-biotin complex method for studying polypeptides hormones with radioimmunoassay antibodies. *Am. J. clin. Pathol.* **75,** 734–738.
32. Hurley K. M., Herbert H., Moga M. M. and Saper C. B. (1991) Efferent projections of the infralimbic cortex of the rat. *J. comp. Neurol.* **308,** 249–276.
33. Jones B. E. (1991) Noradrenergic locus coeruleus neurons: their distant connections and their relationship to neighboring (including cholinergic and GABAergic) neurons of the central gray and reticular formation. In: *Progress in Brain Research* (eds by Barnes C. D. and Pompeiano O.), pp. 15–29. Elsevier, Amsterdam.
34. Jouvet M. (1962) Recherches sur les structures nerveuses et les mécanismes responsables des différentes phases du sommeil physiologique. *Archs ital. Biol.* **100,** 125–206.
35. Kachidian P., Astier B., Renaud B. and Bosler O. (1990) Adrenergic innervation of noradrenergic locus coeruleus neurons. A dual labeling immunocytochemical study in the rat. *Neurosci. Lett.* **109,** 23–29.
36. Krieger M. S., Conrad L. C. A. and Pfaff D. W. (1979) An autoradiographic study of the efferent connections of the ventromedial nucleus of the hypothalamus. *J. comp. Neurol.* **183,** 785–816.
37. Leger L., Degueurce A. M. and Pujol J. F. (1980) (Origin of the serotoninergic innervation of the rat locus coeruleus) Origine de l'innervation serotoninergique du locus coeruleus chez le rat. *C. R. Acad. Sci. D.* **290,** 807–810.
38. Luiten P. G. M., Ter Horst G. J. and Steffens A. B. (1987) The hypothalamus, intrinsic connections and outflow pathways to the endocrine system in relation to the control of feeding and metabolism. *Prog. Neurobiol.* 1–54.
39. Luppi P. H., Aston-Jones G., Akaoka H., Charléty P., Kowelowsky C., Shipley M. T., Zhu Y., Ennis M., Fort P., Chouvet G. and Jouvet M. (1991) Afferents to the rat locus coeruleus (LC) using choleratoxin B subunit (CTb) as a retrograde tracer. *Abstr. Soc. Neurosci.* **17,** 1540.

40. Luppi P. H., Charléty P. J., Fort P., Akaoka H., Chouvet G. and Jouvet M. (1991) Anatomical and electrophysiological evidence for a glycinergic inhibitory innervation of the rat locus coeruleus. *Neurosci. Lett.* **128,** 33–36.
41. Luppi P. H., Fort P. and Jouvet M. (1990) Iontophoretic application of unconjugated cholera toxin B subunit (CTb) combined with immunohistochemistry of neurochemical substances: a method for transmitter identification of retrogradely labeled neurons. *Brain Res.* **534,** 209–224.
42. Machado B. H. and Brody M. J. (1988) Role of the nucleus ambiguus in the regulation of heart rate and arterial pressure. *Hypertension* **11,** 602–607.
43. McCarley R. W. and Hobson J. A. (1975) Neuronal excitability modulation over the sleep cycle: a structural and mathematical model. *Science* **189,** 58–60.
44. Moga M. M., Herbert H., Hurley K. M., Yasui Y., Gray T. S. and Saper C. B. (1990) Organization of cortical, basal forebrain and hypothalamic afferents to the parabrachial nucleus in the rat. *J. comp. Neurol.* **295,** 624–661.
45. Morgane P. J. and Jacobs M. S. (1979) Raphe projections to the locus coeruleus in the rat. *Brain Res. Bull.* **4,** 519–534.
46. North R. A. and Williams J. T. (1985) On the potassium conductance increased by opioids in rat locus coeruleus neurons. *J. Physiol., Lond.* **364,** 265–280.
47. Panula P., Pirvola U., Auvinen S. and Airaksinen M. S. (1989) Histamine-immunoreactive nerve fibers in the rat brain. *Neuroscience* **28,** 585–610.
48. Panula P., Yang H. Y. T. and Costa E. (1984) Histamine-containing neurons in the rat hypothalamus. *Proc. natn. Acad. Sci. U.S.A.* **81,** 2572–2576.
49. Paxinos G. and Watson C. (1986) *The Rat Brain in Stereotaxic Coordinates*, 2nd edn. Academic Press, Sydney.
50. Pieribone V. A. and Aston-Jones G. (1991) Adrenergic innervation of the rat nucleus locus coeruleus arises predominantly from the C1 adrenergic cell group in the rostral medulla. *Neuroscience* **41,** 525–542.
51. Pieribone V. A., Aston-Jones G. and Bohn M. C. (1988) Adrenergic and non-adrenergic neurons in the C1 and C3 areas project to locus coeruleus: a fluorescent double labeling study. *Neurosci. Lett.* **85,** 297–303.
52. Pieribone V. A., Van Bockstaele E. J., Shipley M. T. and Aston-Jones G. (1989) Serotonergic innervation of rat locus coeruleus derives from non-raphe brain areas. *Abstr. Soc. Neurosci.* **15,** 420.
53. Rizvi T. A., Ennis M., Aston-Jones G., Maorong J. and Shipley M. T. (1994) Preoptic projections to Barrington's nucleus and the peri-coerulear region column: Architecture and terminal organization. *J. comp. Neurol.* **347,** 1–24.
54. Robertson B. and Grant G. (1985) A comparison between wheat germ agglutinin- and choleragenoid-horseradish peroxidase as anterogradely transported markers in central branches of primary sensory neurones in the rat with some observations in the cat. *Neuroscience* **14,** 895–905.
55. Ruggiero D. A., Giulano R., Anwar M., Stornetta R. and Reis D. J. (1990) Anatomical substrates of cholinergic-autonomic regulation in the rat. *J. comp. Neurol.* **292,** 1–53.
56. Sakai K. (1985) Anatomical and physiological basis of paradoxal sleep. In, (eds Drucker-Colin R., McGinty D. J., Morrisson A. and Parmeggiani L.), pp. 111–137. Raven Press, New York.
57. Sakai K., Touret M., Salvert D., Leger L. and Jouvet M. (1977) Afferent projections to the cat locus coeruleus as visualized by the horseradish peroxidase technique. *Brain Res.* **119,** 21–41.
58. Saper C. B., Swanson L. W. and Cowan W. M. (1976) The efferent connections of the ventromedial nucleus of the hypothalamus of the rat. *J. comp. Neurol.* **169,** 409–442.
59. Satoh K., Shimizu N., Tohyama M. and Maeda T. (1978) Localization of the micturation reflex center at the dorsolateral pontine tegmentum of the rat. *Neurosci. Lett.* **8,** 27–33.
60. Shimizu N., Katoh Y., Hida T. and Satoh K. (1979) The fine structural organization of the locus coeruleus in the rat with reference to noradrenaline contents. *Expl Brain Res.* **37,** 139–148.
61. Shipley M. T., Fu L., Ennis M. and Aston-Jones G. (1994) Distribution of locus coeruleus extranuclear dendrites. Immunocytochemical LM and EM studies. *J. comp. Neurol.* (in press).
62. Shirokawa T. and Nakamura S. (1987) Antidromic activation of rat dorsomedial hypothalamic neurons from locus coeruleus and median eminence. *Brain Res. Bull.* **18,** 291–295.
63. Simerly R. B. and Swanson L. W. (1988) Projections of the medial preoptic nucleus: a Phaseolus vulgaris leucoagglutinin anterograde tract-tracing study in the rat. *J. comp. Neurol.* **270,** 209–242.
64. Simon H., Le Moal M., Stinus L. and Calas A. (1979) Anatomical relationships between the ventral mesencephalic tegmentum-A10 region and the locus coeruleus as demonstrated by anterograde and retrograde tracing techniques. *J. neural. Transm.* **44,** 77–86.
65. Somogyi P., Minson J. B., Morilak D. A., Llewewellyn-Smith I., McIlhinney J. R. A. and Chalmers J. (1989) Evidence for an excitatory amino acid pathway in the brainstem and for its involvement in cardiovascular control. *Brain Res.* **496,** 401–407.
66. Swanson L. W. (1976) The locus coeruleus: a cytoarchitectonic, Golgi and immunohistochemical study in the albino rat. *Brain Res.* **110,** 39–56.
67. Swanson L. W. (1976) An autoradiographic study of the efferent connections of the preoptic region in the rat. *J. comp. Neurol.* **167,** 227–256.
68. Takagishi M. and Chiba T. (1991) Efferent projections of the infralimbic (area 25) region of the medial prefrontal cortex in the rat: an anterograde tracer PHA-L study. *Brain Res.* **566,** 26–39.
68a. Valentino R. J., Page M. E., Luppi P.-H., Zhu Y., Van Bockstaele E. and Aston-Jones G. (1994) Evidence for widespread afferents to Barrington's nucleus, a brainstem region rich in corticotropin-releasing hormone neurons. *Neuroscience* **62,** 125–143.
69. van der Kooy D., Koda L. Y., McGinty J. F., Gerfen C. R. and Bloom F. E. (1984) The organization of projections from the cortex, amygdala, and hypothalamus to the nucleus of the solitary tract in rat. *J. comp. Neurol.* **224,** 1–24.
70. Villalobos J. and Ferssiwi A. (1987) The differential descending projections from the anterior, central and posterior regions of the lateral hypothalamic area: an autoradiographic study. *Neurosci. Lett.* **81,** 95–99.
71. Williams J. T., North R. A., Shefner S. A., Nishi S. and Egan T. M. (1984) Membrane properties of rat locus coeruleus neurons. *Neuroscience* **13,** 137–156.
72. Yasui Y., Breder C. D., Snaper C. B. and Cechetto D. F. (1991) Autonomic responses and efferent pathways from the insular cortex in the rat. *J. comp. Neurol.* **303,** 355–374.

(*Accepted* 14 *September* 1994)